Establishment of an ELISA and a lateral flow device for detection of European and American foulbrood including genotype-differentiation of the American foulbrood causing agent (ERIC I & ERIC II) in honey bees

I n a u g u r a l d i s s e r t a t i o n

zur

Erlangung des akademischen Grades eines

Doktors der Naturwissenschaften (Dr. rer. nat.)

der

Mathematisch-Naturwissenschaftlichen Fakultät

der

Universität Greifswald

vorgelegt von

Sandra Ehrenberg

Greifswald, 2021

Dekan: Prof. Dr. Gerald Kerth

1. Gutachterin: Prof. Dr. Cornelia Silaghi

2. Gutachter*in: Prof. Dr. Peter Rosenkranz

Tag der Promotion: 01.02.2022

Inhalt

Abbreviation index

°C	degree Celsius
A	ampere
AA	amino acid
Ab	antibody
AFB	American foulbrood
APS	ammonium persulfate
ATCC	American Type Culture Collection
BCCM	Belgian Co-ordinated Collections of Microorganisms
bp	base pairs
BSA	bovine serum albumin
dH_2O	distilled water
DNA	deoxyribonucleic acid
DSM	Deutsche Sammlung von Mikroorganismen und Zellkulturen
ECL	enhanced chemiluminescence
EDTA	ethylene-diamine tetra acetic acid
EFB	European foulbrood
ELISA	enzyme-linked immunosorbent assay
ERIC	enterobacterial repetitive intergenic consensus regions
FCS	foetal calf serum
groEL	gene coding for chaperonin
h	hour
his	histidine
HSP60	heat shock protein 60, chaperonin
HRP	horseradish peroxidase
Ig	immunoglobulin
IP	immunoprecipitation
K	kappa (light chain type of antibodies)
kb	kilo base pairs
kDa	kilo Dalton

LFD	lateral flow device
M	molar
mAb	monoclonal antibody
mg	milligram
min	minutes
mL	milliliter
mM	millimolar
µL	microliter
O/N	overnight
pAb	polyclonal antibody
PAGE	polyacrylamide gel electrophoresis
PCR	polymerase chain reaction
RT	room temperature
SDS	sodium dodecyl sulphate
S-layer	surface layer protein
SplA	surface layer protein of *P. larvae*
V	volt
WB	western blot
x g	gravitational acceleration

Summary

American and European foulbrood (AFB and EFB) are devastating bacterial brood diseases of honey bees (*Apis mellifera*), which cause colony and economic losses worldwide. The causative agent of AFB, *Paenibacillus larvae,* are grouped into different ERIC-genotypes (Enterobacterial repetitive intergenic consensus) the two most common of which are ERIC I and ERIC II. In the field, the differentiation between the symptoms of AFB and EFB (caused by *Melissococcus plutonius*) can be difficult. The differentiation between the ERIC-genotypes in the field based on the symptoms is not possible at all. The differentiation between the ERIC-genotypes of *P. larvae* during diagnosis can help to understand the spread of the AFB disease. Hence, a tool capable of detection and distinction between the bacterial brood diseases and the *P. larvae*-genotypes is needed. For the optimal prevention of disease spread, the diagnosis needs to be fast, cheap and reliable.

This study focuses on the development of a diagnostic sandwich ELISA and a lateral flow device (LFD) for the detection and distinction of EFB and AFB, including the differentiation of the two main occurring *P. larvae* genotypes. The therefore necessary specific monoclonal antibodies (mAbs) were obtained by immunizing mice with *M. plutonius* or *P. larvae* strains belonging to either ERC I or ERIC II. The generated mAbs were characterized for their specificity towards the target bacteria and for their cross reactivity towards other bee-associated bacteria. The screening for suitable mAbs resulted in two specific mAbs against *M. plutonius*, two against *P. larvae* in general and two against ERIC II. In combination with the anti-*P. larvae* mAbs, the anti-ERIC II mAbs were used for genotyping.

In order to evaluate the suitability of the mAbs, their antigens were identified. The target antigens of the produced mAbs turned out to be proteins that could be of further interest as they seem to be involved in the pathogenesis and host-pathogen-interaction. The mAbs with the same antigens were used in the sandwich ELISA for testing the cross reactivity and strain detection. Suitable mAb combinations were used for LFD production. The LFDs were then successfully tested against several field isolates of AFB and EFB causing agents and no cross reactivity with bee-associated bacteria was detected. The *P. larvae* strains used for mAb testing were genotyped to obtain information about the respective genetic variance. In the process atypical *P. larvae* strains were identified and further characterized using the generated mAbs. The ability of the mAbs to also recognise the atypical strains as well indicates that the mAbs bind to an antigen that is common among different *P. larvae* strains.

All in all, a fast tool for detection and differentiation of EFB, AFB and the two ERIC-genotypes was developed that has to be further tested for its reliability in the field.

Zusammenfassung

Die Amerikanische und Europäische Faulbrut (AFB und EFB) sind verheerende bakterielle Brutkrankheiten der Honigbiene (*Apis mellifera*), die weltweit zu Kolonieverlusten und damit auch zu ökonomischen Einbußen führen kann. Verursacher der AFB ist *Paenibacillus larvae*, welcher sich in verschiedene ERIC-Genotypen (Enterobacterial repetitive intergenic consensus) einteilen lässt, von denen die Typen ERIC I und ERIC II am häufigsten auftreten. Die EFB wird durch *Melissococcus plutonius* verursacht. Die Unterscheidung der beiden Faulbrutkrankheiten im Feld am Bienenvolk kann aufgrund der ähnlichen Symptomatik problematisch sein und die Differenzierung der AFB-Genotypen ist im Feld bislang nicht möglich. Da die Genotypunterscheidung relevant für die Verbreitungsanalyse der AFB ist, wäre ein diagnostischer Schnelltest, welcher EFB und AFB detektiert und zusätzlich zwischen den ERIC-Genotypen unterscheiden kann, sehr hilfreich. Um die Verbreitung der Brutkrankheiten möglichst schnell und gezielt eindämmen zu können, sollte ein entsprechender diagnostischer Test schnell, kostengünstig und zuverlässig sein.

Daher war es das Ziel dieser Studie einen Sandwich ELISA und einen Schnelltest für die Diagnose von EFB und AFB, sowie die Unterscheidung der *P. larvae* Genotypen zu entwickeln. Hierzu wurden monoklonale Antikörper (mAks) in Mäusen hergestellt. Die Mäuse wurden entweder mit *M. plutonius* oder *P. larvae,* (separat mit ERIC I oder ERIC II) immunisiert. Die generierten mAks wurden auf ihre Spezifität gegenüber dem Zielbakterium, sowie auf die Kreuzreaktivität mit bienenassoziierten Bakterien getestet. Für die Detektion von *M. plutonius*, *P. larvae* und ERIC II wurden jeweils zwei geeignete mAks für die weitere Anwendung ausgewählt. Die anti-*P. larvae* und anti-ERIC II mAks wurden zusammen für die Genotypisierung verwendet.

Im Verlauf der mAk-Charakterisierung wurden die erkannten Antigene als relevante Proteine für weitere Pathogenese-Untersuchungen und Wirt-Pathogen-Interaktionen identifiziert. Die mAks, welche die gleichen Antigene des jeweiligen Bakteriums erkennen, wurden für die Etablierung des Sandwich ELISAs verwendet und auf ihre Spezifität und Kreuzreaktivität getestet. Geeignete mAk-Kombinationen wurden für die Herstellung der Schnelltests verwendet. Die Schnelltests wurden ebenfalls auf Kreuzreaktivität mit bienenassoziierten Bakterien und verschiedenen Feldstämmen der AFB- und EFB-Erreger erfolgreich getestet. Zudem wurden die verwendeten *P. larvae* Stämme genotypisiert, um die genetische Varianz der getesteten Stämme zu bestimmen. Dabei wurden unter anderem atypische *P. larvae* Stämme identifiziert und mithilfe der mAks charakterisiert. Die erfolgreiche Identifizierung der atypischen *P. larvae* Stämme durch die mAks zeigt, dass die mAks ein Antigen erkennen, welches in den verschiedenen *P. larvae*-Stämmen weit verbreitet ist.

Es wurden Schnelltests für die Detektion und Unterscheidung der EFB, AFB und der zwei hauptäschlich vorkommenden ERIC-Genotypen entwickelt. Jedoch, müssen diese weiterhin auf ihre Zuverlässigkeit im Feld getestet werden.

1. Introduction

1.1 Western honey bee

The western honey bee, *Apis mellifera,* is a eusocial insect that belongs to the order of Hymenoptera and the family *Apidae*. Within a honey bee colony, the different individuals are cooperating with each other and are only able to ensure the survival of the colony and successful reproduction together. The functional specialization of the individual bees of a colony is to some extent comparable to the functional specialization of the individual cells in a multicellular organism. Therefore, honey bee colonies are called superorganisms that consist of three different casts: one fertile queen, several thousand female worker bees and hundreds of male drones (Graham, 1992). The huge number of worker bees is maintaining the food income and the nursing of the honey bee brood, which plays a central role in colony survival and reproduction.

The life cycle of each worker honey bee starts as an egg that is laid by the queen into a brood cell. After three days the larva hatches and is nursed by infertile worker bees that are providing food until the larva pupates on the ~ 6th day after hatching (Winston, 1987; Graham, 1992). Worker bees seal the brood cells with wax and the larva undergoes several pupal stages in a safe environment. After ~ 21 days post hatching, the development into an adult honeybee is completed and the young bee breaks the cap of the brood cell and enters the combs of the colony (Winston, 1987; Graham, 1992). During the developmental phase from egg to adult bee, the larvae are depending on worker bees that provide food, clean and cap the cells. The worker bees are also responsible for feeding the queen and other workers. Although this behaviour has several benefits, it can also enhance the risk of disease transmission and thereby increases the spreading of diseases within the colony, leading to potentially devastating results for the whole colony.

Based on their honey production and even more importantly their role as pollinators, honey bees are considered economically, agriculturally and environmentally important livestock. The agricultural and economical significance of the honey bee mostly comes from their pollination activities of important crop plants. For example, a study in Panama showed that the yields of coffee and some other fruits decreased by more than 90 % when bees were not pollinating the crops (Southwick & Southwick, 1992; Klein *et al.*, 2007). The demand for pollination provided by honey bees increased over the last years, whereas in the same time increasing amounts of colony losses have been reported in some regions of Europe (Klein *et al.*, 2007). In order to prevent discrepancies between pollination demand and supply, it is important to understand which factors can influence the health of a honey bee colony. Such factors can be climate, globalization, agricultural practices, beekeeping practices, local densities of bee colonies and the local spread of different diseases (Hristov *et al.*, 2020). Disease causing agents in

honey bees are ectoparasites, intestinal parasites, fungi, bacteria and viruses, affecting different developmental stages of the bees (Hristov *et al.*, 2020). Diseases that affect the brood can weaken the whole colony due to the lack of healthy offspring that is needed for survival and successful reproduction of the colony.

1.2 Honey bee brood diseases

Honey bee colonies are susceptible to several different brood diseases. These brood diseases can be caused by a number of different agents including mites, fungi, bacteria and viruses. Typical symptoms of brood disease are a change in colour and shape of diseased honey bee larvae and a patchy brood pattern. Some of the most relevant brood diseases are: varroosis, sacbrood, chalkbrood, stonebrood, European foulbrood (EFB) and American foulbrood (AFB). All of these brood diseases can lead to patchy brood pattern. Diseases that are not caused by bacteria typically show additional symptoms such as changes in morphology of diseased/dead larvae that makes the distinction from bacterial brood diseases easy for inspectors and beekeepers.

1.2.1 Bacterial brood diseases

The distinction between the two bacterial brood diseases and the identity of the causative agents was unclear for a long time due to the similarity in symptoms and a lack of suitable methods to distinguish both diseases. The first documented description of foulbrood symptoms in honey bees is reported by Aristotle in the fourth century before Christ (Maassen, 1908). Gottlob Schirach cited by Maassen, 1908 accurately described the disease in 1769 and named it foulbrood, based on its distinctive odour. After several unsuccessful attempts to cultivate the presumably causative agent "*Bacillus alvei*" (Cheshire & Cheyne, 1885) from diseased larvae, White succeeded in cultivating a novel bacterium out of the diseased larvae that he called "*Bacillus larvae*" (White, 1906; Maassen, 1908). Differences in foulbrood symptoms were described in 1906 by White. Due to these differences, the first distinction between the foulbrood diseases, calling them American and European foulbrood in accordance to the origin of the persons who first described the occurring bacteria, was made (White, 1906; Maassen, 1908).

American foulbrood was thought to be caused by two bacteria showing different disease symptoms. "*Bacillus larvae"* (White, 1906) that leads to the degradation of the dead larvae into a ropy mass and "*Bacillus pulvifaciens"* (Katznelson, 1950) causing the development of a powdery scale out of deceased larvae. The causative agent of AFB underwent several phylogenetic reclassifications. In 1993, the genus of *Bacillus* was reclassified referring to 16S rRNA gene sequence analysis and the two American

foulbrood causing bacteria species were reclassified to the new genus *Paenibacillus* (Ash *et al.*, 1993). In 1996, the two bacteria species were identified as one species, which was divided into two subspecies (subsp.), *Paenibacillus larvae* subsp. *larvae* and *Paenibacillus larvae* subsp. *pulvifaciens* (Heyndrickx *et al.*, 1996). However, the clear division into two subspecies was revoked after morphological, metabolic, protein pattern and genomic fingerprinting analyses. The subspecies were reclassified into four genotypes of *P. larvae* with two main clusters (Genersch *et al.*, 2006). For further information about these genotypes, see chapter 1.2.1.2.

The causative agent of European foulbrood was also not clearly identified for a long time. In 1912, White described a new bacterium occurring in diseased larvae, which he named "*Bacillus pluton*". He failed to cultivate this bacterium from diseased larvae, so that the existence of this type of foulbrood was debated in the scientific society (White, 1912; Wharton, 1927; Lochhead, 1928; Burnside, 1934) until in 1956 Bailey successfully cultivated the causative agent of EFB, that he named *Streptococcus pluton* (Bailey, 1957). After further serological and genomic investigations and successful infestation of bee brood the causative agent of EFB was called *Melissococcus plutonius* (Bailey, 1983).

The bacterial brood diseases, EFB and AFB, show common symptoms such as patchy brood pattern and sunken cell-cappings. After a certain amount of larvae have died the eponymous unpleasant "foul" odour develops. Furthermore, the change of larval colour from pearly white to brownish-black can be observed. The larvae/pupae are significantly weakened by the bacterial infection and often die from it. After larval death, the larvae are decomposed by bacteria and lose their tissue integrity (Forsgren, 2010; Fünfhaus *et al.*, 2018a). This can be observed in the field and also in *in vitro* reared larvae as shown in Figure 1 (see arrow).

healthy larva | *M. plutonius* infected larva | *P. larvae* infected larva

Figure 1 In vitro reared and infected honey bee larvae

The in vitro reared honey bee larvae were at the age of seven days post hatching. Freshly hatched larvae were transferred from comb to 24-well plates and were infected with foulbrood causing agents. The larvae were fed and controlled every day. The in vitro rearing was performed in an incubator, maintaining 35 °C and a humidity of 95 %. From left to right: healthy larva, *M. plutonius* infected larva, *P. larvae* infected larva. The infected larvae are smaller than the healthy seven-day old larva. The *M. plutonius* infected larva shows no tissue degradation, whereas the *P. larvae* infected larva died and shows tissue degradation laterally (black arrow).

1.2.1.1 European foulbrood

EFB is distributed worldwide and it is endemic in most parts of the world (Forsgren *et al.*, 2018). In Europe huge increases in EFB incidence have been reported in the United Kingdom and Switzerland in the last decades (Wilkins *et al.*, 2007; Roetschi *et al.*, 2008). In Switzerland the number of infected apiaries increased six-fold in 2006 compared to 1999(~50 infected apiaries in 1999 to ~300 infected apiaries in 2006), whereas the number of cases in the UK increased from 267 cases in 1999 to 429 cases in 2006 (Wilkins *et al.*, 2007; Roetschi *et al.*, 2008). Clinical cases in Finland, France, Greece, Holland, Italy, and Czech Republic have been reported as well (Erban *et al.*, 2017; Forsgren *et al.*, 2018). Because EFB is not a notifiable disease in Germany and the legal authorities do not have to be informed of any EFB suspicions, there is a lack of data about recent EFB outbreaks in Germany.

EFB often occurs seasonally in mid and late spring, when colonies are building up their population (Alippi, 2014; Forsgren *et al.*, 2018). Symptoms of EFB overlap with general brood disease symptoms, for example patchy brood pattern and sunken cappings. A typical sour odour of diseased colonies can be recognized (Forsgren *et al.*, 2013; Forsgren *et al.*, 2018). EFB usually affects young and unsealed brood but cases where sealed brood was infected, have also been reported (Roy & Franco, 2021). The diseased larvae change colour and lose their tissue integrity. The consistency of infected or dead larvae is watery to pasty, sometimes sticky or ropy and stretching granularly (Alippi, 2014). The remaining larvae scales are usually twisted in the cell (Figure 2) and do not adhere tightly to the cell wall (Forsgren *et al.*, 2013; Forsgren *et al.*, 2018).

Figure 2 EFB diseased brood
The arrows indicate brood cells with larvae that show disease symptoms. Larvae have changed colour from pearly white to yellowish-brown and lost their tissue integrity.

The causative agent *M. plutonius* is a gram-positive coccoidal bacterium that can form chains. The bacterium causes EFB, not only in the western honey bee *A. mellifera*, but also in other honey bee species including: the eastern honey bee (*Apis cerana*) and the Himalayan giant honey bee (*Apis laboriosa*) (Forsgren *et al.*, 2018). EFB can also occur in stingless bees (*Melipona* species) that belong to the same family as honey bees (Teixeira *et al.*, 2020). *Melissococcus plutonius* is ingested via larval

food (Takamatsu *et al.*, 2016). Previous studies showed that *M. plutonius* is found in the larval gut and multiplies in the food mass of the gut lumen. At the early stage of infection, *M. plutonius* cells are located on the surface of the peritrophic membrane, which is lining the midgut epithelium and functioning as physical barrier against pathogens (Takamatsu *et al.*, 2016). Bacteria growth extends until bacteria fill the gut lumen almost completely. The bacteria seem to not invade larval tissue actively (Aupperle-Lellbach *et al.*, 2018). Investigations of larval infection with a highly virulent *M. plutonius* strain showed *M. plutonius*-derived substances diffusing into the larval tissues during the course of the infection (Takamatsu *et al.*, 2016; Djukic *et al.*, 2018). The described findings above indicate that *M. plutonius* might only compete for food with the larval host rather than actively harm larval tissue.

EFB is associated with several other bacteria and was therefore believed to be caused by different species. A few of the EFB-associated bacteria were already described in the 19th to 20th century and it is suspected that they have a supplementary pathogenic effect on the causative agent *M. plutonius* but this was not proven so far (Bailey, 1983; Bailey & Ball, 1991; Lewkowski & Erler, 2018; Grossar *et al.*, 2020). Nowadays, several bacteria have been isolated from diseased larvae, such as *Enterococcus faecalis*, *Brevibacillus laterosporus*, *Bacillus pumilus*, *Paenibacillus alvei*, and *Paenibacillus dendritiformis* (Forsgren *et al.*, 2018). Earlier, also *Achromobacter eurydice* was considered to be closely related to European foulbrood outbreaks. However, a recent study revealed that the pleiomorphic bacterium, which was described in 19th century might not have been *A. eurydice* but is more likely to have been a commensal bacterium occurring in honey bee larvae, like *Lactobacillus kunkeei* or *Fructobacillus fructosus* (White, 1912; Erler *et al.*, 2017). In general, the exact role of the different EFB-associated bacteria is still elusive.

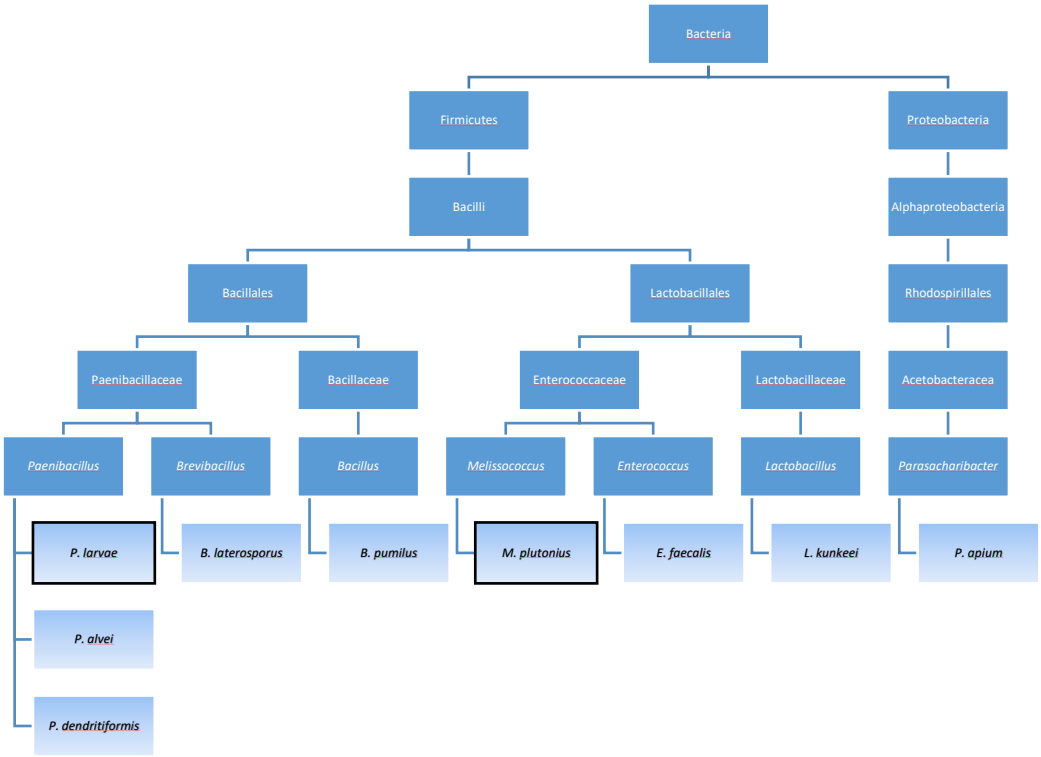

Figure 3 Phylogenetic relation of bacteria occurring in a honey bee hive
Phylogenetic relations of tested bee-associated bacteria. Relations are visualized according to classification into bacterial families and genus using NCBI database (https://www.ncbi.nlm.nih.gov/; 13.05.2019). Light blue boxes show bacteria species that where further analysed within this work. Black framed boxes show the foulbrood causing agents.

1.2.1.1.1. Characteristics and genotyping of *M. plutonius*

Melissococcus plutonius has special requirements when cultivated in the laboratory. The bacterium requires a sodium-potassium ratio smaller or equal to one and shows growth under anaerobic conditions (Arai *et al.*, 2012). When *M. plutonius* is cultured in the laboratory it can lose its virulence (McKee *et al.*, 2004). Overall, the bacterium is considered a morphological, physiological, immunological, and genetically homogeneous species with few exceptions declared as atypical strains (Bailey & Gibbs, 1962; Allen & Ball, 1993; Djordjevic *et al.*, 1999). In 2012, atypical *M. plutonius* strains, which differ phenotypically and metabolically from usual *M. plutonius* strains, have been characterized in Japan (Djordjevic *et al.*, 1999; Arai *et al.*, 2012). DNA-DNA hybridization and 16S rRNA gene analysis demonstrated that the strains were taxonomically identical to typical *M. plutonius* strains. The phenotypical findings of two different groups of *M. plutonius*, typical and atypical were supported by pulsed-field gel electrophoresis analysis (Arai *et al.*, 2012). To refine the genetic grouping of *M. plutonius* strains, next-generation sequencing was performed for identification of highly polymorphic regions (Haynes *et al.*, 2013). These regions were used to establish a modified multi-locus sequence typing (MLST) for *M. plutonius* strains. The MLST consisting of four different non-housekeeping gene loci revealed the existence of 21 sequence types (ST) testing field isolates from

Europe, America, Asia and Australia. Furthermore, the MLST analysis unravelled that the previously detected atypical strain from Japan shows similar MLST types as the strains from Brazil, UK, USA and the Netherlands, suggesting that atypical strains can be found globally (Haynes *et al.*, 2013). So far, 41 different STs of 381 isolates have been added to the MLST database (Jolley *et al.*, 2018). Based on the definition that each ST must share at least three out of four identical alleles, the STs were further grouped into three clonal complexes (CC3; CC12; CC13). Field studies showed that CC3 is the most common of the three CCs, followed by CC13. The complex CC12 is relatively rare in continental Europe and it is mainly detected in the UK and Japan. Strains belonging to CC12 turned out to be more virulent than CC13 in field studies (Budge *et al.*, 2014). These findings were confirmed by *in vitro* infection experiments, where representatives of each CC were tested. CC12 killed all tested bees before pupation. The CC3 strain showed lower virulence than the CC12 strain but higher virulence than the CC13 strain, which was considered as avirulent (Nakamura *et al.*, 2016; Lewkowski & Erler, 2018). The previously described findings indicate that different *M. plutonius* strains are not genetically homogenous across its geographical range and may differ in virulence according to CCs. A recent study, investigating the virulence of sixteen *M. plutonius* strains in an *in vitro* larvae infection experiment showed no correlation between virulence and CC of the field strains (Grossar *et al.*, 2020). The results indicated that differences in virulence correlate more with *in vitro* growth dynamics of the different *M. plutonius* strains than with CC grouping (Grossar *et al.*, 2020). Furthermore, the genotyping of *M. plutonius* strains can be used for identification of multiple infections of a larva or a colony. The existence of infections with different *M. plutonius* strains at the same time has already been reported in one larva (Djukic *et al.*, 2018).

1.2.1.1.2. Virulence factors of *M. plutonius*

Pathogen success is influenced by many different factors. A comparative genomics study demonstrated possible virulence and pathogenicity factors in *M. plutonius*, including an enterococcal polysaccharide antigen, an epsilon toxin, bacteriocins (peptides with antimicrobial activity), proteolytic enzymes, bacteria cell surface-associated, host cell adhesion-associated and capsule-associated proteins (Djukic *et al.*, 2018). All *M. plutonius* strains showed pectin degradation genes that might be useful for pollen perforation to release nutrients from pollen, which are present in the larval gut. This underlines the hypothesis that *M. plutonius* might compete for food with its host and does not actively harm the host (Aupperle-Lellbach *et al.*, 2018; Djukic *et al.*, 2018). The aforementioned hypothesis is further supported by the recent investigation of the function in pathogenesis of peritrophic matrix-degrading proteins of a highly virulent *M. plutonius* strain (Nakamura *et al.*, 2021). In the study it was shown that the peritrophic matrix-degrading proteins are not the main factors for virulence of

the tested strains but might support pathogenesis (Nakamura *et al.*, 2021). The bacteriocins present in some *M. plutonius* strains additionally suggest that other bacteria present in the larval gut might be competitors for *M. plutonius*. Furthermore, genes for tyramine production (a biogenic amine) have been identified in *M. plutonius* (Djukic *et al.*, 2018). It was shown that tyramine causes similar symptoms in larvae as EFB does, when tyramine is expressed by *E. faecalis,* so that it could potentially be toxic for honey bee larvae (Kanbar *et al.*, 2004; Kanbar *et al.*, 2005). The presence of a putative toxin, melissotoxin A, might also be important for the development of the high pathogenicity of some *M. plutonius* strains (Grossar *et al.*, 2020). The loss of pathogenicity of *M. plutonius* after several cultivation cycles in the laboratory can be explained by the loss of the plasmid (pMP19) that harbours the gene of melissotoxin A (McKee *et al.*, 2004; Djukic *et al.*, 2018; Grossar *et al.*, 2020). The potential virulence factors described above have to be studied further for their functionality and relevance in pathogenicity to determine reliable virulence factors of *M. plutonius in vivo*.

1.2.1.2 American foulbrood

The AFB is more devastating for the honey bee colony than EFB. In contrast to EFB, it is not associated with secondary bacterial infection. The AFB is spread worldwide (Forsgren *et al.* (2018). In Germany, an average of 268 *P. larvae* outbreaks were reported per year over the last 25 years (Tiergesundheitsjahresbericht, 2019). AFB is a bacterial honey bee brood disease that is notifiable or must be reported to governmental authorities in many countries. Honey bee colonies suffering from AFB show typical symptoms of brood diseases, such as patchy brood pattern, scattered capped brood and sunken cappings (Ebeling *et al.*, 2019). Diseased larvae undergo colour change from pearly white over light brown to almost black. The diseased brood loses its integrity and is drawing a brownish, semi-fluid, glue-like colloid mass (=ropy mass) (Alippi, 2014). The larval scales usually adhere strongly to cell wall and a solid and dry mass may be present. In the diseased colonies a slight to pronounced glue odour develops (Alippi, 2014).

Figure 4 AFB diseased brood
On the left side the typical ropy mass of dead larvae is shown (black arrow). On the right side the hard larvae scales (white arrow) that are brownish-black are shown.

The AFB is caused by the spores of the rod-shaped and gram-positive bacterium *P. larvae.* The vegetative bacterial cells are not infectious to larvae (White, 1920; Tarr, 1937; Woodrow, 1942; Bailey & Ball, 1991). Honey bee larvae are most susceptible to AFB in the first ~12-36 h after hatching (Woodrow, 1942; Bamrick & Rothenbuhler, 1961; Brodsgaard *et al.*, 1998; Genersch, 2010). The susceptibility of larvae to *P. larvae* spores decreases with age of the larva. Young larvae (< 24 h after hatching), can be successfully infected with fewer than ten *P. larvae* spores, whereas 24 h old larvae require millions of spores for successful infection (Woodrow & Holst, 1942; Bamrick & Rothenbuhler, 1961; Chantawannakul & Dancer, 2001). Spores of *P. larvae* are ingested by swallowing contaminated food. Roughly, 12 h after the spore ingestion, the spores germinate and vegetative cells proliferate in the larval mid gut following a commensal life style in this stage of infection (Bamrick, 1967; Yue *et al.*, 2008; Genersch, 2010). As soon as the larval gut is filled with vegetative cells of *P. larvae*, the bacteria attack the gut epithelium. After breaching the epithelium, *P. larvae* invades the hemocoel and secretes several proteases that are involved in the degradation of the honey bee larvae (Genersch, 2010). The larvae die after the gut epithelium is breached by the bacterium. Dead larvae are either removed from the cells by worker bees or the larvae are digested by the bacteria into a brownish ropy mass. Finally, the ropy mass dries to a hard scale that contains a high number of spores and is attached the bottom of the brood cell. The infectious spores are highly resistant to environmental factors and remain infectious for years (Haseman, 1961). Spores are driving disease transmission and can be spread via adult honey bees to larvae, honey stores and other parts of the hive (Genersch, 2010).

1.2.1.2.1. Characteristics and genotyping of *P. larvae*

The historical classification of *P. larvae* into two sub-species indicates that a higher diversity of *P. larvae* exists compared to the diversity of *M. plutonius.* The current classification of *P. larvae* is as it is shown in Figure 3. One of the main methods for distinction of sub-groups in *P. larvae* species is a

genetic differentiation based on enterobacterial repetitive intergenic consensus regions (ERIC). Therefore, a repetitive element polymerase chain reaction (rep-PCR) with primers binding the ERIC regions is used. The examination of strain-specific DNA band patterns can be used for typing purposes of different species (Olive & Bean, 1999). The AFB causing agent, *P. larvae*, can be sub-grouped into five different ERIC-genotypes (ERIC I, II, III, IV and V) (Genersch *et al.*, 2006; Beims *et al.*, 2020). Additionally, two special ERIC-genotypes, ERIC * and ERIC **, have been described that show high similarities in band pattern of rep-PCR compared to ERIC II. The band pattern of ERIC * is lacking the upper band at ~2500 bp, whereas ERIC ** is lacking a band at ~2000 bp (Figure 11). Further investigations using MALDI Biotyper, showed that ERIC * seems more related to ERIC II, whereas ERIC ** forms a separate group, when comparing them to ERIC I and II isolates (Schäfer *et al.*, 2016). The identified ERIC-genotypes, ERIC I to ERIC V, differ in distribution, morphology, pathogenesis and virulence to the honey bee larvae or on honey bee colony level. In the field, the most commonly found genotypes are ERIC I and ERIC II. The genotypes ERIC III and IV have not been reported for decades (Genersch, 2010; Forsgren *et al.*, 2018) and so far, only one strain of ERIC V was isolated from a Spanish honey sample (Beims *et al.*, 2020). In comparison, ERIC I shows lower virulence in *in vitro* reared larvae than ERIC II, killing the larvae after ~12 days, whereas ERIC II causes earlier larvae death after ~ 7 days (Ashiralieva & Genersch, 2006; Genersch, 2010; Genersch, Ashiralieva, & Fries, 2005). The virulence on colony level negatively correlates to virulence on larval level. ERIC I infected colonies suffer more from infection than ERIC II infected ones due to slower/later removal of ERIC I infected larvae by nurse bees (Rauch, Ashiralieva, Hedtke, & Genersch, 2009).

For a detailed understanding of epidemiological connections, outbreaks and cross-transmission of diseases, sub-typing the pathogenic bacterium is a significant advantage (Olive & Bean, 1999). Therefore, several investigations based on differences of genetic properties and protein levels have been conducted (Genersch *et al.*, 2006; Schäfer *et al.*, 2014; Morrissey *et al.*, 2015; Descamps *et al.*, 2016). MLST analysis, as it is used for *M. plutonius*, was also established for *P. larvae* using seven gene loci (Morrissey *et al.*, 2015). The MLST analysis sub-divided 400 *P. larvae* isolates from five different continents into 42 STs (Jolley *et al.*, 2018). The tested ERIC I strains, showed higher diversity than the tested ERIC II strains (Morrissey *et al.*, 2015). Even though, MLST is a useful method for epidemiology and source tracking, the necessity for a labour-intensive sequencing step makes it an unsuitable method for large scale screening. To lower the costs of sub-typing, multiple locus variable number of tandem repeats analysis (MLVA), another method for DNA-typing, was adapted for *P. larvae* sub-typing (Descamps et al., 2016). MLVA is based on a multiplex PCR and DNA band pattern analysis to distinguish the different MLVA-types. The targets of this genotyping are variable-number tandem repeats (VNTR) targeting five different loci in the DNA of *P.* larvae (van Belkum, 1999; Descamps *et al.*, 2016). VNTRs

are caused by slipped strand mispairings (Torres-Cruz & van der Woude, 2003). The MLVA typing of more than 200 strains unravelled the existence of 21 MLVA-genotypes thus refining the ERIC-genotyping (Descamps *et al.*, 2016). Recently, based on their band patterns, more than 40 new MLVA-genotypes have been discovered in the laboratory of Bee Diseases of the Friedrich-Loeffler institute (Schäfer, unpublished). The MLVA is used for refined typing of the target species for more accurate epidemiological approaches compared to ERIC-genotyping.

1.2.1.2.2. Virulence factors of *P. larvae*

Paenibacillus larvae possesses several potential virulence factors, like bacteria cell surface-associated proteins, AB toxins, cytolysins, chitinases and serine proteases (Fünfhaus *et al.*, 2009; Djukic *et al.*, 2014). Chaperonins, also known as heat shock proteins have been described to play an important role for pathogenesis of pathogenic bacteria and are highly conserved among bacteria, mammals and plants (Kumar *et al.*, 2015). All representatives of the five ERIC-genotypes show sequence identity of a chitin-degrading enzyme (PlCBP49) and two toxins (Plx2 and C3 larvin) (Beims *et al.*, 2020). The AB toxins Plx1 and Plx2 were proven to be important virulence factors of *P. larvae* (Fünfhaus *et al.*, 2013; Ebeling *et al.*, 2017). The gene of Plx1, is predominantly present in ERIC I, III, and IV, whereas parts of Plx2 also exist in ERIC II but they are incomplete (Djukic *et al.*, 2014). Another virulence factor occurring only in strains of ERIC II and ERIC V genotype is the surface layer protein (SplA). The SplA surrounds the bacteria cells, supports cell adhesion to host cells and plays a key role in pathogenesis of ERIC II strains (Fünfhaus & Genersch, 2012; Poppinga *et al.*, 2012; Djukic *et al.*, 2014). The presence of the SplA in ERIC II strains might explain the differences in virulence of ERIC I and II mentioned earlier. The differences in the presence of virulence factors could partially explain the difference in virulence of the ERIC-genotypes but further investigation is needed.

1.3 Diagnostics of foulbrood

A fast and reliable diagnosis of foulbrood is important to prevent disease spread and maintain bee health. Up to now, the field diagnosis of foulbrood outbreaks is based on the detection of the characteristic clinical symptoms upon visual inspection of brood combs. Furthermore, the presence of the causative agent is usually confirmed in the laboratory. Cultivation of the pathogens, microscopy, PCR-based and immunological methods are the main methods used in the laboratory to confirm the presence of the foulbrood causing agents. Cultivation of the bacteria on specific selective agar followed by visual inspection is usually a prior step to further molecular analyses. *Melissococcus plutonius* forms

small, round and white colonies (Figure 5). The *P. larvae* ERIC I strain shows flat and transparent colonies, whereas the ERIC II strain shows round and white colonies (Figure 5).

Figure 5 Foulbrood causing bacteria on culture agar
Bacteria colonies cultivated on specific agar plates. For *M. plutonius* modified basal medium according to Lewkowski and Erler (2018) was used. The *P. larvae* strains were cultivated on Columbia-Agar with 5 % sheep blood (Otto Nordwald GmbH).

Microscopical examination is used for detection of both foulbrood diseases. Although it can be challenging to identify either the typical spores and flagellar bundles of *P. larvae* or the coccoidal chains formed by *M. plutonius* under the light microscope, it is possible with some experience to successfully confirm the presence of the foulbrood causing agents in larval samples. The *P. larvae* spores can be difficult to identify due to morphological similarities to other spores from bacteria of the same genus (Chantawannakul & Dancer, 2001; OIE, 2016). To eliminate uncertainty about the identity of observed spores and bee-associated bacteria, several methods based on molecular and protein biology of the causative agents have been developed. Recently, a multiplex polymerase chain reaction (PCR) was developed for diagnosis of EFB and AFB in one sample (Dainat *et al.*, 2018). The multiplex PCR requires appropriate equipment with three fluorophore channels for probe detection of potential *P. larvae*, *M. plutonius* and honey bee DNA as control. The needed equipment might not be present in all diagnostic labs, which makes a widespread use of the method difficult (Dainat *et al.*, 2018). Matrix-assisted laser desorption/ionization time-of-flight mass spectrometry (MALDI-TOF-MS) is another approach for diagnosis of EFB and AFB. MALDI-TOF-MS is a reliable tool that is relatively cheap when the machine is already available in the laboratory. However, it requires a time-consuming cultivation of the bacteria (Schäfer *et al.*, 2014; Pomastowski *et al.*, 2019).

1.3.1 Diagnostic methods for detection of European foulbrood

Several methods are established to detect the EFB-causing agent. Cultivation of *M. plutonius* on selective media is insensitive, detecting less than 0.2 % of microscopically counted bacteria cells (Djordjevic *et al.*, 1998; Hornitzky & Smith, 1998; Forsgren, 2009). For molecular diagnosis of EFB, several PCR protocols for *M. plutonius* detection have been developed in the past. Conventional, hemi-nested and real-time PCR, detecting either 16S rRNA or sodA gene of *M. plutonius*, are in use for EFB-

diagnosis (Djordjevic *et al.*, 1998; Govan *et al.*, 1998; Roetschi *et al.*, 2008; Budge *et al.*, 2010; Forsgren *et al.*, 2013). *M. plutonius* DNA can be extracted from different samples, like adult bees, larvae/pupae, honey and hive debris (McKee *et al.*, 2003; Forsgren *et al.*, 2013; Biova *et al.*, 2021). Furthermore, two molecular based methods that can be evaluated visually were established for EFB-diagnosis. A loop-mediated isothermal amplification (LAMP) method using DNA intercalating dyes after successful amplification of the molecular marker and a nanodiagnostic method that is using gold nanoparticles for direct detection of unamplified *M. plutonius* DNA have been developed (Nguyen *et al.*, 2012; Saleh *et al.*, 2012). The distinction between typical and atypical *M. plutonius* strains can be performed using duplex PCR (Arai *et al.*, 2013). Additionally, immunological diagnostic methods based on antibodies were established for EFB-diagnosis. The use of antibodies in an amperometric immunosensor based on a sandwich assay was developed for detection of *M. plutonius* on a gold surface (Mikušová *et al.*, 2019). Furthermore, two Enzyme-linked immunoassays (ELISA) and an upconversion-linked immunoassay (ULISA) using polyclonal antibodies (pAbs) from rabbits and chicken have been set up (Pinnock & Featherstone, 1984; Mohan Rao *et al.*, 2011; Poláchová *et al.*, 2019). For field use, a lateral flow device (LFD) using one specific monoclonal antibody (mAb) against *M. plutonius* is accessible, but it is not licensed for the diagnostic use in Germany (Tomkies *et al.*, 2009).

1.3.2 Diagnostic methods for detection of American foulbrood

For the detection of AFB, similar methods as mentioned for EFB have been established and will be described in the following part. The cultivation of *P. larvae* on selective media is more reliable and causes less bacteria losses compared to *M. plutonius* cultivation. For AFB diagnosis, several PCRs have been established including conventional, quantitative and nested approaches (de Graaf *et al.*, 2006; Rossi *et al.*, 2018). Usually, the targets of PCR are the 16S rRNA gene of *P. larvae*. Aside PCR other molecular methods such as SDS-PAGE of whole cell proteins of *P. larvae* and gas chromatography of methylated fatty acids lead to successful *P. larvae* identification (Hornitzky & Djordjevic, 1992; Drobníková *et al.*, 1994). Several immunological diagnostic methods are available for AFB detection. The utility of immunological diagnostic tests is depending on the specificity of the antibodies used for the assay. Historical approaches are an immunodiffusion test and an immunofluorescence assay, where pAbs are used for detection (Otte, 1973; Peng & Peng, 1979; de Graaf *et al.*, 2006). Furthermore, one ELISA using a mAb and one ULISA using pAb for AFB diagnosis have been developed (Olsen *et al.*, 1990; Pastucha *et al.*, 2021). Similar to EFB, there is a LFD test kit for AFB detection available (Vita, Hants, UK), but there is no information about the used antibodies and their antigens. It has been reported that the AFB-LFD might not detect *P. larvae* belonging to the ERIC II genotype (Saville, 2011;

Fünfhaus *et al.*, 2018b). In conclusion, it can be noted that so far there is no reliable tool for diagnosis of AFB in the field available.

The difference in virulence of the ERIC-genotypes on colony level can make the diagnosis of ERIC I more difficult than ERIC II because symptoms of ERIC I infected larvae usually occur later than in ERIC II infected larvae. Furthermore, the distinction of the two main ERIC-genotypes can be helpful to understand disease spread between colonies and apiaries. Therefore, the demand for diagnostic distinction between the two main ERIC-genotypes of *P. larvae* increased in the laboratories. So far, ERIC-genotyping using rep-PCR, a multiplex PCR targeting plx1 in ERIC I strains and MALDI-TOF are used for detection of the different ERIC-genotypes. All methods are time consuming due to prior cultivation steps and require certain equipment and expertise for analysis (Genersch *et al.*, 2006; Schäfer *et al.*, 2014; Beims *et al.*, 2020).

1.4 Antibodies in diagnostics

Antibodies are also known as immunoglobulins (Ig). Depending on their own amino acid sequence, antibodies bind to specific sequences of other proteins. These proteins to which the antibodies bind are called antigens Antibodies can occur as monomers, heterodimers and pentamers that are composed of a basic structure of four polypeptide chains. The peptide chains consist of two identical heavy (H) chains (50-60 kDa) and two light (L) chains (23 kDa). The different polypeptide chains are linked by interchain disulphide bridges (Nezlin, 1998). Five different Ig classes are known in rodents (IgA, IgD, IgE, IgG IgM), which differ in primary structure, carbohydrate content, and antigenic properties of their heavy chains. Additionally, Igs can be further sub-classified by determination of the light chain type (kappa light chain or lambda light chain). The kappa light chain is more common. The Ig classes IgD and IgE are relatively rare in serum. The IgA is mainly involved in mucosal immunity (Nezlin, 1998). The IgM molecules are appearing during early phases of immune response. IgM Molecules are larger than the other Ig molecules as they consist of five subunits, each of the five subunits again consists of two heavy and two light chains. Due to their structure, IgM antibodies can bind up to ten antigens (Nezlin, 1998). The region where antibodies bind the antigens is defined as the epitope of the antigen, whereas the binding region of the antibody is defined as paratope (Sela-Culang *et al.*, 2013). The strength of the epitope-paratope binding is called affinity. IgG is the major class of Igs, covering about three quarters of all serum Ig molecules (Nezlin, 1998). After secondary immunization, B lymphocytes secrete predominantly IgG molecules, belonging to four IgG subclasses (IgG_1, IgG_{2a}, IgG_{2b}; IgG_3) that differ in structure of their heavy chains. mAbs are derived from a single B lymphocyte clone, whereas pAbs are secreted by different B lymphocyte lineages within the body

(Nezlin, 1998). The Ig preparations from sera are heterogeneous and are grouped to pAbs. They differ in most of their physical, chemical and immunological properties recognizing several epitopes of an antigen, whereas mAbs bind only one epitope (Nezlin, 1998). This specificity makes it possible to use Igs in diagnostic tools for highly sensitive and specific pathogen detection.

So far, antibodies play no big role in the diagnostic routine of bee diseases. The main diagnostic methods for the detection of bee diseases are PCR for virus and bacteria detection and microscopic examinations to detect endoparasites and bacteria. A few approaches using antibodies were developed for diagnosis of AFB and EFB such as ELISAs, ULISAs and LFDs (Pinnock & Featherstone, 1984; Tomkies *et al.*, 2009; Poláchová *et al.*, 2019; Pastucha *et al.*, 2021). A detailed description of these methods can be found in chapter 1.3. However, the previously developed AFB- and EFB-LFDs are the only tools that are commercially available for the diagnostics. Unfortunately, these tools have no approval for diagnostic use in Germany.

1.4.1 Enzyme-linked Immunosorbent Assays

One method taking advantage of the favourable properties of antibodies for diagnostic purposes are Enzyme-linked Immunosorbent Assays (ELISA). ELISAs are fast tools for direct detection of antigens using specific antibodies. ELISAs can be used for large-scale analysis of various samples with a good sensitivity and easy applicability in the laboratory. The principle of ELISA is to detect the antibody-antigen binding using a colorimetric detection method. The antibody-antigen binding is usually detected using a label or enzyme bound to the antibody (Crowther, 2009). The conjugated enzymes convert an applied chemical compound (substrate) to a coloured product. The reaction can be detected either visually or using a photometer. For confirmation of antigen-antibody binding, different approaches can be used, for example enzyme conjugation, fluorescence or nanoparticle conjugation. Commonly used enzymes in ELISA are horseradish peroxidase (HRP) and alkaline phosphatase (AP). The enzymes react with different substrates. HRP reacts with the substrate 3,3',5,5'-tetramethylbenzidine (TMB), whereas AP reacts with p-nitrophenyl phosphate (PNPP). In this study HRP was used with TMB as substrate. For improvement of the ELISA sensitivity, biotin can be conjugated to the antibody. One end of the biotin molecule is bound to the antibody and the other end binds the streptavidin (SA) molecule. The SA is conjugated with an enzyme, thereby the signal caused by the conversion of the substrate by the enzyme can be increased due to multiplex binding of enzyme to the antibody. There are three main types of ELISA: direct, indirect and sandwich ELISA (Figure 6).

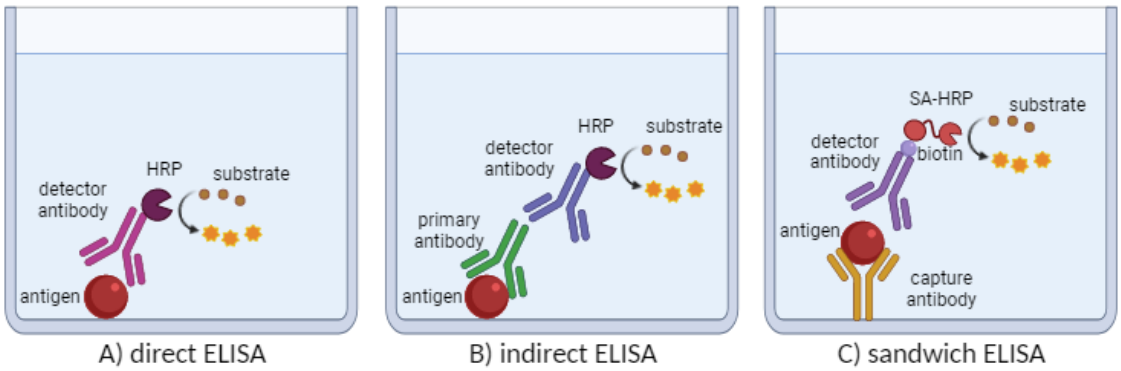

Figure 6 Schematic description of ELISA types using enzymes

Reactions are presented schematically in one well for each type. The direct ELISA (A) is performed with one directly conjugated antibody that detects the immobilized antigen on the plate. The conjugated enzyme (e.g. HRP) reacts with a substrate (e.g. TMB) and leads to colour development that can be detected visually or using a photometer. In the indirect ELISA (B) antigens are also immobilized on the plate surface and primary antibodies bind the antigen. Primary antibodies are then detected by a species-specific enzyme-conjugated secondary antibody. The enzyme (e.g. HRP) reacts with substrate (e.g. TMB) that leads to colour development and can be detected visually or using a photometer. In the sandwich ELISA (C) so called capture antibodies are immobilized on the plate surface. The bacteria samples are applied and the capture antibody binds the specific antigens. The biotin-coupled detector antibody binds to the antigen as well and due to non-covalent interaction of biotin and SA-HRP the HRP is bound to the molecule complex. The HRP-enzyme reacts with substrate (TMB) that leads to colour development and can be detected visually or using a photometer. The Figure was created with the use of BioRender.

For direct and indirect ELISAs the antigen of interest is immobilized to the bottom of a 96-well plate. The antigen is detected either directly with an enzyme-conjugated antibody (direct ELISA) or indirectly with an unlabelled primary antibody, that is bound by an enzyme-conjugated secondary antibody (indirect ELISA). The enzyme reacts with the substrate. The measured signal gives information about the general presence of the antigen and with a further analysis it is even possible to get information about the quantity of the antigen. Although, for highly concentrated samples it might be necessary to dilute the sample in order to obtain quantitatively accurate results. For the sandwich ELISA, antibodies (capture antibody) that are binding the target antigen are immobilized onto the plate. The antigen, which has been bound by a capture antibody is bound by a second antibody (detector antibody). The detector antibody can be enzyme-conjugated as described for direct ELISA or it can be detected with a secondary enzyme-conjugated antibody (Crowther, 2009). The capture and detector antibodies used in sandwich ELISA have to bind the same antigen on different binding sites (epitopes) for a successful detection of the antigen. At least one of the two antibodies has to be antigen-specific to avoid false positive signals.

In general, ELISAs are easy applicable tools for high through put diagnostics with a high specificity, sensitivity and the possibility of a quantitative analysis of the pathogen of interest (Sakamoto *et al.*, 2018). Furthermore, the assay is relatively cheap when the suitable antibodies have already been produced. Nonetheless, ELISAs can only be applied in the laboratory. Furthermore, they require labour intensive washing steps and also the processing of duplicates or even triplicates is necessary to achieve

a sufficiently high accuracy. The reliability of ELISAs strongly depends on the characteristics and stability of the specific antibodies (Sakamoto *et al.*, 2018).

1.4.2 Lateral Flow Devices

The principle of sandwich ELISA is also used for LFDs that are fast tests for the direct use in the field. For the development of an LFD, two antibodies binding the antigen of interest are necessary. The immunoassay takes place on a nitrocellulose stripe where one antibody is adsorbed in one line to the nitrocellulose, forming the so called test line (Figure 7) (Lee *et al.*, 2013). The second antibody is conjugated with a reporter entity, usually gold nanoparticles. The sample material is mixed with the buffer. By then applying this solution to the nitrocellulose stripe, the conjugated antibodies are desorbed by the sample buffer and bind the sample of interest. The antigen-antibody complex flows along the nitrocellulose until the antigen is bound by the immobilized antibodies. The accumulation of particle-conjugated antibodies leads to colour development and can be visually detected as a coloured line. Usually, there is an additional control line located upstream of the test line. The Control line consists of immobilized antibodies, that are binding the gold-labelled antibodies. The gold-labelled antibodies accumulate and can be visually detected at the control line as well. The binding of gold-labelled antibodies by the antibodies immobilized at the control line verifies the successful mobilization of the gold-labelled antibodies and is an important indicator for the successful assay, preventing falsely interpreting a malfunctioning test as a negative result (Lee *et al.*, 2013).

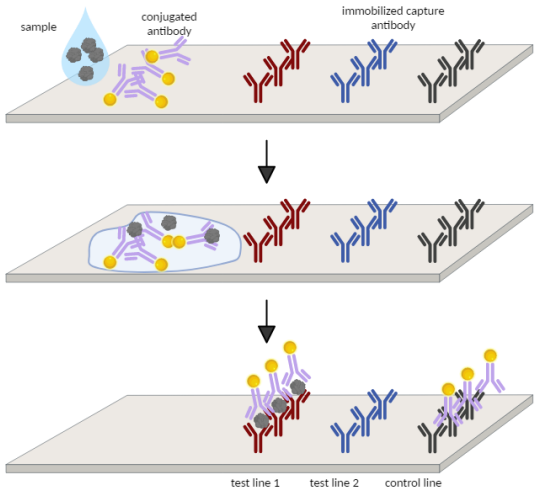

Figure 7 Principle of lateral flow device
Different steps during LFD application are shown schematically. The first part shows the sample application and the general construction of an LFD. The capture antibodies are immobilized on a nitrocellulose membrane and detector antibodies are conjugated with nanoparticles (in this study with silver-nanoparticles). The figure was created with the use of BioRender.

Testing in the field with LFDs has become a popular way of diagnosis in clinical analysis, food safety monitoring and environmental monitoring (Ngom *et al.*, 2010). LFDs can be constructed to detect different target molecules. For detection of disease and food contamination, LFDs target molecules of bacteria, related toxins or viruses (Ngom *et al.*, 2010). Currently, a LFD against certain honey bee viruses is in development in a new research project (BLE, 2021). Furthermore, the number of applications for the detection of chemical contaminants using LFD rises. For example, the B-good project is involved in the development of LFDs that detect residues of pesticides in honey and other hive products (Xu *et al.*, 2019). Beyond the application in bee research LFDs are for example used in human diagnosis of COVID-19 or as pregnancy tests (Kasetsirikul *et al.*, 2020; Matsuda *et al.*, 2021).

LFDs are portable and fast diagnostic tools based on a one-step assay without tedious sample pre-treatment. LFDs are fast and reliable tools for diagnosis in the field that require little to no experience in order to conduct fast and reliable diagnosis. The devices are inexpensive and have a relative long shelf life (several months to years) (Bahadır & Sezgintürk, 2016). Thanks to relatively new technical developments, multiplex testing of different target molecules in one device is possible (Sajid *et al.*, 2015). Nonetheless, LFDs struggle with low signal intensity and a poor quantitative discrimination, mainly giving qualitative information (Bahadır & Sezgintürk, 2016). In contrast to ELISA, the desired application of LFDs in the field necessitate special requirements of reagents used for the assay. For example, the used reagents should not be toxic to the applicant and to the environment. Furthermore, the sample buffer should not denature proteins to maintain antibody-antigen binding in the sample buffer.

Similar to ELISA, the functionality of LFDs strongly depends on the characteristics of the antibodies used in the assays. The sensitivity and the specificity are measures of the quality of a diagnostic test. The sensitivity describes the ratio of correctly diagnosed positive samples to the overall number of positive samples. The specificity describes the ratio of correctly diagnosed negative samples to the overall number of negative samples. Sensitivity and specificity are linked to each other and the assays have to be adapted to achieve the optimal sensitivity and specificity. The sensitivity of the described assays depends on the ability of the antibody to bind the antigen. Usually, highly specific antibodies show a lower sensitivity due to their distinct epitope recognition. Furthermore, stability and antigen-specificity are important in order to develop a highly sensitive and specific assay for reliable diagnosis. In order to thoroughly evaluate the specificity and the sensitivity of a given diagnostic tool, it has to be tested with a series of different bacteria strains that are not the target pathogen and with a series of different field strains of the actual target pathogen. The sensitivity and specificity of the assays are not only depending on the suitability of the antibody but also on the characteristics of the target antigen. The target antigen has to be specific for the disease, which should be detected. In general, the more

of the antigen is present in the sample and the easier the antigen is accessible for the antibody, the higher is the sensitivity of the diagnostic tool. In order to reliably diagnose a certain pathogen in all stages of the disease, the target antigen has to be present in all of these stages. Furthermore, the general accessibility and stability of the antigen after cell lysis also plays a crucial role for the sensitivity of a diagnostic assay. Moreover, the presence of the antigen in different bacteria strains of the same pathogen species/genotype is another factor influencing the reliability of the diagnostic tool. Therefore, the characterization of target antigen is of great value for the appraisal of antibody suitability for disease diagnosis.

1.5 Study objective

So far, diagnosis of EFB and AFB, including the ERIC-genotyping takes several days in the laboratory and it is cost intensive. After a suspected foulbrood outbreak, it is important to quickly take appropriate action to prevent further disease spread. Therefore, a fast, reliable and inexpensive tool for diagnosis of EFB and AFB including ERIC-genotyping is needed. One very promising type of tools for such applications are LFDs.

The development of an immunological diagnostic method requires antibodies that fulfil certain requirements such as specificity, high reactivity (sensitivity), stability and reproducibility. Therefore, highly specific and sensitive mAbs are necessary to minimize false positive or false negative results. Previous studies showed that specific mAb generation against the causative agents of EFB and AFB is possible (Olsen *et al.*, 1990; Tomkies *et al.*, 2009). So far, none of the previously established ELISAs is commercially available for diagnostic purposes. The production of an ERIC-genotype specific antibody was not tried so far. The high similarity of the *P. larvae* ERIC-genotypes on protein level lowers the number of possible ERIC-genotype specific antigens as well as the number of specific antibody candidates.

The aim of the study was to generate specific antibodies for the development of an all-in-one diagnostic approach to detect and differentiate between the foulbrood diseases and the two main ERIC-genotypes. Ideally, such a tool makes the diagnosis and ERIC-genotyping easier, faster and cheaper than the use of the so far available approaches.

2. Materials

2.1 Chemicals

A table with a detailed list of the used chemicals can be found in the appendix (Table S 1).

Table 1 Kits

Kit name	Supplier
BigDye Terminator v1.1 Cycle Seq. Kit	ThermoFisher Scientific, Lithuania
Dynabeads™ Co-Immunoprecipitation Kit; 14321D	ThermoFisher Scientific, Lithuania
EZ-Link Sulfo-NHS-LC-Biotin, No-Weigh Format	ThermoFisher Scientific, USA
HotStarTaq Plus DNA Polymerase Kit	Qiagen, Hilden
InstaGene™ Matrix (DNA extraction)	Bio-rad, UK
NucleoSEQ™ Kit	Macherey-Nagel
Phusion High-Fidelity DNA Polymerase Kit	Thermo Scientific, Lithuania
Pierce Rapid ELISA Mouse mAb Isotyping Kit	ThermoFisher Scientific, USA
QIAprep Spin Miniprep Kit	Qiagen, Hilden
QIAquick Gel Extraction Kit	Qiagen, Hilden
QIAquick PCR Purification Kit	Qiagen, Hilden
QuantiTect Multiplex PCR NoROX Kit	Qiagen, Hilden
Rat Monoclonal Antibody Isotyping Test Kit RMT1	Bio-rad, UK

The primers mentioned in Table 2 were ordered from the metabion international AG (Planegg, Germany).

Table 2 Primer

Name	Sequence 5'-3'	Modification	Reference
Slp773_NcoI-for	aatcaCCATGGCGAGGAATATGGGCTCCGCTATTTCC		
Slp773_XhoI-re	aatcaCTCGAGTTAAAGGTTTTTAACAAGATTACCAG		Poppinga et al, 2012
Slp773_NdeI-for	aatcaCATATGGCGAGGAATATGGGCTCCGCTATTTCC		Poppinga et al, 2012; modified
plx1-NcoI for	actgacCCATGGCACTGCAAAAAATGAATATCATGGTAAAAAAAACG		
plx1-XhoI rev	actgacCTCGAGTTACTTTGTGTCCGTAAATTTTTTAAATTGTTCTAGC		
MP-groEL-NcoI for	actgacCCATGGCAAAAGAAATCAAATTTGCAGAAGATGC		
MP-groEL-XhoI rev	actgacCTCGAGTTACATCATACCGCCCATCATTGATGG		
PL-groEL-NcoI for	actgacCCATGGCAAAAGATATTAAGTTCAGTGAAGACG		
PL-groEL-XhoI rev	actgacCTCGAGTTACATCATGCCGCCCATTCCACCCATGC		
SplA-F1	ATGAGGAATATGGGCTCCG		
SplA-R1	CTGTTTTTTCGTTAAGCATGGTT		
SplA-F2	ACTATCAGCAAATCGTTATTGAAGG		
SplA-R2	TCAACTGTTGTTGCACCGG		this work

SplA-F3	TATTAAACCTGGAAAAGTAGATGTCC		
SplA-R3	TTAAAGGTTTTTAACAAGATTACCAGC		
SplA-F4	GGTTAGCCAATATTGAAGCTCTG		
SplA-R4	AATCCGCAGAACCTTTAGCA		
SplA-F5	AAGATTTAATTGAAACTCTTAATGCAG		
SplA-R5	TCGGTACTGCAGAAAACTTTG		
MP-groEL-F1	CAAAAGAAATCAAATTTGCAGAAGATG		
MP-groEL-F2	GCAATTGTTCGTGAAGGCCT		
MP-groEL-F3	GCTGATGATGTAGATGGTGAAGC		
MP-groEL-F4	CGCTGTTGAAGAAGGCATGG		
MP-groEL-R1	ACCAGATGAAACAGCAGCGA		
PL-groEL-F1	AGTTCAGTGAAGACGCTCGC		
PL-groEL-F2	CTGAAAAACGTGACTGCCGG		
PL-groEL-F3	AGCTCTGCTGATCATTGCTGA		
PL-groEL-F4	TACTCGTGCAGCTGTGGAAG		
PL-groEL-R1	TCGCCTACTTCGTCATCTGC		
T7-for	TAATACGACTCACTATAGG		pET28a vector map, Novagen
16S-V1-V3 F	GAGTTTGATCNTGGCTCAG		
16S-V1-V3 R	GTNTTACNGCGGCKGCTG		
16S-V6-V8 F	AAACTYAAAKGAATTGACGG		Engel et al, 2013
16S-V6-V8 R	ACGGGCGGTGTGTRC		
ERIC1R	ATGTAAGCTCCTGGGGATTCAC		Versalovic et al, 1994
ERIC2	AAGTAAGTGACTGGGGTGAGCG		
VNTR A-For	GAGGGATATACCCCACCTCTTT	6-Fam	
VNTR A-Rev	GGGGAAGTATGATCCCGAAG		
VNTR B-For	CCGGAATAATCCGCTTATGA	Atto550	
VNTR B-Rev	ATCACCAGAGTTGGCGATTC		
VNTR C-For	TGGTTTAGGAACCGGTGTTG	Atto 565	
VNTR C-Rev	CACATTAAAGCCTGTGCAGGTA		
VNTR D-For	ATCATGGCGGTTGGGATG	Yakima YellowTM	
VNTR D-Rev	CACAGGCTCGACAACCACTA		
VNTR E-For	TGTTCAATTTTGATTGTTTTGTTCA	6-Fam	
VNTR E-Rev	TATATGGCGGTCGGCTTAAT		
VNTR F-For	TACCCCAATCTGCCTTGTTG	Atto550	
VNTR F-Rev	CATGCTCCTGCGTGGTATAA		
VNTR G-For	GTCATTACGGCCCAGGTG	Atto 565	Descamps et al, 2016
VNTR G-Rev	TGAGGCTGCAAAGACAGATG		

The commercially available antibodies listed in Table 3 were used for characterization of the generated mAbs in this study.

Table 3 Commercially available antibodies

Antibody	Company	Antigen	Conjugate	Added chemicals
AffiniPure Goat anti-rat IgG	ImmunoJackson, West Grove	rat IgG (H+L)	peroxidase	glycerol
AffiniPure Goat anti-mouse IgG	ImmunoJackson, West Grove	mouse IgG (H+L)	peroxidase	glycerol
AffiniPure Goat anti-rabbit IgG	ImmunoJackson, West Grove	rabbit IgG (H+L)	peroxidase	glycerol
AffiniPure Goat anti-mouse IgG	ImmunoJackson, West Grove	mouse IgG (subclass 1+2a+2b+3)	peroxidase	glycerol
Mouse Anti-poly-Histidine	Merck, Darmstadt	poly-Histidine	none	none

For recombinant protein expression, target genes were cloned into a vector using the reagents listed in Table 4.

Table 4 Reagents for cloning

Reagent	Supplier	Application
10X FastDigest buffer	ThermoFisher Scientific	restriction enzyme digestion
FastDigest NdeI	ThermoFisher Scientific	
FastDigest XhoI	ThermoFisher Scientific	
FastDigest NcoI	ThermoFisher Scientific	
fastAP	ThermoFisher Scientific	dephosphorylation of DNA
T4 ligase	ThermoFisher Scientific	ligation of DNA
10X T4 DNA Ligase Buffer	ThermoFisher Scientific	
T4 DNA Ligase	ThermoFisher Scientific	

2.2 Devices

The electronic equipment and lab devices used within this study are listed in the appendix (Table S 2 and Table S 3).

2.3 Scientific software

The scientific software used for this study is listed in Table 5.

Table 5 Scientific software

Name	Company	Application
BioRender	BioRender, Canada	visualization
BLAST	National Center for Biotechnology Information, USA	sequence analysis
Chromas 2.6.6	Technelysium Pty Ltd.	sequence analysis
Geneious Prime® 2021.0.1	Biomatters Ltd.	primer design, cloning
Image Lab 6.1	Bio-Rad Laboratories, Inc.	WB and agarose gel analysis
Microsoft Office	Microsoft, Redmond, USA	Data analysis

3. Methods

3.1 Animals, bacteria strains and cells

Animal experiments were approved by the supervisory authority (LALLF, 7221.3-2-042/17) and conducted in compliance with the German animal welfare law, the German guidelines for animal welfare and the EU Directive 2010/63/EU. All experiments were performed in accordance with relevant guidelines and regulations.

Rabbits, mice and rats were used for antibody generation against the causative agents of AFB and EFB (Table 6).

Table 6 Immunized animals

Species	Animal ID	Antigen for immunization
rabbit (cross breed: New Zealand White X Chinchilla Bastard)	5534	ERIC I (DSM 25719)
	8414	ERIC II (DSM 25430)
	6754	*M. plutonius* (mixture: CH 40.2; CH 49.3; CH 54.1; LMG 20360)
	7499	ERIC II (DSM 25430)
mouse BALB/c	288	ERIC I (203-13)
	289	ERIC II (198-13)
	678	ERIC I (DSM 25719)
	679	ERIC I (DSM 25719)
	680	ERIC II (DSM 25430)
	681	ERIC II (DSM 25430)
	682	*M. plutonius* (mixture: CH 40.2; CH 49.3; CH 54.1; LMG 20360)
	683	*M. plutonius* (mixture: CH 40.2; CH 49.3; CH 54.1; LMG 20360)
rat (Sprague Dawley)	0034	ERIC I (DSM 25719)
	035	ERIC I (DSM 25719)
	0036	ERIC II (DSM 25430)
	037	ERIC II (DSM 25430)
	0038	*M. plutonius* (mixture: CH 40.2; CH 49.3; CH 54.1; LMG 20360)
	039	*M. plutonius* (mixture: CH 40.2; CH 49.3; CH 54.1; LMG 20360)

For hybridoma production the myeloma cell line Sp2/0 from the American Type Culture Collection (ATCC: CRL-2016) was used and cultivated in RPMI medium (ThermoFisher Scientific, Germany; Table 7). The origin of the bacteria reference strains is the German Collection of Microorganisms and Cell Cultures (DSMZ) for *P. larvae* strains and the Belgian Coordinated Collections of Microorganisms (BCCM) for the *M. plutonius* reference strain. The bacteria described below were cultivated in different media (Table 7) at 37 °C with addition of 5 % CO_2.

Table 7 Cultivation media for cell culture and bacteria

Medium	Ingredients	pH	Cultivation of	Supplier/ Reference
Columbia-Agar with 5 % sheep blood	see supplier information		*P. larvae, E. faecalis, B. pumilus, B. laterosporus*	Otto Nordwald GmbH
MYPGP	1 % Mueller-Hinton broth 1.5 % yeast extract 0.3 % K2HPO4 0.1 % sodium pyruvate 2 % agar 0.2 % glucose after autoclaving	7.2-7.6	*P. larvae*	de Graaf et al, 2015
modified basal medium	0.5 % yeast extract 1 % glucose 0.2 % saccharose 0.1 % L-cysteine 0.675 % KH2PO4 0.675 % K2HPO4	6.60	*M. plutonius*	Lewkowski & Erler, 2018
Sabouraud-dextrose broth	0.5 % peptone from meat 0.5 % peptone from casein 2 % D (+) glucose 1.5 % agar	5.60	*P apium*	DSMZ
Man, Rogosa and Sharpe (MRS) agar	5.1 % MRS broth (Sigma) 1 mL Tween-80 15 % agar		*L. kunkeei*	DSMZ
Luria-Bertani (LB) agar	0.5 % yeast extract 1 % tryptone 0.5 % NaCl 1.5 % agar	7.00	*E. coli, E. faecalis, B. pumilus, B. laterosporus*	DSMZ modified
Medium for P. alvei	0.5 % Peptone 0.3 % Meat extract 0.05 % fructose 0.05 % D (+) glucose 1.5 % agar	7.00	*P. alvei*	DSMZ
Medium for P. dendritiformis	0.5 % Peptone 1.5 % pancreatic digest from casein 0.5 % NaCl 1.5 % agar	7.30	*P. dendritiformis*	DSMZ
RPMI 1640 Medium	RPMI 1640 10 % foetal calf serum (FCS) 1x HAT Media Supplement		Sp2/0, hybridoma cells addition for complete RPMI medium Selection of hybridoma	ThermoFisher Scientific, Germany Merck, Darmstadt

1x BM Condimed H1	hybridoma growth stimulation	Merck, Darmstadt

3.1.1 *Melissococcus plutonius*

The used *M. plutonius* strains (Table 8) were cultivated on modified basal agar (Forsgren *et al.*, 2013) or basal medium with addition of larvae homogenate (Lewkowski & Erler, 2018) under micro aerobic conditions using an atmosphere generation system (Oxoid AnaeroJar, Thermo Scientific). The bacteria were incubated at 37 °C for 4-10 days until growth was observed. Benjamin Dainat from the Swiss Bee Research Centre, Agroscope, Liebefeld-Bern in Switzerland provided the *M. plutonius* field strains.

Table 8 M. plutonius strains

Reference number	Species	Virulence	Origin	Reference
2013_02	*M. plutonius*		Switzerland	
2013_27	*M. plutonius*		Switzerland	
2013_30	*M. plutonius*		Switzerland	
2013_35	*M. plutonius*		Switzerland	
2013_51	*M. plutonius*		Switzerland	
CH 21.1	*M. plutonius*	high	Switzerland	Grossar et al., 2020
CH 40.2	*M. plutonius*	low- intermediate	Switzerland	Grossar et al., 2020
CH 41.4	*M. plutonius*		Switzerland	
CH 46.1	*M. plutonius*	low- intermediate	Switzerland	Grossar et al., 2020
CH 48.1	*M. plutonius*		Switzerland	
CH 49.3	*M. plutonius*	high	Switzerland	Grossar et al., 2020
CH 54.1	*M. plutonius*	low- intermediate	Switzerland	Grossar et al., 2020
CH 60	*M. plutonius*	high	Switzerland	Grossar et al., 2020
CH 90	*M. plutonius*		Switzerland	
CH 119	*M. plutonius*	low- intermediate	Switzerland	Grossar et al., 2020
LMG 20360	*M. plutonius*		United Kingdom	

3.1.2 *Paenibacillus larvae*

In this study, the reference strains obtained from DSMZ and the different field isolates (Table 9) of *P. larvae* were cultivated either on Columbia sheep blood agar or in MYGP-medium for 2-3 days. All used strains were genotyped using repetitive element PCR (rep-PCR) for ERIC-fingerprinting (Genersch & Otten, 2003) and MLVA PCR followed by gel electrophoresis (Descamps *et al.*, 2016).

Table 9 P. larvae strains

Reference number	Species	Genotype
DSM 7030	*P. larvae*	ERIC I
DSM 25719	*P. larvae*	ERIC I

DSM 25430	*P. larvae*	ERIC II
DSM 8443	*P. larvae*	ERIC III
DSM 3615	*P. larvae*	ERIC IV
DSM 106052	*P. larvae*	ERIC V
122-13	*P. larvae*	ERIC I
131-13	*P. larvae*	ERIC I
135-13	*P. larvae*	ERIC I
151-13	*P. larvae*	ERIC I
204-13	*P. larvae*	ERIC I
222-13	*P. larvae*	ERIC I
255-13	*P. larvae*	ERIC I
277-13	*P. larvae*	ERIC I
329-13	*P. larvae*	ERIC I
489-13	*P. larvae*	ERIC I
35-14	*P. larvae*	ERIC I
66-14	*P. larvae*	ERIC I
92-14	*P. larvae*	ERIC I
99-14	*P. larvae*	ERIC I
190-14	*P. larvae*	ERIC I
208-14	*P. larvae*	ERIC I
235-14	*P. larvae*	ERIC I
299-14	*P. larvae*	ERIC I
412-14	*P. larvae*	ERIC I
528-14	*P. larvae*	ERIC I
46-15	*P. larvae*	ERIC I
56-15	*P. larvae*	ERIC I
183-15	*P. larvae*	ERIC I
223-15	*P. larvae*	ERIC I
250-15	*P. larvae*	ERIC I
278-15	*P. larvae*	ERIC I
365-15	*P. larvae*	ERIC I
442-15	*P. larvae*	ERIC I
500-15	*P. larvae*	ERIC I
542-15	*P. larvae*	ERIC I
129-13	*P. larvae*	ERIC II
172-13	*P. larvae*	ERIC II
182-13	*P. larvae*	ERIC II
262-13	*P. larvae*	ERIC II
274-13	*P. larvae*	ERIC II
292-13	*P. larvae*	ERIC II
324-13	*P. larvae*	ERIC II
353-13	*P. larvae*	ERIC II
443-13	*P. larvae*	ERIC II
487-13	*P. larvae*	ERIC II
01-14	*P. larvae*	ERIC II
05-14	*P. larvae*	ERIC II

40-14	*P. larvae*	ERIC II
64-14	*P. larvae*	ERIC II
145-14	*P. larvae*	ERIC II
204-14	*P. larvae*	ERIC II
240-14	*P. larvae*	ERIC II
253-14	*P. larvae*	ERIC II
307-14	*P. larvae*	ERIC II
431-14	*P. larvae*	ERIC II
41-15	*P. larvae*	ERIC II
76-15	*P. larvae*	ERIC II
172-15	*P. larvae*	ERIC II
197-15	*P. larvae*	ERIC II
236-15	*P. larvae*	ERIC II
291-15	*P. larvae*	ERIC II
301-15	*P. larvae*	ERIC II
400-15	*P. larvae*	ERIC II
427-15	*P. larvae*	ERIC II
510-15	*P. larvae*	ERIC II
341-13	*P. larvae*	ERIC *
493-13	*P. larvae*	ERIC *
456-13	*P. larvae*	ERIC **
1201-14	*P. larvae*	ERIC **
252-18	*P. larvae*	atypical
282-18	*P. larvae*	atypical
100-19	*P. larvae*	atypical

3.1.3 Bee-associated bacteria

The honey bee-associated bacteria (Table 10) were selected according to association with honey bee larvae and European foulbrood disease (Forsgren, 2010; Corby-Harris *et al.*, 2014). The bacteria were cultivated on different media (Table 7).

Table 10 Bee-associated bacteria

Reference number	**Species**
DSM 101882	*Parasaccharibacter apium*
DSM 12361	*Lactobacillus kunkeei*
DSM 18844	*Paenibacillus dendritiformis*
DSM 20478	*Enterococcus faecalis*
DSM 25	*Brevibacillus laterosporus*
DSM 27	*Bacillus pumilus*
DSM 29	*Paenibacillus alvei*

3.1.4 Confirmation of bacterial identity and genotype

After cultivation of bacteria on the respective agar plates (Table 7), bacteria were harvested and their DNA was isolated.

3.1.4.1 DNA extraction

Bacteria DNA was extracted using the InstaGene Matrix reagent (Bio-Rad, UK). Bacteria colonies were sampled and solved in 200 µL dH_2O. The solution was centrifuged at 15300 x g for 2 min, the supernatant removed and the resulting pellet was solved in 150 µL of InstaGene matrix solution. The reaction was incubated at 56 °C for 20 min, mixed and incubated at 99 °C for 8 min. Finally, the bacteria solution was centrifuged at 15300 x g for 3 min. The resulting supernatant contained DNA and was stored at -20 °C until use.

3.1.4.2 16S rDNA sequencing

16S rRNA is currently a target molecule for identification and taxonomic clarification of different bacteria species (Engel *et al.*, 2013). The gene for 16S RNA (16S rDNA) is present in every cell and codes for a highly conserved molecule among different species with highly variable species-specific regions (Arnemann, 2019). The identity of the bee-associated bacteria strains was confirmed using 16S-PCR followed by Sanger sequencing (Engel *et al.*, 2013). The following reagents were mixed per reaction (Table 11).

Table 11 16S rDNA-PCR reagents

PCR reagent	**V in µL**
HotStarTaq Master Mix Kit	12.5
10 µM Primer for (V1-V3 region or V6-V8 region)	0.75
10 µM Primer rev (V1-V3 region or V6-V8 region)	0.75
25 mM $MgCl_2$	3
dH_2O	3
DNA (total ~100 ng)	5
∑	25

Table 12 16S rDNA-PCR temperature profile

	Initial denaturation	**Denaturation**	**Annealing**	**Elongation**	**Final elongation**	**Pause**
temperature	95°C	94 °C	60 °C	72 °C	72 °C	4 °C
time	15 min	30 s	40 s	1 min	10 min	∞
		25 cycles				

The whole PCR reaction (Table 12) was purified using QIAquick PCR purification kit (Qiagen, Hilden) following the instructions of the manufacturer with minor modifications using 1 min centrifugation steps at 17900 x g. First, five volumes of PB buffer were added to one volume PCR reaction and the mixture was applied to the provided QIAquick Spin column. Loaded spin columns were centrifuged and the flow-through was removed. DNA, bound to QIAquick Spin column, was washed with 750 µL of the provided PE buffer (ethanol was added before use) followed by two centrifugation steps to dry the membrane. The column was transferred to the collection tube and 30 µL of the provided EB buffer was applied, incubated for 1 min and centrifuged. The flow-through then contains the purified PCR product. Sequencing of PCR products was performed according to the principle of Sanger (Sanger F, 1977) which is based on fluorescent labelled dideoxynucleotide triphosphates (ddNTPs). Purified 16S-PCR product was prepared for chain-termination PCR using the BigDye™ Terminator Cycle Sequencing Kit (ThermoFisher Scientific, Lithuania). The chemicals and conditions used for the chain-termination reaction are given in Table 13 and Table 14 respectively.

Table 13 Chain-termination PCR reagents

PCR reagent	**V in µL**
Big Dye	2
5x BigDye buffer	1
10 µM Primer (according to gene)	1
H_2O	5
DNA template (up to 150 ng)	1
∑	10

Table 14 Chain-termination PCR temperature profile

	Initial denaturation	**Denaturation**	**Annealing**	**Elongation**	**Pause**
temperature	96°C	96 °C	50 °C	60 °C	4 °C
time	15 min	10 s	40 s	1 min	∞
		25 cycles			

The resulting and purified reaction product was analysed with in house sequencing using AB Hitachi 3500 Genetic Analyzer (Applied Biosystems, Weiterstadt). The sequences were analysed with the programs Chromas 2.6.6 (Technelysium Pty Ltd.; http://technelysium.com.au/wp/chromas/) and Geneious Prime® 2021.0.1 (Biomatters Ltd.; https://www.geneious.com). Sequences were trimmed, meaning that non-valid characters and not clearly determined nucleotides (mainly at the sequence ends) were removed. Bacteria identity was verified using nucleotide Basic Local Alignment Search Tool (nBLAST) (Coordinators, 2018). The BLAST e-value is the number of expected hits of similar quality that could be found just by chance. The alignment length shows how many residues were aligned to a sequence of the database and gives insights into the reliability of the result. The pairwise sequence

identity describes the percentage of pairwise residues that are identical in the alignment. The bacteria identity was considered to have been confirmed, if the top five hits according to pairwise sequence identity were the expected bacteria species and the sequence identity was above 97 % (Johnson *et al.*, 2019).

3.1.4.3 ERIC-genotyping of *P. larvae*

The resulting DNA pattern after rep-PCR and gel electrophoresis can be used to describe the relatedness of bacteria strains and draw conclusions about epidemiological distribution of the pathogen (Olive & Bean, 1999). The rep-PCR reaction and primers in this study were used as described in literature (Genersch & Otten, 2003; De Graaf *et al.*, 2013). The bacteria DNA was extracted as described in 3.1.4. Extracted DNA was used for ERIC-genotyping using rep-PCR reaction (Table 15, Table 16).

Table 15 rep-PCR reagents for ERIC-genotyping

PCR reagent	**V in µL**
HotStarTaq Master Mix Kit	12.5
10 mM Primer for (ERIC1R)	0.75
10 mM Primer rev (ERIC2)	0.75
25 mM $MgCl_2$	3
dH_2O	3
DNA (total ~100 ng)	5
∑	25

Table 16 rep-PCR temperature profile

	Initial denaturation	**Denaturation**	**Annealing**	**Elongation**	**Final elongation**	**Pause**
temperature	95°C	94 °C	53 °C	72 °C	72 °C	4 °C
time	15 min	1 min	1 min	2.5 min	10 min	∞
		35 cycles				

The resulting PCR-products were mixed with loading dye (ThermoFisher Scientific) and applied to a 0.8 % agarose gel (containing 0.5 µg/mL ethidium bromide) in TAE buffer (40 mM Tris, 20 mM glacial acetic acid, 1 mM EDTA). The gel electrophoresis reaction was carried out at 85 V for 70 min and visualized under UV light using the Imaging system ChemiDoc (Bio-Rad Laboratories, Germany). Resulting DNA band patterns were examined visually and classified according to the known ERIC-genotypes (Figure 11, Table 9).

3.1.4.4 Multiple locus variable number of tandem repeats analysis of *P. larvae*

The multiple locus variable number of tandem repeats analysis (MLVA) is another method for DNA-typing of different bacteria strains (Descamps *et al.*, 2016). In this study, MLVA was used to get an impression of the variance in the tested field strains for better assessment of strain detection of the produced mAbs and the developed assays for *P. larvae* detection.

The same *P. larvae* DNA, which was used for rep-PCR, was also used for MLVA-PCR reactions (Table 17, Table 18).

Table 17 MLVA-PCR reagents for genotyping

PCR reagent	**V in µL**
HotStarTaq Plus DNA-Polymerase (5 U/µL)	0.3
10 mM dNTPs	0.5
50 µM VNTR-A for	0.2
50 µM VNTR-A rev	0.2
50 µM VNTR-B for	0.1
50 µM VNTR-B rev	0.1
50 µM VNTR-C for	0.1
50 µM VNTR-C rev	0.1
50 µM VNTR-D for	0.1
50 µM VNTR-D rev	0.1
100 µM VNTR-E for	0.5
100 µM VNTR-E rev	0.5
25 mM $MgCl_2$	1.25
5x Q-Solution	2.5
10x PCR buffer	1.25
dH_2O	2.2
DNA (total ~100 ng)	2.5
∑	12.5

Table 18 MLVA-PCR temperature profile

	Initial denaturation	**Denaturation**	**Annealing**	**Elongation**	**Final elongation**	**Pause**
temperature	95°C	94 °C	52 °C	72 °C	72 °C	4 °C
time	5 min	1 min	1 min	1 min	10 min	∞
		30 cycles				

The resulting PCR-products were mixed with loading dye (ThermoFisher Scientific) and applied to a 3 % agarose gel (containing 0.5 µg/mL ethidium bromide) in TAE buffer (40 mM Tris, 20 mM glacial acetic acid, 1 mM EDTA). The gel electrophoresis reaction was carried out at 85 V for 150 min and visualized under UV light using the Imaging system ChemiDoc (Bio-Rad Laboratories, Germany). Resulting DNA band patterns were examined visually and classified according to MLVA genotypes. Due to the discovery of more than 50 new MLVA types by the laboratory of Bee Diseases of the Friedrich-Loeffler

institute, a new nomenclature for MLVA types was used, which was then compared to the 23 already described MLVA-types (Descamps *et al.*, 2016).

3.2 Antibody production

For production of specific antibodies either one target protein or whole cell lysates of the target pathogen can be used. So far, in existing studies (Fünfhaus *et al.*, 2009) on the topic of ERIC I and ERIC II differentiation, the existence of potential specific antigen candidates was only proven in only a few representative strains of the respective genotypes. Therefore, it is not fully clear whether these antigens are present in all field strains of the respective genotype. Furthermore, some antigens were only proposed based on results from analyses on the genetic level (Fünfhaus *et al.*, 2009), which makes it questionable whether the antigen is actually expressed on protein level in detectable amounts. On the protein level contrary findings have been reported for the potential genotype-specific antigens (Fünfhaus & Genersch, 2012; Erban *et al.*, 2019). These findings make it difficult to choose one potential genotype-specific antigen for mAb production. To avoid these shortcomings of the previous works, whole bacteria cells were used for immunization within this study. With this approach a higher number of mAbs can be produced, detecting different antigens that potentially are expressed in larger amounts in the field strains. This increases the chance to find a mAb against the most frequently occurring antigens in the different strains. Furthermore, the detection of whole bacteria cells is closer to the natural conditions in the field. Therefore, there is a higher probability that the generated mAbs detect antigens that are easily accessible and the mAbs are not disturbed by the presence of other proteins of the bacteria.

3.2.1 Immunization & polyclonal antibody extraction

Cultivated bacteria for immunization were removed from agar plates with 1x Phosphate buffered saline buffer (PBS) buffer under sterile conditions. For this purpose, a sterile spatula was used and plates were washed three times with PBS. After centrifugation, the resulting pellet was solved in PBS and bacteria were counted under the microscope using a Helber Bacteria Counting Chamber (Hawksley, UK). The bacteria solutions were diluted to the designated concentration of $1x10^8$ cells/mL. For calculation of bacteria concentrations, bacteria of 48 little squares of the counting chamber were counted. Each small square has an area of 1/400 mm and a depth of 0.02 mm. For calculation of bacteria concentrations per mL, following equation was applied:

$$c_{bacteria} = \frac{bacteria\ counts}{48 \times \left(\frac{1}{400} \times 0.02\ mm^2\right)} = \frac{bacteria\ counts}{(48 \times 5 \times 10^{-8}) cm^3} \qquad (1)$$

Mice (BALB/c mice), rats (Sprague Dawley) and rabbits (cross breed: New Zealand White x Chinchilla Bastard) were immunized with $1x10^8$ cells/mL bacteria solution in PBS (mouse: 50 µL; rat: 100 µL; rabbit: 500 µL), mixed with equal volume of either GERBU Adjuvant MM™ (GERBU Biotechnik GmbH, Heidelberg) for mice and rats or Freund Adjuvants (FCA+FICA; Sigma-Aldrich, Steinheim) for rabbits. After three antigen boosts, the antibody titre of immunized animals was tested using serum in an indirect ELISA (see 3.3.2) and WB analysis (see 3.4.1). After verification of antibody titres, a final boost was performed three days before the animals were euthanized. Final blood samples were harvested for pAb extraction using S-Monovette tubes (Sarstedt Inc., USA) and the blood samples were centrifuged after clotting for 10 min at 2000 x g. Spleen cell extraction was performed from rats & mice using RPMI 1640 Medium (ThermoFisher Scientific, Germany) (Table 7) without FCS for hybridoma fusion at the day of euthanasia.

3.2.2 Screening for monoclonal antibodies

Hybridoma fusion was performed as previously described in literature (Bussmann *et al.*, 2006). The hybridoma were produced in cooperation with Dr. Sven Reiche (Laboratory for the Generation of Monoclonal Antibodies of the FLI). For hybridoma production, spleen cells were separated using a Corning membrane filter with a diameter of 100 µm (Thermo Fisher Scientific, Germany). The resulting cell suspension was washed twice with 50 mL RPMI medium (centrifuging 10 min for 340 x g) followed by cell pellet suspension in RPMI medium. Meanwhile, SP2/0 myeloma cells were washed in the same way as described for the spleen cells. The myeloma cells were resuspended in RPMI medium without FCS. The prepared and alive cells were diluted, stained using trypan blue staining (Sigma-Aldrich, Steinheim) and counted under the microscope. For cell fusion, $1x\ 10^8$ spleen cells were fused with fourfold of SP2/0 myeloma cells. The cell mixture was centrifuged at 800 x g for 5 min and resuspended in 1 mL PEG 1500 (Sigma-Aldrich, Steinheim) under constant stirring (Köhler & Milstein, 1975). After slow addition of 15 mL RPMI medium, cells were incubated for 30 min at 37 °C with additional 35 mL of complete RPMI containing 10 % FCS. Cells were washed using centrifugation (10 min; 340 x g). The cells were diluted in complete RPMI medium, which was supplemented with BM Condimed H1 (Merck, Darmstadt) for stimulating growth of fused cells. The resulting cell suspension was diluted to different cell concentrations (1 x 96-well plate with 30 000 cells/well; 2 x 96-well plates with 15 000 cells/well; 1 x 96-well plate with 7 500 cells/well). Each well was prepared with 100 µL cell suspension. The cells were cultivated at 37 °C with 8 % CO_2 addition and saturated humidity overnight. On the first and on the sixth day after cell fusion 100 µL of selection medium (complete RPMI, 1x BM Condimed H1, 1x HAT-Media supplement) was added to the growing cells. The remaining cells from the cell fusion were

washed and stored in freeze-medium (complete RPMI medium with 10 % DMSO). Cells were frozen and stored in the vapour phase of liquid nitrogen.

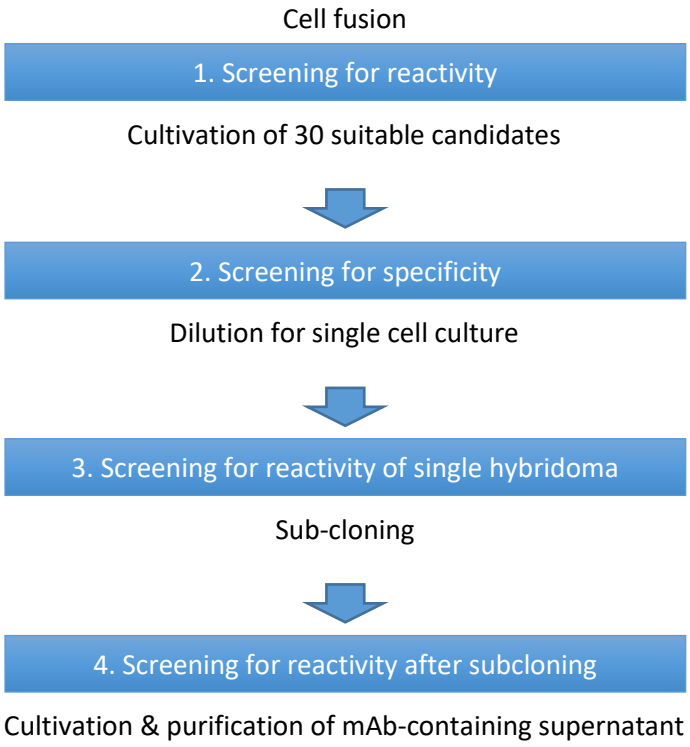

Figure 8 Screening scheme for hybridoma candidates
The workflow of mAb-screening shows the four screening steps for selection of suitable mAb producing hybridoma/well. Furthermore, the major steps for hybridoma separation aiming to produce monoclonal hybridoma cultures for mAb generation are shown.

After 10 days post cell fusion, different hybridoma populations were screened for anti-*M. plutonius,* anti-*P. larvae*, anti-ERIC I and anti-ERIC II specific mAbs using indirect ELISA (see 3.3.1) (Figure 8). Per fusion 30 positive clones were selected, further cultivated and screened for mAb reactivity to the pathogen, which was used for immunization, and screened for cross reactivity with the respective other two bacteria not used for immunization. Non-cross reacting clones were selected and plated with different concentrations (1 x 96-well-plate: 3 cells/well; 1 x 96-well-plate: 1 cell/well; 2 x 96-well-plates: 0.3 cell/well). After 10 days, the third screening was performed. The supernatants of the cell dilutions were tested for positivity against the bacteria species/genotype, which were used for immunization. Three positive wells (preferred wells with low number of cells per well) were selected and one of the these wells was directly cultivated with selection medium, while the others were stored in freeze-medium in the vapour phase of liquid nitrogen. After sub-cloning and final screening, the supernatants were tested for reactivity and all suitable hybridoma were cultivated in large scale resulting in ~ 150 mL of cell supernatant that contained the mAbs of interest.

3.2.3 Monoclonal antibody preparation

3.2.3.1 Monoclonal antibody purification

The mAb containing supernatants were purified using HiTrap Protein G HP 1mL columns (Cytiva, USA) following the manufacturer´s instructions. Supernatant of hybridoma candidates was centrifuged (10000 x g, 4 °C, 15 min), filtered (0.45 µm diameter) and diluted 1:1 with binding buffer (Table 19). Protein G column was activated with ten column volumes of binding buffer prior to sample application (1 mL/min flow rate). After bound mAbs were washed with 20 column volumes of binding buffer, elution buffer (Table 19) was applied to the column and the sample was incubated for 10 min. Elution into tubes with 200 µL of neutralizing buffer (Table 19) was performed with six 1 mL-fractions. Protein content of different fractions was measured using NanoDrop 2000C (Thermo Scientific). Purified mAbs were adjusted to a concentration of 1 mg/mL, aliquoted (100 µL) and stored at -20 °C until mAb characterization (3.3.). Used columns were washed with ten column volumes of binding buffer followed by five column volumes of 20 % ethanol and stored in 20 % ethanol at 4 °C until reuse.

Table 19 Solutions for mAb purification with protein G column

Buffer	Ingredients	pH
binding buffer	20 mM sodium phosphate	7.0
elution buffer	100 mM glycine-HCl	2.7
neutralizing buffer	1 M Tris	9

3.2.3.2 Monoclonal antibody biotinylation

Prior to antibody biotinylation, the storage buffer of purified antibodies (1 M Tris buffer) was exchanged using pierce protein concentrators 30K (Thermo Scientific, USA). For this, 1 mL of mAb in Tris buffer was diluted with 19 mL PBS using the 20 mL vial of protein concentrator and centrifuged at 4000 x g until the desired concentration of mAb was reached in PBS.

For biotinylation of mAbs, the covalent binding between biotin and proteins was used. EZ-Link Sulfo-NHS-LC-Biotin kit (ThermoFisher Scientific, USA) was used to label the mAbs with biotin. NHS-activated biotins react efficiently with primary amino groups (-NH2) of antibodies and stable amide bonds are formed. Biotinylation was performed following the manufacturer's protocol. The provided 1 mg biotin was dissolved in 180 µL water immediately before use to prepare a 10 mM biotin solution. Biotin is added in a 20-fold molar excess to the mAbs. The required mAb and biotin volumes were calculated as described in the manufacturer´s protocol. The equation (2) was used to calculate millimoles of biotin reagent for addition to the biotinylation reaction for a 20-fold molar excess.

$$mmol\ biotin = mL\ mAb \times \frac{mg\ mAb}{mL\ mAb} \times \frac{mmol\ mAb}{mg\ mAb} \times \frac{20\ mmol\ biotin}{mmol\ mAb} \qquad (2)$$

Next step was to calculate the desired volume (µL) of 10 mM biotin reagent solution for addition to the biotinylation reaction (3).

$$\mu L\ biotin = mmol\ biotin \times \frac{1000000\ \mu L}{L} \times \frac{L}{10\ mmol} \quad (3)$$

After addition of calculated biotin, the reaction was incubated at room temperature (RT) for 30 min. The removal of excess unconjugated biotin was performed using pierce protein concentrators as described above. Biotinylated mAbs were used in sandwich ELISA as detector mAbs (3.3.3).

3.3 Monoclonal antibody characterization

3.3.1 Monoclonal antibody isotyping

The isotyping of the mouse mAbs was performed with the Pierce Rapid ELISA Mouse mAb Isotyping Kit (ThermoFisher Scientific, USA) following the manufacturers' protocol. The Kit contains a pre-coated ELISA plate with immobilized antibodies specific for the isotypes. Purified antibodies were diluted in Tris buffered saline (TBS), which was delivered with the Pierce isotyping Kit, to a final concentration of 250 ng/mL (supernatant was diluted 1:50 in TBS). The diluted antibody and the HRP-conjugate anti-mouse antibody delivered with the kit were applied using 50 µL of each reagent to the ELISA plate and mixed using the microplate shaker Wallace 1296-001 (Heidolph, Schwabach). The reaction was incubated for 1 h at RT. The plate was washed three times with 250 µL of the delivered washing buffer. After 75 µL addition of provided TMB and further incubation for 10 min, the reaction was stopped with the same volume of the provided stop solution. The successful reaction for isotype was examined optically to determine the strongest reaction.

For the rat antibody isotyping, the Rat Monoclonal Antibody Isotyping Test Kit RMT1 (Bio-rad, UK) was used. For this, the purified antibody was diluted in PBS containing 1 % BSA to a final concentration of 1 µg/mL. Mixing of 150 µL of the antibody dilution was followed by incubation at RT for 30 s. The test strip was placed in the vial and after 10 min of incubation, the isotype-specific bands occurred and were examined visually.

3.3.2 Indirect ELISA

The indirect ELISA was used for screening of suitable hybridoma and the characterization of the produced mAbs. For indirect ELISA target bacteria and bee-associated bacteria were immobilized on a 96-well plates. The generated mAbs were used as primary antibodies.

The coating solution for indirect ELISA was prepared using different cultivated bacteria belonging to *M. plutonius*, *P. larvae* or bee-associated bacteria (Table 8, Table 9 and Table 10). Bacteria were washed twice with PBS, solved in coating buffer and counted under the microscope to prepare a working solution with a concentration of $1x10^7$ cells/mL. The further steps of the solution preparation were analogous to the steps described for the preparation of bacteria solution used for immunization (3.2.1.). For the indirect ELISA transparent 96-Well plates were used. Well were plated with $5x10^5$ cells/well (Table 20) overnight at 4 °C or for 2 h at RT.

Table 20 Solutions for indirect ELISA

Buffer	Ingredients	pH
coating buffer	100 mM Na_2HPO_4 x $2H_2O$	9
blocking buffer	PBST 1 % BSA	7.0-7.2
dilution buffer	PBST	7.0-7.2
washing buffer	0.05 % BSA PBST	7.0-7.2
substrate	TMB	
stop solution	2M sulfuric acid	

The primary antibodies (serum, hybridoma supernatant or mAb) and the secondary antibodies (HRP-conjugated goat antibodies) were prepared for indirect ELISA according to Table 21. The indirect ELISA was performed as shown in a short protocol (

Table 22).

Table 21 Antibodies and their dilutions used in indirect ELISA

Antibody	Dilution factor
polyclonal rabbit serum rabbit	1 : 16 000
polyclonal mouse serum	1 : 800
polyclonal rat serum	1 : 2 000
hybridoma supernatant	1 : 1
goat anti-rabbit IgG (H+L)	1 : 5 000
goat anti-mouse IgG (H+L)	1 : 1 000
goat anti-rat IgG (H+L)	1 : 5 000
goat anti-mouse IgG (subclass 1+2a+2b+3)	1 : 4 000

Table 22 Short protocol for indirect ELISA

V [µl]	Action	t [min]	Temp [°C]
1 x 50	coating bacteria (1 x 10^7 cells/mL in coating buffer)	O/N	4
1 x 200	washing (PBST)	-	RT
1 x 200	blocking	60	RT
3 x 200	washing (PBST)	-	RT
1 x 50	primary antibody (dilution in 0.5 % BSA in PBST; Table 21)	60	RT
3 x 200	washing (PBST)	-	RT
1 x 50	secondary antibody HRP-conjugated (dilution in 0.5 % BSA in PBST; Table 21)	60	RT
3 x 200	washing (PBST)	-	RT
1 x 50	substrate (TMB) incubation in the dark	25	RT
1 x 50	stopping (2 M H_2SO_4)	-	RT
	read OD450 and OD620		

After stopping the enzymatic reaction and photometric examination, the ELISA results were normalized by subtracting the reference absorbance measured at OD_{650} from values measured at OD_{450}. The limit of detection (LOD_{OD}) was calculated using normalized values from 12 blanks (with dilution buffer (Table 20) instead of primary antibody) according to the equation shown below (Shrivastava & Gupta, 2011) .

$$LOD_{OD} = \bar{x}_{blank} + 3 \times SD_{blank} \qquad (4)$$

The variable $\bar{x}_{blank}$ represents the mean of 12 blank measurements and SD_{blank} stands for the standard deviation of the same 12 blank measurements.

A twofold mAb dilution series (from 1.56 to 100 µg/mL) was performed to find the most suitable working concentration of the generated mAbs aiming for a high sensitivity, specificity and economical mAb consumption. For the anti-*M. plutonius* mAbs one of the four *M. plutonius* strains, which were used for immunization of the mice, was chosen as positive control. The closest phylogenetic relative of the bee-associated bacteria, which is the bacterium *E. faecalis*, was used as negative control. For anti-*P. larvae* mAbs the ERIC I strain was used as positive control and *P. alvei* served as negative control. The anti-ERIC mAbs were tested in the dilution series against ERIC I and ERIC II. The aim was to find the best working concentration of the mAbs for distinction between negative and positive controls. The suitable mAb concentrations were used for testing cross reactivity and specificity of the mAbs against different bee-associated bacteria and several field isolates of the target strains.

3.3.3 Sandwich ELISA

The sandwich ELISA was developed in cooperation with the project partner Senova (Industriestraße 8, 99427 Weimar). Developing a sandwich ELISA is an important step towards the LFD development. The capture antibody adsorbs to the plate, bacteria samples (antigens) were applied and bound by capture antibody, followed by an antigen binding detector antibody that is conjugated with biotinFigure 6. Due to high affinity of biotin and streptavidin, HRP-conjugated streptavidin binds biotin-conjugated antibody and enables enzymatic colour development with TMB as substrate.

For testing the mAb candidates in combination with each other for specific pathogen detection, the sandwich ELISAs were performed testing the detection of field isolates and cross reactivity with bee-associated bacteria. The provided reagents by Senova (Table 23) were applied with the in-house produced mAbs targeting *M. plutonius*, *P. larvae* or ERIC II.

Table 23 Solutions used for sandwich ELISA

Buffer	Ingredients	pH
coating buffer	100 mM CBB supplied by Senova	9.5
sample buffer	supplied by Senova	
washing buffer	PBS 0.1 % BSA 0.05 % Tween-20	7.2-7.5
substrate	sTMB supplied by Senova	
stop solution	1.4 % H_2SO_4	

The sandwich ELISA was processed following the manufacturer's (Senova) protocol (Table 24).

Table 24 Short protocol for sandwich ELISA

V [µl]	Concentration	Action	t [min]	Temp [°C]
1 x 100	2.5 µg/mL	coating *P. larvae:* 3B3; *M. plutonius:* pAb; ERIC II: 5B2 (CBB)	O/N	4
1 x 200		blocking (sample buffer)	30	RT
3 x 200		washing (washing buffer)	-	RT
1 x 100	1x 10^5 cells/mL	bacteria sample (sample buffer)	60	RT
3 x 200		washing (washing buffer)	-	RT
1 x 100	2.5 µg/mL	*P. larvae:* 5B1-biotin; *M. plutonius:* 6F10-biotin; ERIC II: 2D12-biotin (sample buffer)	30	RT
3 x 200		washing (washing buffer)	-	RT
1 x 100	1: 10 000	SA-HRP (sample buffer)	30	RT
3 x 200		washing (washing buffer)	-	RT
1 x 100		substrate (sTMB)	8	RT
1 x 50		stop solution (1,4 % H_2SO_4)	-	RT
		read (OD450 and OD620)		

After stopping the enzymatic reaction and photometric examination, the ELISA results were normalized by subtracting the reference values measured at OD_{620} from values measured at OD_{450}. The limit of detection (LOD_{OD}) was calculated using normalized values from 12 blanks (with sample buffer instead of bacteria) according to the equation shown in 3.3.2 (Shrivastava & Gupta, 2011). For comparison of detection limits, the detectable concentrations of bacteria were calculated ($LOD_{cells/mL}$). Therefore, a linear regression of bacteria dilutions with low bacteria numbers for each mAb combination was performed. The resulting equations were used for $LOD_{cells/mL}$ calculation using the previously determined LOD_{OD}.

The cross reactivity against the bee-associated bacteria and the specificity to field isolates was also tested in the sandwich ELISA using the same bacteria used for indirect ELISA.

3.4 Antigen characterization and identification

The antigen characterization is an important step towards the sandwich approach. For application in sandwich assay, two antibodies that bind the same antigen at different epitopes are required. A first indication that the mAbs possibly bind the same antigen is given when the antibodies detect antigens with the same molecular weight. Therefore, antibodies were tested in the WB. The antigens of the produced mAbs were characterized to gain more information of antigen quantity in the pathogen. WB analysis and mass spectrometry were used for identification of the antigens of interest.

3.4.1 SDS-PAGE & Western Blot

SDS-PAGE followed by WB was performed to test whether the antibodies detect the denatured form of the antigen and to determine the size of the antigen. Buffers for SDS-PAGE and WB were prepared, sterilized and stored at RT. The TBST-milk was prepared immediately before use.

The bacteria for protein extraction were cultivated and harvested as described before (3.1, 3.2). The bacteria pellets were solved in water and an equal volume of 2x extraction buffer (Table 25) was applied to the sample. The sample was mixed and incubated for 15 min at RT. Bacteria cells were disintegrated by repeated sonication (three times for 30 s) using Branson sonifier 450 (G. Heinemann Ultraschall- und Labortechnik, Germany). Bacteria lysates were mixed again and centrifuged for 20 min at 10600 x g at RT. The resulting protein lysates were incubated at 96 °C for 10 min prior to application to SDS-PAGE and 12 µL per sample were applied on the SDS-gel.

Table 25 Solutions for SDS-PAGE & Western Blot

Buffer	Ingredients	pH
2x extraction buffer	8 M urea 20 % (v/v) glycerine 125 mM Tris 4 % (w/v) SDS 0.01 % (w/v) bromophenole blue 7 % β-mercaptoethanol 1x protease inhibitor cocktail	6.8
running gel buffer	1.5 M tris-base	8.8
stacking gel buffer	1 M tris-base	6.8
PAGE-running buffer	25 mM tris-base 250 mM glycine 3.5 mM SDS	
Coomassie staining	50 % (v/v) ethanol 7. 5 % (v/v) acetic acid 0.2 % (w/v) Coomassie	
distaining solution	40 % (v/v) methanol 10 % (v/v) acetic acid	
transfer buffer	25 mM tris-base 150 mM glycine 10 % (v/v) methanol	
TBST buffer	10 mM tris-base 150 mM NaCl 0.05 % Tween-20	8
TBST-milk	TBST 5 % (w/v) milk powder	

The SDS-gels were prepared according to Table 26 with 12.5 % acrylamide.

Table 26 Preparation of acrylamide gels for SDS-PAGE

chemical	running gel (12.5 %)	stacking gel (5 %)
dH2O	1.53 mL	1.41 mL
30 % acrylamide	2.08 mL	0.33 mL
running/stacking gel buffer	1.3 mL	0.25 mL
20 % SDS	25 µL	10 µL
10 % APS	50 µL	20 µL
temed	4 µL	2 µL

The SDS-PAGE was run at 30 mA until the samples reached into the stacking gel using the power supply Power Pac basic (Bio-Rad Laboratories, Germany). When the samples reached the running gel, the current was increased to 40 mA. Gel electrophoresis was performed until the extraction buffer reached the bottom of the gel. For visualization of the proteins, the SDS-gels were stained for 1 h in Coomassie

staining (Table 25) under continuous shaking. gels were distained overnight exchanging distaining solution (Table 25) several times.

For WB analysis, the proteins from the SDS-gels were transferred to a nitrocellulose membrane (0.45 µm) using a semi-dry Blotting system Major Science MP-3AP (biostep GmbH, Jahnsdorf) with 70 mA per gel for 35 min. Further incubation and antibody application per membrane were performed according to Table 27.

Table 27 Short protocol for WB

V [ml]	Action	t [min]
1 x 10	blocking (TBST-milk)	60
3 x 10	washing (TBST)	2
1 x 10	primary antibody (concentration according Table in TBST)	60
3 x 10	washing (TBST)	2
1 x 10	secondary antibody-HRP (concentration according Table in TBST)	60
3 x 10	washing (TBST)	2
1 x 1	ECL Blotting Substrate	-
	detection of chemiluminescence (ChemiDoc)	

After detection of stained proteins using the Imaging system ChemiDoc MP (Bio-Rad Laboratories, Germany), the WB was analysed with Image Lab 6.1 (Bio-Rad Laboratories, Inc.) and Microsoft PowerPoint.

3.4.2 Immunoprecipitation & Mass spectrometry

The immunoprecipitation (IP) was used to purify the antigens of the produced mAbs. This is important in order to identify the detected antigens via mass spectrometry. For IP, Dynabeads™ Co-Immunoprecipitation Kit with M-270 Epoxy magnetic beads (ThermoFisher Scientific, Lithuania) was used. The M-270 Epoxy magnetic beads have a hydrophilic surface, which ensures covalent non-specific binding with primary sulfhydryl groups of the ligand antibody. The antibodies coupled with beads can be used to bind the target antigen and extract the target antigen from the crude protein lysate performing several washing steps. The elution ensures that the antibody-antigen link is unbound and only antigen is eluted in elution solution for further analysis.

Prior to antibody coupling, the buffer of purified antibodies, which are stored in 1 M Tris buffer, was exchanged due to interactions between Tris and the magnetic beads. For buffer exchange, pierce protein concentrators (Thermo Scientific, USA) were used as described before (3.2.3). Centrifugation was performed until desired concentration of mAb was reached. For mAb-magnetic bead coupling,

7 µg mAb/mg beads were used. The coupling procedure was performed according to the manufacturer's protocol using the delivered buffers. Beads for coupling were washed in 1 mL C1 buffer using the DynaMag™-2 Magnet (ThermoFisher Scientific, Norway) for bead accumulation. The mAbs were diluted with C1 buffer, added to washed magnetic beads and mixed gently. For coupling reaction C2 buffer was added. The coupling reaction was performed at RT on a roller overnight. Coupled beads were washed once with HB buffer and once with LB buffer followed by two washes with SB buffer. Antibody-coupled beads were stored with a concentration of 10 mg beads/mL in SB buffer at 4 °C until use.

The pathogenic bacteria of interest (*P. larvae* ERIC I: DSM 25719 & ERIC II: DSM 25430 and *M. plutonius*: BK-350-17) were cultivated on agar plates (3.1.1) and removed with a spatula in 5 mL of sterile water per plate. Bacteria of three agar plates were fused and the bacteria were centrifuged (15 min; 4000 x g). The resulting bacteria pellet was washed twice with 5 mL sterile water and once with 1 mL 20 mM HEPES buffer (pH 7.4). The washed pellet was centrifuged (15 min; 4000 x g) and solved in residual buffer. The solved pellet was immediately frozen with liquid nitrogen and stored at -80 °C until use.

Shortly before IP, the stored pellets were put on ice and 0.5-1 g bacteria cells were solved in 5-10 mL lysis buffer (100 mM NaCl, 1x IP buffer provided with the kit and protease inhibitor cocktail). The cells were disintegrated by repeated sonication (three times for 30 s) using Branson sonifier 450 (G. Heinemann Ultraschall- und Labortechnik, Germany). Bacteria lysate was incubated for 1 h on ice and cell debris was removed via centrifugation (2600 x g, 10 min at 4 °C). For antibody-antigen binding, 1 mL of the resulting bacteria supernatant were mixed with 3 mg of antibody-coupled beads. After Incubation of 1 h at RT on a roller, the bead-antibody-antigen complex was washed several times according to manufacturer's instructions, three times with lysis buffer and once with 0.05 % Tween-LWB buffer incubating 5 min on a roller. Elution was performed in 60 µL EB buffer incubating the reaction for 10 min at RT. During the elution process, the antigen, which is bound by the antibody, is released into the EB buffer but the antibody stays bound to the magnetic beads. Finally, the antigen is separated from the antibody and can be analysed in SDS-PAGE, WB and mass spectrometry. For SDS-PAGE and WB 6 µL of IP-eluate was mixed with equal volume of 2x extraction buffer (Table 25) and incubated at 96 °C for 10 min. The denatured protein was applied to the acrylamide gel. For detailed description of SDS-PAGE and WB see 3.4.1.

After verification of IP success, the samples were identified wire mass spectrometry using MALDI-TOF/TOF (matrix-assisted laser desorption/ionization, time of flight). MALDI is a three-step process. First samples are immobilized on a matrix, then a pulsed laser is used for desorption of molecules and

the molecules are ionized. Samples are accelerated in a mass spectrometer and the time of flight is analysed based on mass-to-charge ratio (Chandrasekhar *et al.*, 2014). Identification of proteins was performed in cooperation with the laboratory for Biochemistry and Proteomics of the FLI (head: Axel Karger). The IP eluates were run on acrylamide gel without prior boiling of the proteins. Protein bands were cut out, digested with trypsin and analysed with MALDI-TOF/TOF mass spectrometry. The fragment spectra were analysed with the help of MASCOT Server and the resulting spectra were compared to a peptide database of species, from which the target proteins/antigens are originated. The database (Swissprot) was searched by using peptide mass fingerprinting (PMF), which allowed to identify the analysed antigens.

3.4.3 Antigen Cloning and recombinant protein expression

Recombinant protein expression was performed to verify the identity of antigens analysed by mass spectrometry and to test different antibodies for recognizing the antigen of interest. Therefore, the gene DNA sequences (Table 28) of the identified antigens from mass spectrometry were extracted from NCBI (https://www.ncbi.nlm.nih.gov/). The sequences were taken from the bacteria strains *M. plutonius* (LMG 20360), *P. larvae* ERIC I (DSM 25719) and ERIC II (DSM 25430).

Table 28 List of genes for recombinant protein expression

Gene	Species	Genotype	Strain ID	Gene ID	size [bp]
groEL	*M. plutonius*	-	LMG 20360	57043026	1635
groEL	*P. larvae*	-	DSM 25719	64217281	1629
S-layer	*P. larvae*	ERIC II	DSM 25430	JQ353714	3024

For cloning the ERIC II specific antigen, the protocol and primers of a published article (Poppinga et al., 2012) were used. The primer for the species-specific antigen amplification were designed using the program Geneious Prime® 2021.0.1 (Biomatters Ltd.; https://www.geneious.com). The primers mentioned in Table 2 were ordered from the metabion international AG (Planegg, Germany). For all conducted protein expression experiments the vector pET28a (Merck, Darmstadt) was used.

3.4.3.1 Amplification of antigen DNA

The primer for gene amplification were designed with restriction sites at 3´-end of the target gene with NcoI sequence and at 5´-end for XhoI using the software Geneious Prime® 2021.0.1 (Biomatters Ltd.; https://www.geneious.com). For expression of the ERIC II-specific antigen with a histidine tag (His-tag),

another forward primer was designed containing a NdeI restriction site to include the 6x-His-tag present in the pET28a vector (Figure 9).

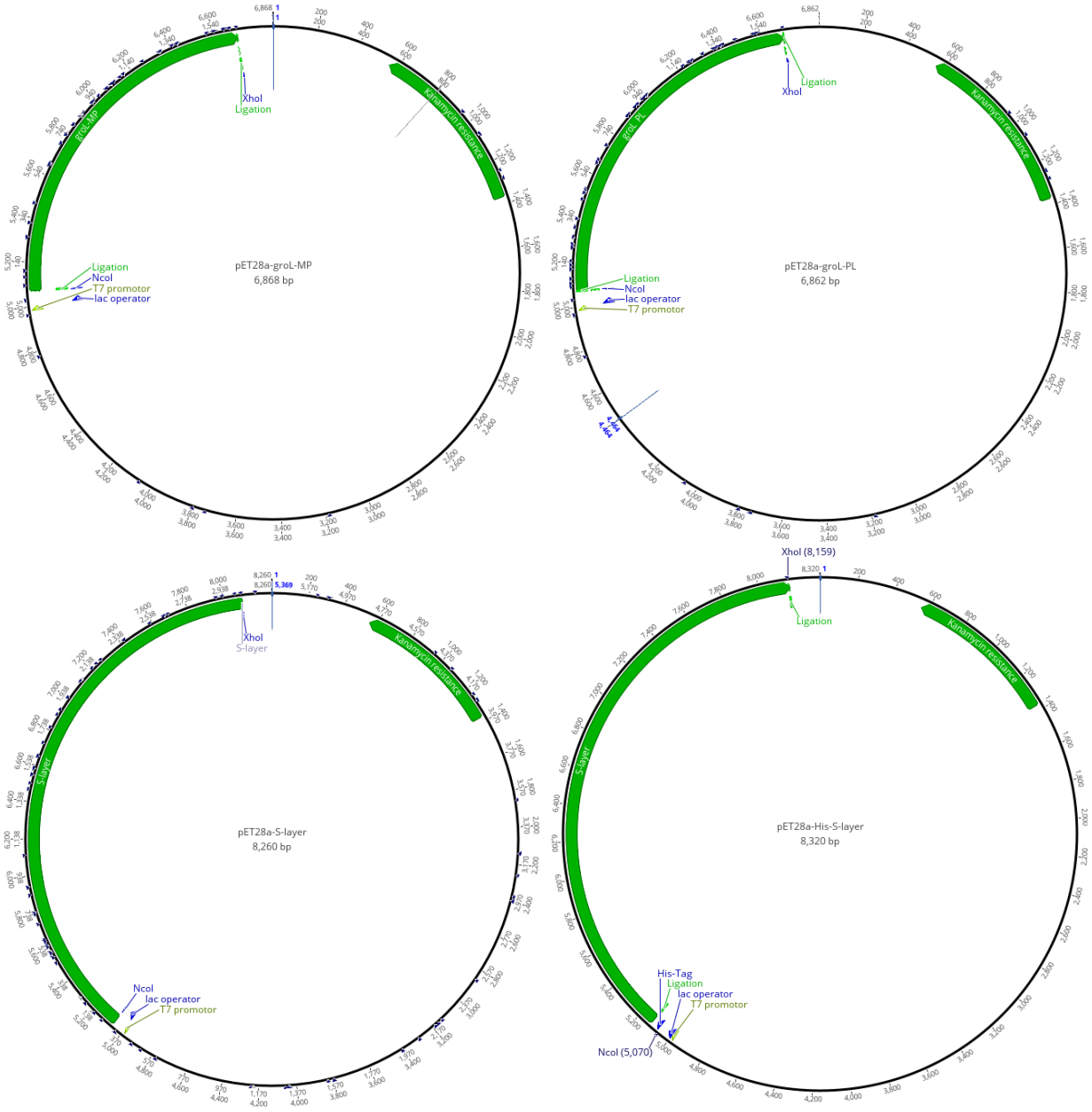

Figure 9 Vector maps of pET28 with different inserts

The plasmid for recombinant protein expression of species-specific antigen of *M. plutonius* (pET28a-groEL-MP: 6868 bp) and *P. larvae* (pET28a-groEL-PL: 6862 bp) are shown in the upper part of the figure. The downer part of the figure shows the plasmids used for S-layer expression with (pET28a-His-S-layer: 8320 bp) and without (pET28a-S-layer; 8260 bp) a histidine tag. Important Sequences are marked in the vector map: the insert gene (groEL or S-layer) with the restriction sites used for cloning, the gene for kanamycin resistance, T7 promotor and lac operator for protein expression.

The DNA amplification of the target gene was performed with the Phusion High-Fidelity DNA Polymerase Kit (Thermo Scientific, Lithuania) with a proofreading function to obtain high sequence identity (Table 29, Table 30).

Table 29 Phusion PCR reagents for cloning

PCR reagent	V in µL
Phusion high fidelity polymerase	0.5
5x Phusion GC buffer	10
10 µM Primer for (RE: NcoI/NdeI)	2.5
10 µM Primer rev (RE: XhoI)	2.5
10 mM dNTPs	1
dH_2O	32.5
DNA (50-250 ng)	1
∑	50

Table 30 Phusion PCR temperature profile

	Initial denaturation	Denaturation	Annealing	Elongation	Final elongation	Pause
temperature	98°C	98 °C	58 °C	72 °C	72 °C	4 °C
time	30 s	30 s	80 s	80 s	10 min	∞
		35 cycles				

PCR products were mixed with loading dye (ThermoFisher Scientific) prior to loading on gels. The success of PCR was confirmed through gel electrophoresis (100 V; 70 min) using 1.5 % agarose gel stained with 1x GelRed (Biotium, USA) and visualized under UV light using the Imaging system ChemiDoc (Bio-Rad Laboratories, Germany). Resulting DNA-bands were cut out and DNA was extracted using QIAquick Gel Extraction Kit (Qiagen, Hilden) following the manufacturer's instructions with minor changes. All centrifugation steps were conducted at RT with 17900 x g for 1 min. After the weight of the DNA-gel slices was determined, three volumes of QG buffer were added and incubated for 10 min at 50 °C until the gel slice completely dissolved. Isopropanol was added, mixed, the solution was applied to the provided column and centrifuged for 1 min. The flow-through was discarded. The DNA was washed with 500 µL of QG buffer and centrifuged again. Another washing step was performed with 750 µL of PE buffer provided with the kit. After additional centrifugation of 1 min to dry membrane, the provided column was transferred to an elution tube and 30 µL of EB buffer were added, incubated for 4 min and eluted via centrifugation. Purified DNA was quantified using NanoDrop 2000C (Thermo Scientific).

3.4.3.2 Restriction enzyme digestion and ligation

Purified DNA was digested with FastDigest restriction enzymes (ThermoFisher Scientific) The vector was additionally treated with a phosphatase (FastAP) to prevent self-ligation. For recombinant protein expression, target genes were cloned into a vector using following reagents (Table 4).

Table 31 Reaction of restriction enzyme digestion

Reagent	V in µL
FD buffer 10x	2
Enzyme NcoI or NdeI	1
Enzyme XhoI	1
FastAP (vector digest)	1
dH_2O	x
DNA (~1µg vector; 500 ng insert)	y
∑	20

y = volume of DNA solution in dependence on the DNA concentration
X = volume in dependence on inserted volume of DNA (y)

For verification of successful restriction enzyme digest, gel electrophoresis (100 V; 70 min, 1.5 % agarose gel with 1x GelRed (Biotium, USA) was performed with the digest reaction (Table 31), bands of interest were cut out and purified using QIAquick Gel Extraction Kit (Qiagen, Hilden) as described in 3.4.3.1.

Purified digested vector and insert were used for ligation with a T4 ligase (ThermoFisher Scientific; Table 32). The ligation reaction was incubated for 30 min at room temperature and continued at 4°C overnight.

Table 32 Reagents for ligation

Reagent	V in µL
Ligase buffer T4 10x	2
T4 ligase	1
vector	2
insert	4
dH_2O	11
∑	20

3.4.3.3 Transformation and verification of successful cloning

Competent *Escherichia coli* cells (BL21) were produced using calcium chloride (100 mM $CaCl_2$). A pre-culture was incubated overnight and transferred into 50 mL of fresh LB medium until bacteria growth reached OD_{600} of 0.4-0.5. The bacteria culture was pre-cooled and centrifuged (1700 x g, 4 °C, 10 min). Bacteria were resuspended with cold 100 mM $CaCl_2$, incubated for 30 min and centrifuged again

(1000 x g, 4 °C, 2 min). Bacteria were resuspended (100 mM $CaCl_2$, 16.7 % glycerol), aliquoted (50 µL per tube) and stored at -80 °C until use.

Competent cells were incubated for 30 min on ice prior transformation. Half of the ligation reaction (10 µL) was added to bacteria cell and further incubated for 30 min on ice. Stimulation for plasmid uptake was performed at 42 °C in a water bath for 45 s following 2 min incubation on ice. Cells were incubated with 1 mL LB medium for 1 h, and centrifuged at 800 x g for 2 min. Bacteria pellets were solved in 200 µL LB medium. The bacteria solution (100 µL) were plated on LB-kanamycin agar plates (50 µg/mL kanamycin) and incubated at 37 °C overnight. Grown colonies were transferred to mini cultures (4 mL LB with 50 µg/mL kanamycin) and incubated for ~6 h or overnight. Glycerine stocks of the different clones were prepared (100 µL 100 % glycerine and 450 µL bacterium culture) and plasmid DNA was extracted using QIAprep Spin Miniprep Kit (Qiagen, Hilden) following the manufacturers protocol. All centrifugation steps were performed at RT with 17900 x g. Cells were centrifuged, supernatant removed and pellet was solved in 250 µL P1 buffer with RNase A and lyse blue. P2 buffer (250 µL) and 350 µL N3 buffer were added and mixed. The lysate was transferred to QIAprep spin column and centrifuged for 1 min, the flow-through was discarded and the column was washed with 750 µL PE buffer. After an additional centrifugation step to dry membrane, the column was transferred into elution tube and 30 µL of EB buffer were added. After 4 min incubation, elution was performed via centrifugation and resulting plasmid DNA was quantified using NanoDrop 2000C (Thermo Scientific). Resulting plasmid DNA was digested using the restriction enzymes, which were used for cloning (Table 31). Successful plasmid digests were verified with gel electrophoresis and candidates were prepared for sequencing following the process described in 3.1.4.2) with the according primer for target gene sequencing (Table 2)

For purification of sequencing reaction, 1 µL 3 M sodium acetate and 25 µL pure ethanol were added per 10 µL PCR-reaction. After incubation of 10 min at 4 °C a centrifugation step followed (18400 x g, 4 °C, 20 min). DNA was washed twice with 75 % ethanol, DNA was resuspended in 20 µL form amide and stored at 4 °C until sequencing. The purified sequences were analysed with in house sequencing using AB Hitachi 3500 Genetic Analyzer (Applied Biosystems, Weiterstadt). Resulting DNA sequences were analysed with the software Geneious Prime® 2021.0.1 (Biomatters Ltd.; https://www.geneious.com) comparing the sequence to the target sequence. Clones containing the correct sequences were stored at -80 °C until use.

For sequencing the groEL gene of the atypical *P. larvae* strains the same primers were used as for cloning. The resulting PCR products were prepared for sequencing performing same procedure described before (3.1.4.2). Resulting sequences were mapped to reference sequence, the genetic

distances have been calculated and a phylogenetic tree was build using the software Geneious Prime® 2021.0.1 (Biomatters Ltd.; https://www.geneious.com). The phylogeny was depicted by neighbour-joining method. Therefore, genetic distances have been calculated pairwise using the Tamura-Nei genetic distance model.

3.4.3.4 Recombinant protein expression

Recombinant protein expression is induced by activating lac operon followed by T7-polymerase activation. The induction is performed by addition of IPTG a structural analogue of lactose. For protein expression, overnight cultures of *E. coli* BL21 cells containing the corresponding plasmid were used. For inoculation of bacteria 100 mL fresh LB medium with kanamycin addition (50 µg/mL) was used. When the bacteria culture reached OD_{600} of 0.5-0.6, protein expression was induced with the addition of 0.5 mM IPTG. After further incubation of 4 h, cells were harvested (centrifugation 5000 x g, 4 °C, 15 min). Bacteria cells were used either for SDS-PAGE (3.4.1), WB (3.4.1), IP (3.4.2) or, when containing a His-Tag, for immobilized metal affinity chromatography (IMAC).

3.4.3.5 Immobilized metal affinity chromatography (IMAC)

Histidine (His) is an aromatic amino acid that attracts positively charged metal ions. A string of His amino acids (often 6x-His) can be attached to proteins of interest. The binding of His to metal ions is used for purification purposes. His-tagged proteins were purified with HisTrap HP Ni^{2+} column (Thermo Scientific, Sweden). Bacteria cells were solved in lysis buffer (Table 33), sonicated three times for 30 s using Branson sonifier 450 (G. Heinemann Ultraschall- und Labortechnik, Germany) and chilled on ice in between. After 30 min incubation on ice, the cell lysate was centrifuged (5000 x g, 4 °C, 30 min) and the supernatant was sterile filtered (0.22 µm) prior application to HisTrap HP Ni^{2+} column.

Table 33 Solutions for IMAC

Buffer	Ingredients	pH
lysis & binding buffer	20 mM sodium phosphate 500 mM NaCl 40 mM imidazole 1x protease inhibitor cocktail (for lysis only)	7.4
elution buffer	20 mM sodium phosphate 500 mM NaCl 500 mM imidazole	7.4

Protein extracts were diluted 1:1 with binding buffer (Table 33). The protein-binding buffer mix was applied to column (1 mL/min flow rate) after column equilibration with ten column volumes of binding

buffer. The column was washed with 20 column volumes of binding buffer. The bound protein was eluted with five column volumes of elution buffer (Table 33) in six fractions. The different fractions were analysed for purity using SDS-PAGE (3.4.1). Purified His-labelled protein was sent to project partners for sandwich ELISA optimization. The HisTrap HP Ni^{2+} column was washed with ten column volumes of binding buffer and stored with 20 % ethanol at 4 °C until reuse.

3.5 Lateral flow device application

LFDs are fast tests for the direct use in the field. The principle of LFDs is based on sandwich ELISA. For the production of the LFDs by Senova (Industriestraße 8, 99427 Weimar), the suitable mAbs against *M. plutonius*, *P. larvae* and ERIC II were used. The detector antibodies, which were conjugated with silver nanoparticles, were stabilized in a sucrose solution. The capture antibodies were immobilized on the nitrocellulose membrane where the reactions with the samples takes place. After the membrane dried, free active sites on the membrane are blocked with chemicals such as polyvinyl alcohol (Bahadır & Sezgintürk, 2016). The sample pad, the conjugation pad with the conjugated detector mAbs and the absorption pad were fixed on the nitrocellulose membrane (Bahadır & Sezgintürk, 2016). After insertion of this membranes into a plastic cassette, the LFD is ready for use. The applied sample moves via capillary forces towards the end of the LFD strip (Bahadır & Sezgintürk, 2016). The result of the LFD can be read out by naked eye due to colour development by the accumulated silver nanoparticles.

The implementation of the mAbs to the LFD in the field is connected with a few challenges. It has to be considered that the produced mAbs are stable for long-term storage at room temperature. Furthermore, the use of buffers that are harming the environment or dangerous to the applicant have to be avoided. Additionally, the buffers that are used, have to be compatible to the nitrocellulose membrane and nanoparticle conjugated mAbs and must not have denaturing abilities due to the use of the buffer as reaction space.

Two AFB-LFD prototypes were produced, one with only the anti-*P. larvae* mAbs (3B3 and 5B1) and one with the anti-*P. larvae* mAbs and the anti-ERIC II (AFB-EII-LFD: 1A6 and 2D12) mAbs in one device. For the EFB-LFD production the 6F10 mAb with the rabbit anti-*M. plutonius* pAb was used. To test the developed LFDs from Senova for AFB and EFB detection, frozen bacteria cell solutions stored in PBS or coating buffer (used for indirect ELISA; 3.3.2) were used. Bacteria were diluted 1:10 or directly solved in lysis buffer after centrifugation (30 mM potassium phosphate, 2 mg/mL lysozyme, 1 % tergitol). The lysis reaction was mixed and incubated for at least 2 min. The cell lysates were diluted in sample buffer (provided by Senova) to a final concentration of $5x10^5$ cell/mL, if not designated differently. Finally, 100 µL of bacteria lysate in sample buffer were applied to each LFD-type (AFB- and EFB-LFD separate).

The results were read out after 15 min incubation by naked eye. The AFB-EII-LFD showed two occurring bands when testing with ERIC I bacteria (one was the control band and the other one was the positive reaction with the anti-*P. larvae* mAbs) and three bands when testing with ERIC II bacteria (Figure 10 A) and B)). The EFB-LFD developed two bands when *M. plutonius* was successfully detected (Figure 10 C).

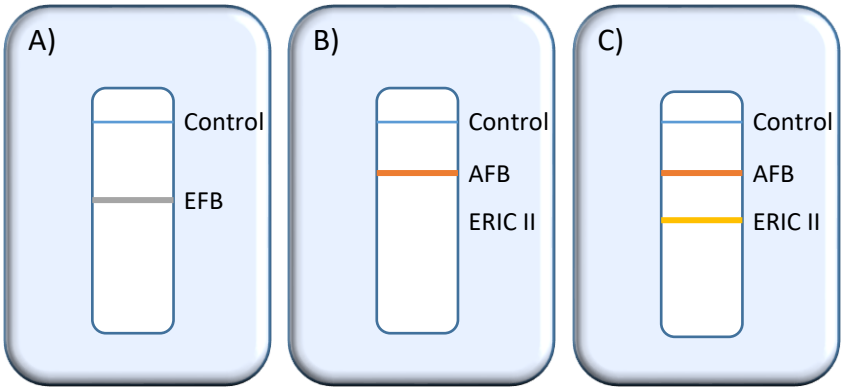

Figure 10 Scheme for possible LFD results
Schematic illustration of AFB-EII-LFD and EFB-LFD. A) shows a positive result for EFB-LFD.B) and C) show schematic results of AFB-EII-LFD; AB shows positive sample with ERIC I and C) shows positive sample with ERIC II.

For determination of the LFD-LOD a dilution series of the bacteria in sample buffer ($1x10^7$ cells/mL; $5x10^6$ cells/mL; $1x10^6$ cells/mL; $5x10^5$ cells/mL; $1x10^5$ cells/mL; $5x10^4$ cells/mL) was performed and applied to the different LFDs. For EFB-LFD the strain CH21.1 and for AFB-EII-LFD the ERIC I and ERIC II reference strains were used. The AFB- and EFB-LFDs were tested for cross reactivity with bee-associated bacteria using a bacteria concentration of $5x10^5$ cells/mL. For detection ability of the different target field strains the bacteria concentrations of $5x10^5$ cells/mL were used for AFB-LFD and $1x10^7$ cells/mL were used for EFB-LFD.

In a former PhD thesis from Saville, 2011 it was declared that the current available test kit (Vita Europe Ltd., Basingstoke, UK) is not detecting the ERIC-genotypes II, III and IV. For this reason, a comparison of the two test kits was performed. Therefore, bacteria pellets with the same undetermined number of cells were solved in the provided buffers of the kits, mixed and applied to the test kits according to manufacturer's recommendations. For the AFB-LFD produced by Senova, bacteria pellets were solved in lysis buffer and diluted in the provided sample buffer. The bacteria pellets were solved with the provided buffer of the Vita-LFD and diluted in the same ratio as performed for the Senova AFB-LFD kit. The bacteria samples (100 µL) were applied to each LFD, respectively.

4. Results

4.1 Bacteria characterization

The nine bacteria species used in this study belong to seven different genera and five different bacteria families. All used bacteria are gram positives. The closest relatives of the AFB causing agent *P. larvae* are *P. alvei* and *P. dendritiformis*, whereas the closest related bacterium of the EFB causing agent *M. plutonius* is *E faecalis*. The close phylogenetic relations of the bacteria to the causative agents of EFB and AFB implies a higher probability for cross reactivity in immunological assay due to shared protein families of the bacteria, which can be recognized by the generated mAbs.

4.1.1 *Melissococcus plutonius*

4.1.1.1 16S sequence verification

To test anti-*M. plutonius* antibodies for their suitability for the use in the LFD for EFB-diagnosis, different *M. plutonius* strains were cultivated and the bacteria identity was verified by 16S-sequencing (Table 34). Sequences were analysed using nBLAST (3.1.4.2). When the comparison with BLAST resulted in a sequence identity higher than 97 %, a threshold also used in literature (Johnson *et al.*, 2019), and the first hits were with *M. plutonius*, the *M. plutonius* identity was considered to be verified. The identities of all successfully cultivated *M. plutonius* strains were confirmed (Table 34).

Table 34 BLAST result of used M. plutonius strains after 16S sequencing

Strain	BLAST result	Accession	Pairwise identity in %	Alignment length in bp	e-value
2013_02	*M. plutonius*	X75751	100	491	0
2013_27	*M. plutonius*	X75751	100	466	0
2013_30	*M. plutonius*	X75751	100	490	0
2013_35	*M. plutonius*	X75751	100	254	2.77 E-128
2013_51	*M. plutonius*	X75751	100	452	0
CH 21.1	*M. plutonius*	X75751	100	453	0
CH 40.2	*M. plutonius*	X75751	100	417	0
CH 41.4	*M. plutonius*	NR_113314	98.5	452	0
CH 46.1	*M. plutonius*	NR_113314	99.8	503	0
CH 48.1	*M. plutonius*	X75751	100	464	0
CH 49.3	*M. plutonius*	X75751	100	468	0
CH 54.1	*M. plutonius*	X75751	100	417	0
CH 60	*M. plutonius*	X75751	100	297	1.74E-135
CH 90	*M. plutonius*	NR_113314	99.6	503	0
CH 119	*M. plutonius*	NR_113314	99.6	503	0
LMG 20360	*M. plutonius*	NR_113314	99.8	497	0

4.1.2 *Paenibacillus larvae*

In recent years, atypical ERIC-genotypes were discovered by the laboratory of Bee Diseases of the Friedrich-Loeffler institute. The atypical strains have different origin coming from Germany (ERIC * and ERIC **) or Latin America (Table 35). The identity of the atypical strains from Latin America was confirmed via 16S-PCR sequencing (Table 35), whereas the strains of ERIC * and ERIC ** were already previously identified as *P. larvae* (Schäfer *et al.*, 2016). The further characterization of these strains and other *P. larvae* field strains was performed using ERIC-genotyping with rep-PCR analysis (4.1.2.1).

Table 35 Atypical P. larvae strains and their origin

Reference number	ERIC-genotype	Origin	Accession	Pairwise identity in %	Alignment length in bp	e-value
341-13	ERIC *	Germany	n.d	n.d.	n.d.	n.d.
493-13	ERIC *	Germany	n.d	n.d.	n.d.	n.d.
456-13	ERIC **	Germany	n.d	n.d.	n.d.	n.d.
1201-14	ERIC **	Germany	n.d	n.d.	n.d.	n.d.
252-18	atypical	Argentina	MK618560	100	482	0
282-18	atypical	Argentina	NR_115120	99.9	461	0
100-19	atypical	Mexico	KT363743	99.5	484	0

n.d. stands for not determined samples

4.1.2.1 ERIC-genotyping of *P. larvae*

For testing the specificity of the ERIC-genotype specific mAbs 30 field strains of the two main genotypes ERIC I and ERIC II were randomly chosen out of the in-house strain collection of the laboratory of Bee Diseases from three different years (ten strains from each genotype out of 2013, 2014 and 2015). The identity of all used *P. larvae* strains (3.1.1) was confirmed to match the genotypes as declared in Table 9 by ERIC-genotyping. The DNA band patterns of different genotypes are shown in Figure 11 exemplary for ERIC I to ERIC V and the other *P. larvae* strains belonging to ERIC *, ERIC ** and the atypical strains from Latin America.

The rep-PCR results showed band patterns that differed from the band patterns of the already known ERIC-genotypes I to V (Figure 11).

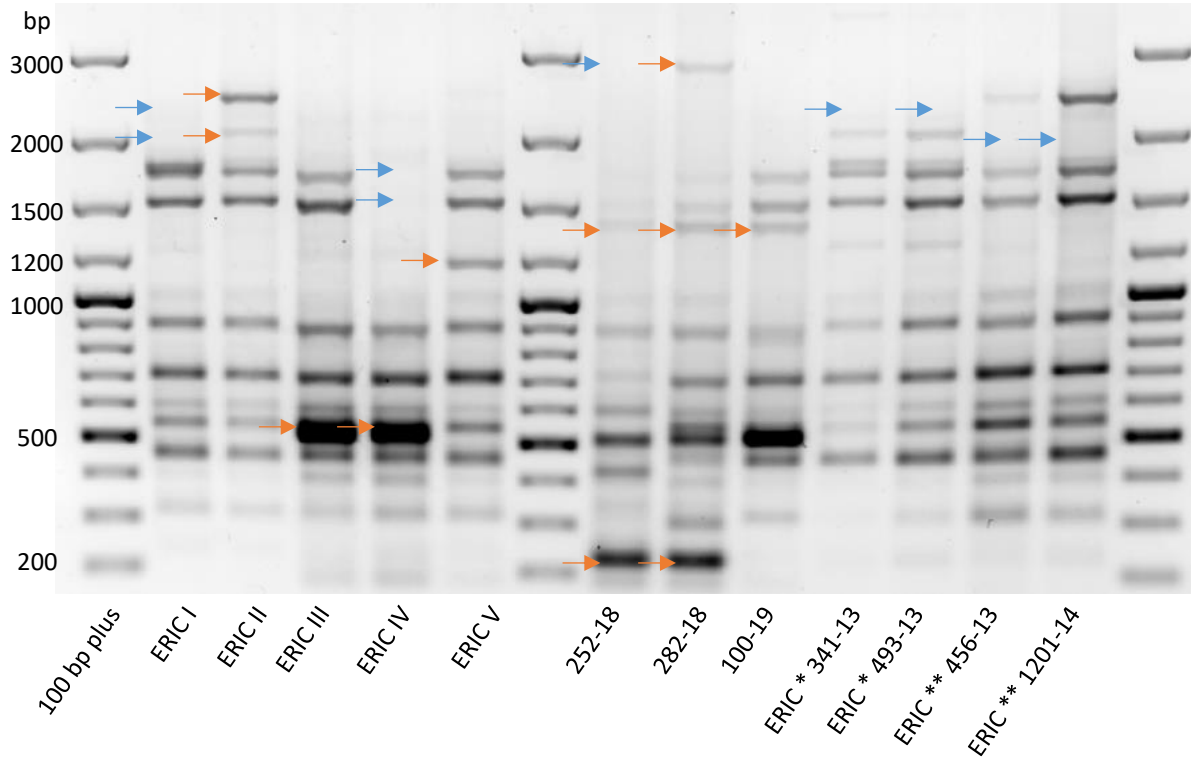

Figure 11 ERIC-genotyping via rep-PCR of P. larvae strains
The DNA ladder 100 bp plus was used. The blue arrows represent missing bands compared to the ERIC-genotypes I to V and the orange arrows represent typical bands for the certain genotype.

The strains belonging to ERIC * and ERIC ** have a similar band pattern compared to ERIC II but they are missing one of the two upper bands between 2000 and 3000 bp. When the 3000 bp band is missing, the strains genotype is named as ERIC * and when the lower band is missing, the strains genotype is named ERIC ** (Schäfer *et al.*, 2016). The band patterns of the atypical strains from Latin America (252-18; 282-18; 100-19) differ even more from the band patterns of ERIC I and ERIC II. From the three atypical strains, the Mexican strain (100-19) has the highest similarity in band pattern when comparing it to the ERIC III and IV. The Mexican strain shows the prominent band at ~500 bp, which is typical for ERIC III and IV. However, it has an additional band close to 1500 bp, which is not present in the known genotypes. The two Argentinian field strains (252-18 and 282-18) show relative similar band patterns when comparing them to each other. The Argentinian strains show a prominent band at ~200 bp, but the strain 282-18 has an additional band at 3000 bp and a double band at ~500 bp (Figure 11).

4.1.2.2 Multiple locus variable number of tandem repeats analysis of *P. larvae*

The MLVA-PCR was performed to get a better impression of the variance in the selected field strains of *P. larvae*. New MLVA-types that have not been described in Descamps et al. (2016), were discovered by the laboratory of Bee Diseases (oral communication, Schäfer, M.). The designation of the new

MLVA-types was performed according to differences to band patterns of known MLVA-types. In total, 30 different MLVA-types were discovered testing the 72 *P. larvae* strains used in this study (Figure 12). The MLVA types from 1 to 17 were grouped to ERIC I, whereas the MLVA-types 18 to 21 belong to ERIC II genotype. The genotypes ERIC III to V, ERIC * and ERIC ** described by Schäfer et al (2016) and the atypical strains from Latin America are designated here as others.

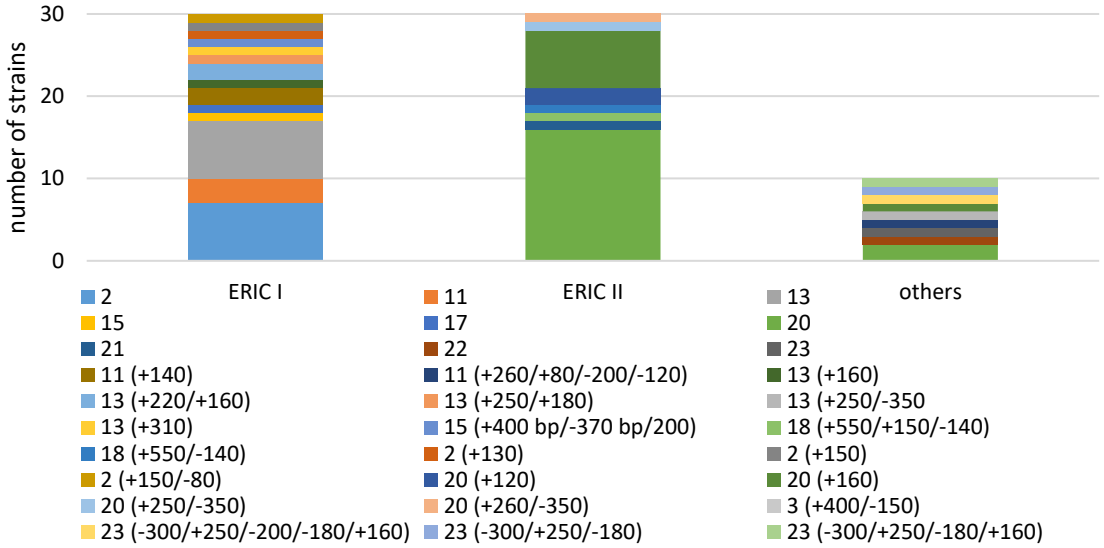

Figure 12 MLVA types of the analysed P. larvae field strains
The genotypes ERIC III to V, ERIC * and ERIC ** and the atypical strains from Latin America are designated here as others on the x-axis. New MLVA-types were characterized in comparison to band patterns of the known MLVA-types (from 1 to 23). Additional occurring bands compared to known MLVA-types were marked with a (+) and the missing bands were marked with (-) at the certain fragment size in bp.

The ERIC I and ERIC II field strains were sampled from 2013 to 2015 in Germany. The samples from 2014 consisted of twelve different MLVA types, while samples of 2013 and 2015 consist of ten different MLVA-types. The ERIC I field strains showed a higher variance with fifteen different MLVA-types compared to ERIC II field strains with only eight different MLVA-types (Figure 12). The most common ERIC I strains were identified as MLVA-type 2 (n= 7) and 13 (n= 7). Most of the ERIC II strains belonged to MLVA-type 20 (n= 16), followed by MLVA type 20 with an additional band at 160 bp (n= 7). The ERIC I reference strain used for immunization belonged to a MLVA-type that could not be found again in the analysed ERIC I field strains and it was also not described by Descamps *et al* (2016). In the group, which was designated as others, every strain belonged to a separate MLVA-type except of the two ERIC ** strains that showed the same band pattern (MLVA type 20) that is known to exist for ERIC II strains.

4.1.2.3 Characterization of atypical strains using SDS-PAGE

For further investigation of the atypical *P. larvae* strains on the protein level, the protein lysates of the strains belonging to the different ERIC-genotypes and the atypical *P. larvae* strains were analysed using SDS-PAGE followed by Coomassie staining (Figure 13).

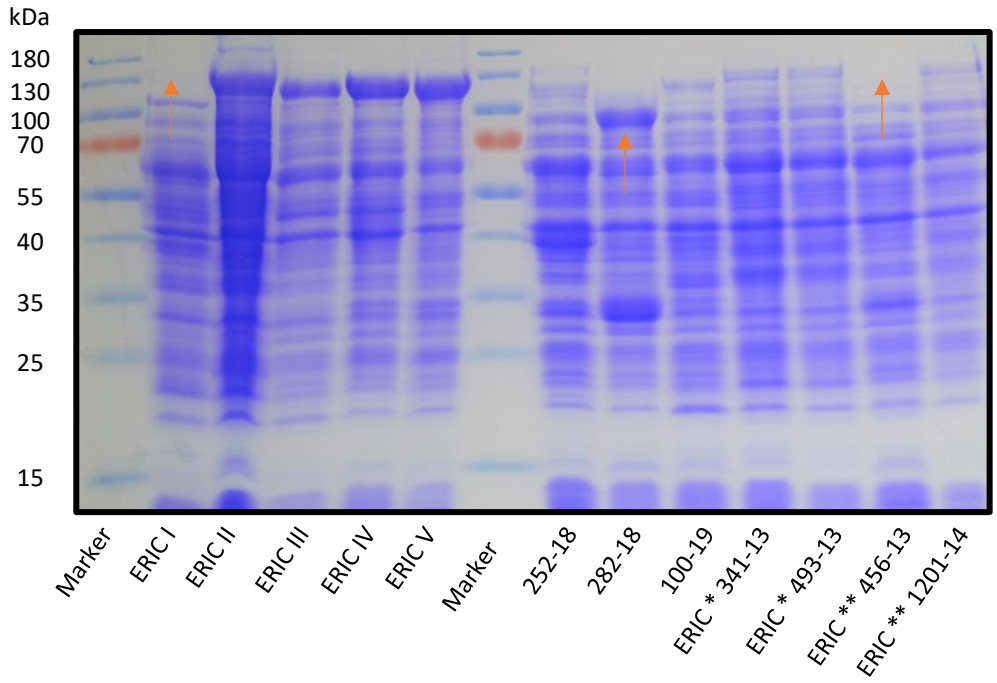

Figure 13 SDS-PAGE of atypical P. larvae strains

The SDS-PAGE followed by Coomassie staining was performed (3.4.1) with the bacteria lysates from the reference strains of the known ERIC-genotypes (Table 9), the ERIC *, ERIC ** and the atypical *P. larvae* strains. The protein band patterns show differences, especially in the expression of a protein at 130 kDa band. The blue arrows represent the lack of the 130 kDa band. The orange arrows mark a prominent band at 100 kDa.

The protein lysates of all tested *P. larvae* strains showed a band at ~ 60 kDa that fits well to the size of the described antigen, which is detected by the specific anti-*P. larvae* mAbs (3B3 and 5B1; 4.4.1.2). Comparing the protein patterns of the well described ERIC I and ERIC II genotypes, ERIC I was missing a prominent band at ~130 kDa, which was present in ERIC II protein lysate. This band fits well in size to the protein, which was detected by the produced anti-ERIC II mAbs (4.4.1.4). The genotypes ERIC III to V showed similar bands as ERIC II at 130 kDa. The general protein patterns of the ERIC I to V strains were similar to each other (Figure 13). The ERIC * and ERIC ** protein band patterns showed similar distribution of bands compared to ERIC I and ERIC II but ERIC * and ERIC ** strains showed less prominent bands at 130 kDa. However, the ERIC * genotypes (341-13; 493-13) and one ERIC ** genotype (1201-14) showed a weak band at 130 kDa, whereas the ERIC ** strain 456-13 showed no such band. The protein band patterns of the atypical Latin American strains differed more from the genotypes ERIC I to V. The protein band pattern of strain 100-19 showed more similarities to the known genotypes than to the other two atypical Latin American strains, which is well in line with the rep-PCR

results (Figure 11 and Figure 13). The 100-19 strain showed a weak band below the 130 kDa marker, whereas the 282-18 strain had a prominent band at ~100 kDa. The 252-18 strain showed a weak band at 130 kDa as it was also the case for ERIC * and one ERIC ** (1201-14). Both Argentinian *P. larvae* strains showed additional bands compared to the other *P. larvae* strains. The strain 252-18 had an additional band at ~40 kDa and the strain 282-18 showed an additional prominent band at ~30 kDa (Figure 13). The findings of the protein pattern comparison underline the differences found in rep-PCR analysis.

4.1.3 Identification of bee-associated bacteria

The identity of the bee-associated bacteria was confirmed after cultivation of the bacteria on different media (Table 7) using 16S-Sequencing (4.1.1). All of the cultivated bee-associated bacteria were identified as the ones expected/inoculated (Table 36).

Table 36 BLAST result of used bee-associated bacteria

strain	BLAST result	Accession	pairwise identity in %	alignment length in bp	e-value
DSM 101882	*P. apium*	NR_133042	99.6	368	0
DSM 12361	*L. kunkeei*	MT381736	99.9	468	0
DSM 18844	*P. dendritiformis*	NR_042861	99.9	455	0
DSM 20478	*E. faecalis*	MW816501	99.9	464	0
DSM 25	*B. laterosporus*	MW736875	99.7	450	0
DSM 27	*B. pumilus*	MW799918	100	452	0
DSM 29	*P. alvei*	NR_113577	99.7	438	0

4.2 Antibody production and analysis

Antibodies were produced by the immunized animals. The pAbs were taken from blood of immunized animals. The mAbs were characterized after hybridoma production, sub-cloning and purification. The two antibody types were further analysed with indirect ELISA and WB (3.3.2).

4.2.1 Polyclonal antibodies (pAbs)

The pAbs were isolated after immunization of rat, mice and rabbit blood of each animal. Blood was centrifuged to separate serum from plasma and the serum was further diluted in buffer according to the method used for analysis.

4.2.1.1 Indirect ELISA

Blood samples were taken from all immunized animals before 1st immunization (except for rats) and the resulting serum was considered as negative sample (primary serum). On the day of euthanization, blood was taken again for serum extraction (end serum). To verify that the immunization was successful, primary sera and end sera were tested in different concentrations against their target pathogen (the bacteria the animals have been immunized with) using indirect ELISA.

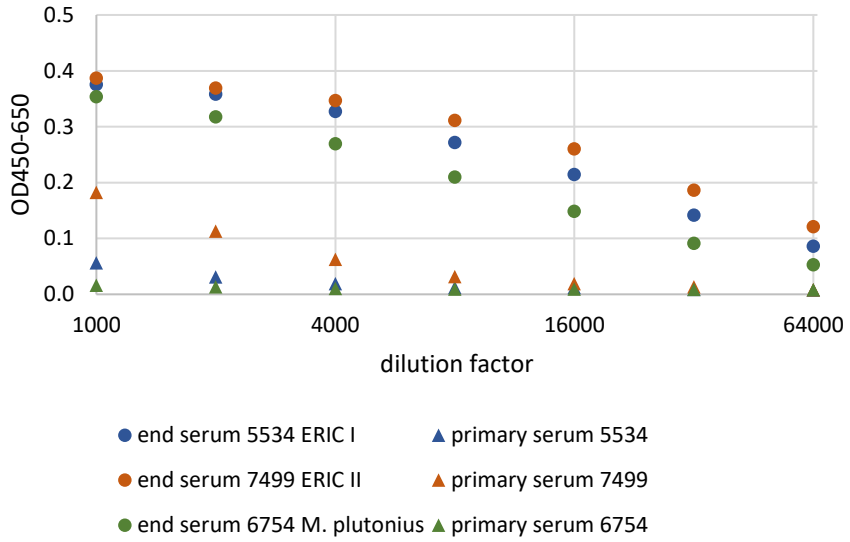

Figure 14 Dilution series of rabbit sera in indirect ELISA
The sera were tested against the bacteria, which were used for the immunization of the respective animal. Primary and end sera were diluted (see x-axis). The numbers next to the sera represent the animal ID (Table 6) followed by the bacterium they have been immunized with. The y-axis depicts the difference of the measured OD values at 450 nm and 650 nm. The Symbols represent mean of three technical replicates (triangles: primary sera; dots: end sera).

Rabbit end sera showed a clear signal with a two to fourfold higher signal (Figure 14) compared to the respective primary sera. Therefore, the immunization was declared to have been successful. In general, primary sera showed a lower signal compared to end sera. The primary serum of the rabbit 7499 (later immunized with ERIC II) showed a two times higher signal than the other primary rabbit sera (Figure 14).

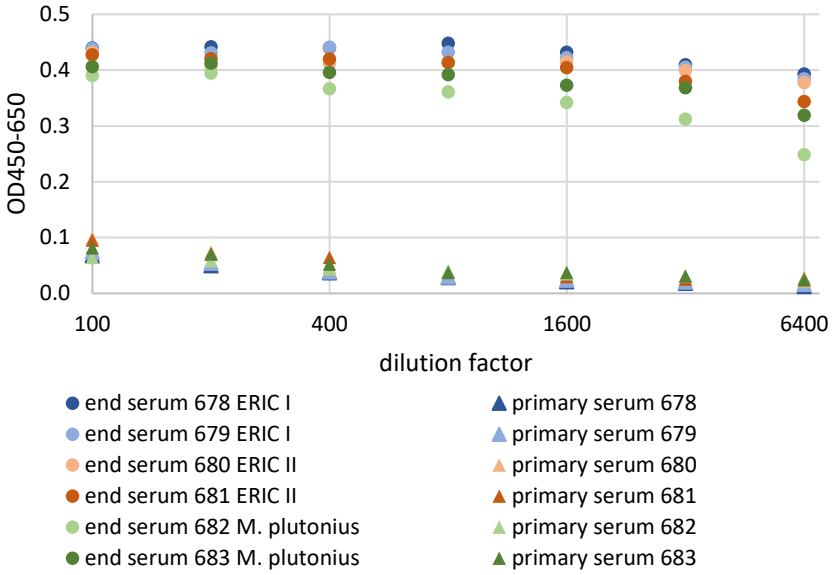

Figure 15 Dilution series of mouse sera

The sera were tested against the bacteria, which were used for the immunization of the respective animal. Primary and end sera were diluted (see x-axis). The numbers next to the sera represent the animal ID (Table 6) followed by the bacterium they have been immunized with. The y-axis depicts the difference of the measured OD values at 450 nm and 650 nm. The Symbols represent mean of three technical replicates (triangles: primary sera; dots: end sera).

The mouse end sera showed fourfold higher absorbance compared to the primary mouse sera. All tested primary sera had similar absorbance heights. Same absorbance heights were also observed for the end sera, except for mouse 682. The mouse 682 was immunized with *M. plutonius* and had a lower response to *M. plutonius* antigen in the indirect ELISA (Figure 15) than mouse 683, which was immunized with *M. plutonius* as well.

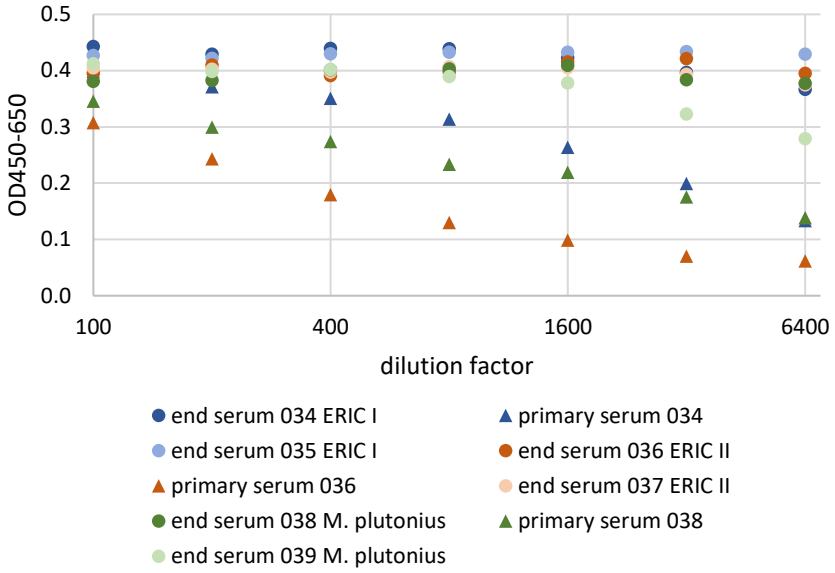

Figure 16 Dilutions series of rat sera
The sera were tested against the bacteria, which were used for the immunization of the respective animal. Primary and end sera were diluted (see x-axis). The numbers next to the sera represent the animal ID (Table 6) followed by the bacterium they have been immunized with. The y-axis depicts the difference of the measured OD values at 450 nm and 650 nm. The Symbols represent mean of three technical replicates (triangles: primary sera; dots: end sera).

The rat sera were tested in the same way as the mouse sera. Unfortunately, the primary sera of only three of the six immunized rats were taken one day after first immunization. It is visible that even shortly after the first immunization the rats show slight reactivity towards their injected antigens (Figure 16). Nevertheless, in the lower concentrated reactions of the ELISA the difference between "primary" and end sera increases. In general, the "primary" rat sera show larger variation in absorbance height compared to the primary sera of rabbits and mice. The lowest signal of the end sera against the immunized antigen is achieved by a rat serum, where the rat was immunized with *M. plutonius*. The other end sera showed similar absorbance height when compared to one another.

4.2.1.2 Western blot

The band patterns of ERIC I and ERIC II bacteria lysates were compared to one another, when both lysates were detected with the same pAbs of antiserum. The application of anti-ERIC I-pAb to protein lysates of ERIC I and ERIC II could show that specific bands are occurring for ERIC I protein lysate. The application of anti-ERIC II pAb to both protein lysates can unravel specific bands occurring for ERIC II protein lysate. This is also the case when comparing the occurring protein bands of anti-*M. plutonius* pAbs.

In general, the WBs with anti-ERIC I and anti-ERIC II pAbs against ERIC I and ERIC II protein lysates showed similar band patterns for the two ERIC-genotypes with only a few specific bands. The pAbs of

the different animals immunized with the two *P. larvae* strains showed no or only low reactivity towards *M. plutonius* protein lysates. The anti-*M. plutonius* pAbs also showed no or only low reactivity towards protein lysates of *P. larvae* (Figure 17, Figure 18 and Figure 19). All anti-*M. plutonius* pAbs indicated a low number of immunogenic proteins of *M. plutonius* compared to the pAbs of animals immunized with *P. larvae*.

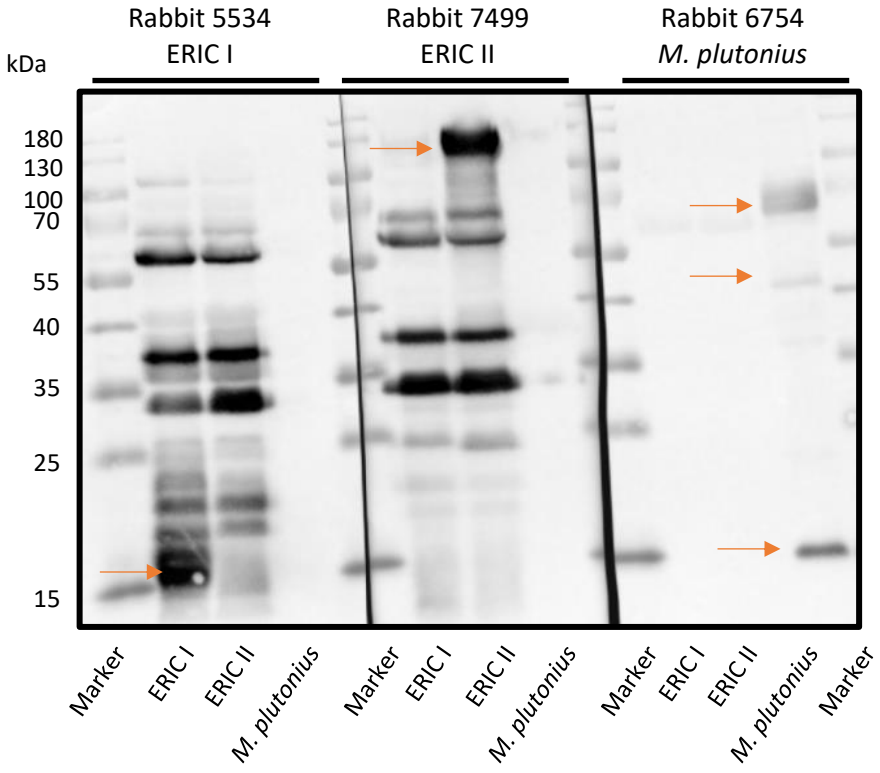

Figure 17 WB: rabbit sera detecting antigens of immunized pathogens
pAbs out of serum were tested against the protein lysates of the three pathogen strains used for immunization. The arrows mark specific protein bands occurring for each pathogen.

The rabbit and mouse pAbs (Figure 17, Figure 18) showed a higher number of antigens towards the bacteria that were used for immunization than the rat pAbs. This is indicated by the higher dilution (factor 1: 5000 for mice and rabbit sera instead of 1:1000 for rat sera) of mouse and rabbit sera when used in WB. Comparing the rabbit and mice pAbs with the rat pAbs, the rabbit and the mice pAbs showed higher variability of detected antigens according to protein size (Figure 17). The rabbit pAbs unravelled one specific protein band for ERIC I (15 kDa) and one for ERIC II (130 kDa). For *M. plutonius* three different specific protein bands occurred (70 kDa, 45 kDa, 15 kDa).

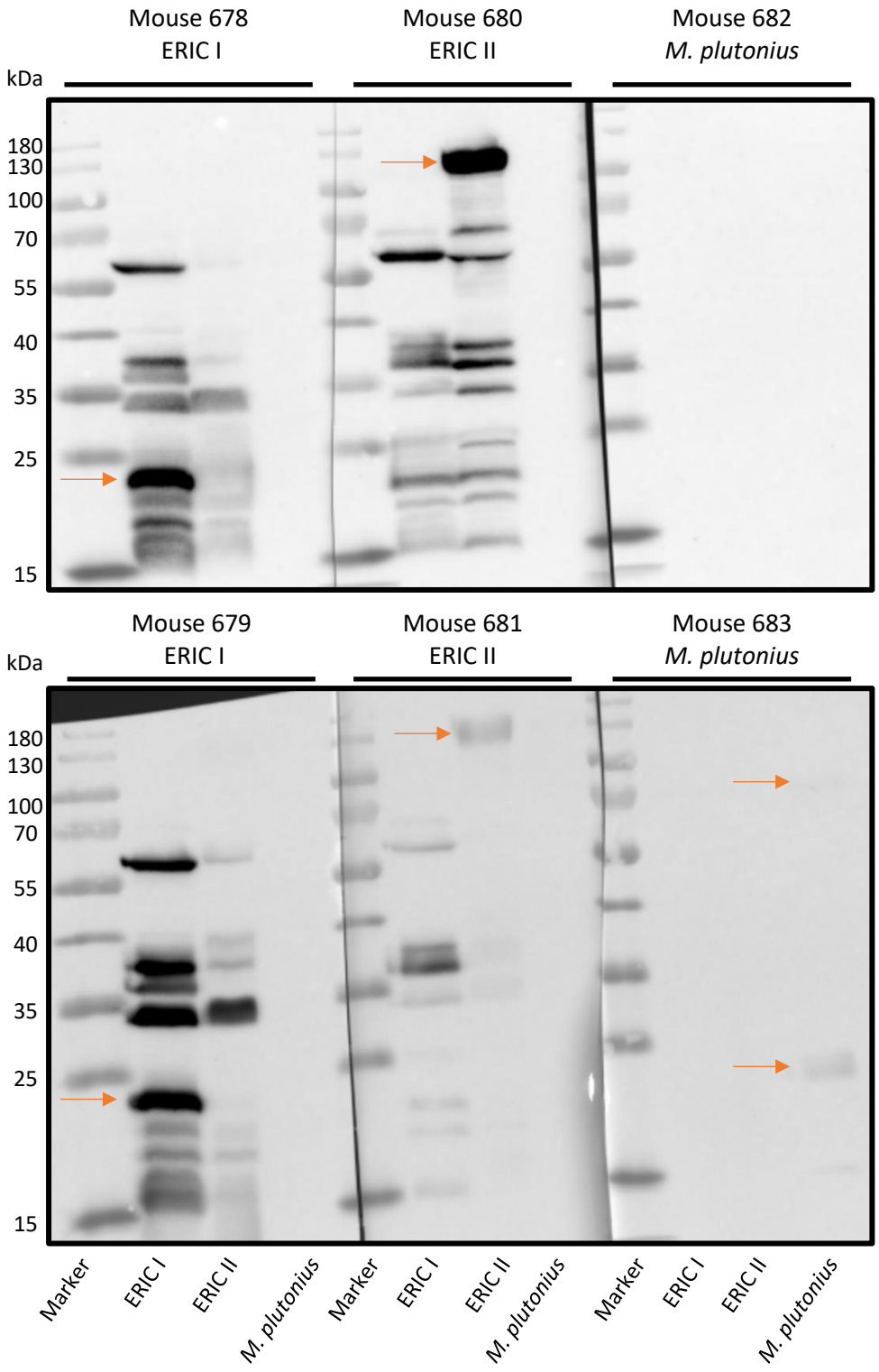

Figure 18 WB: mouse sera detecting antigens of the immunized pathogens
pAbs out of serum were tested against the protein lysates of the three pathogen strains used for immunization. The arrows mark specific protein bands occurring for each pathogen.

Comparing the mouse pAbs, which were tested with the same bacteria that were used for immunization, differences between the individuals occurred. The pAbs of mouse 681 generally showed

weaker bands than pAbs of the mouse 680. When comparing the protein lysates of ERIC I and ERIC II that are detected by pAbs of the mouse 681, it seems that, unexpectedly, specific bands for ERIC I appeared (Figure 18).

Further investigating the rat pAbs in order to identify specific antigens, one antigen for ERIC I (~25 kDa), one for ERIC II (~130 kDa) and three different specific antigens for *M. plutonius* can be identified (60 kDa, 55 kDa, 15 kDa). The rat anti-ERIC I and anti-ERIC II pAbs show a higher cross reactivity with *M. plutonius* protein lysates than the corresponding mouse and rabbit pAbs (rat 035; Figure 19).

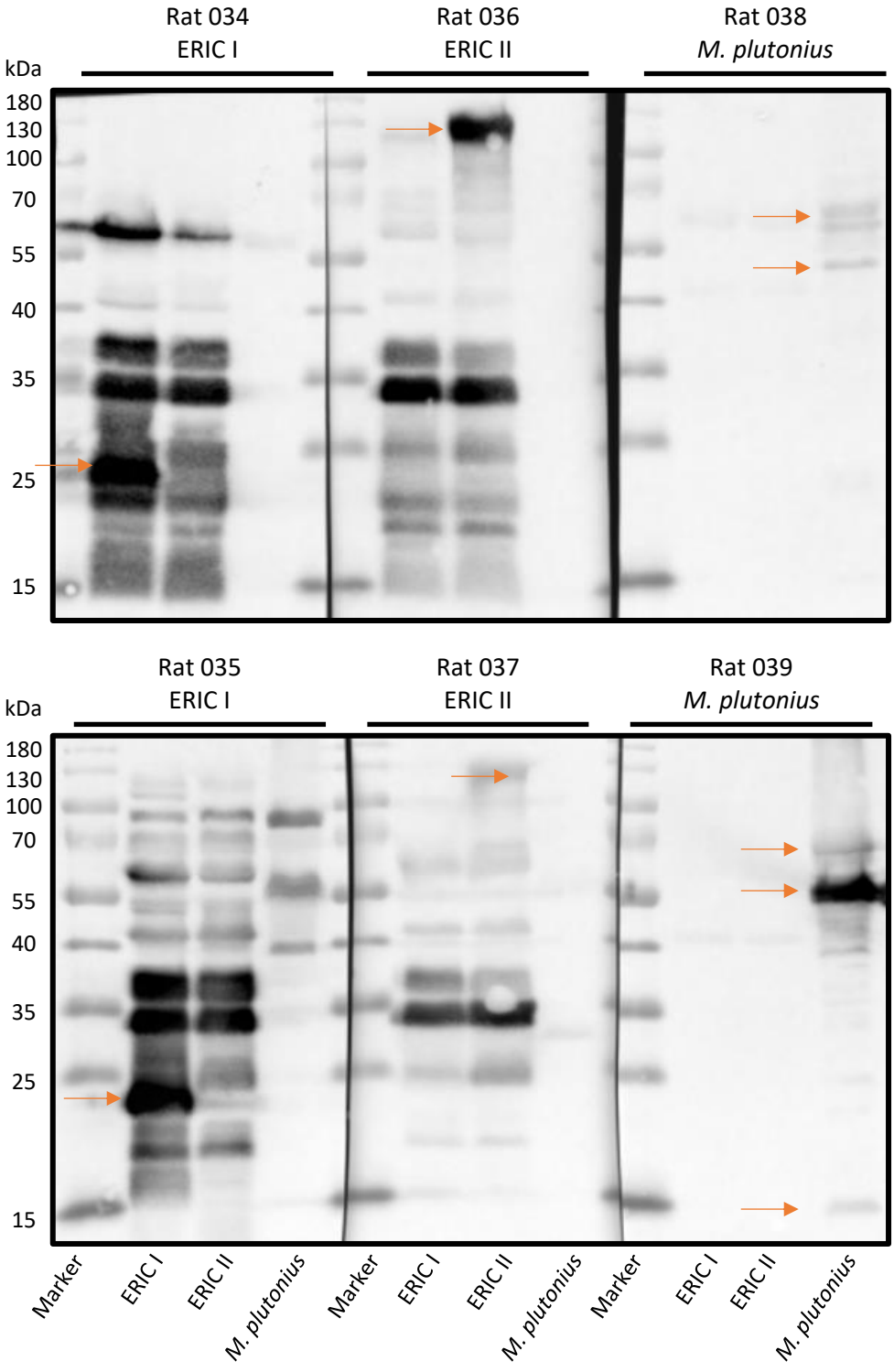

Figure 19 WB: rat sera detecting antigens of the immunized pathogens
pAbs out of serum were tested against the protein lysates of the three pathogen strains used for immunization. The arrows mark specific protein bands occurring for each pathogen.

From the specific bands occurring in all the tested pAbs, it can be concluded that some specific antigens were detected. Anti-*M. plutonius* pAbs detected three possible antigens at ~60 kDa, ~55 kDa and ~15 kDa (Figure 17, Figure 18 and Figure 19). From this one can conclude that for *M. plutonius,* at least

three possible specific antigens exist that can be used for mAb generation. Two specific antigen candidates were found for ERIC I (~25 kDa and ~15 kDa) and one for ERIC II (~130 kDa). When comparing anti-ERIC I pAbs of the different animals, specific bands occur for ERIC I at ~25 kDa tested with rat and mouse pAbs (Figure 12, Figure 13), whereas a band at ~15 kDa occurs when tested with anti-ERIC I rabbit pAbs (Figure 11). The absence of further specific bands does not exclude the possibility that further specific antigens exist. Specific antigens could have similar sizes as non-specific antigens resulting in only one protein band in the WB.

4.2.2 Screening for specific monoclonal antibodies

For antibody screening, the mAbs were screened in four steps after cell fusion of myeloma and spleen cells (3.2.2). The mAbs characterized in 4.3 resulted from five different screenings. One of these screenings was performed with cells of rat spleen for detection of specific anti-ERIC I mAbs. After cell fusion, cells were diluted to eight 96-well plates (2 x 30000 cells/well, 4 x 15000 cells/well, 2 x 7500 cells/well). The supernatant of each well was tested for reactivity against antigens used for immunization by performing indirect ELISA. In the first screening step the proportion of positive wells ranges from 3.6 % (for anti-*M. plutonius* mAb) to 27.8 % (for anti-ERIC I mAb). The resulting anti-*P. larvae* and anti-ERIC II mAbs originated from the same cell fusion and were processed together until second screening (Figure 20). For the second screening step 24 to 30 positive wells were selected for further cultivation. The supernatant of surviving hybridoma was screened for reactivity towards the target antigen (protein of the bacteria, which were used for immunization of the animal) and cross reactivity with the other two pathogens used for immunization. For example, when screening for anti-ERIC I mAbs, hybridoma supernatants were tested for reactivity with ERIC I and tested for cross reactivity against ERIC II and *M. plutonius*. The second screenings of mouse mAbs showed a proportion of positives between 60-70 %, whereas the screening of rat anti-ERIC I mAbs had a proportion of 22 % positive hybridoma supernatants (Figure 20). Roughly 10-25 % of the hybridoma tested in the second screening step were specific for their target bacterium.

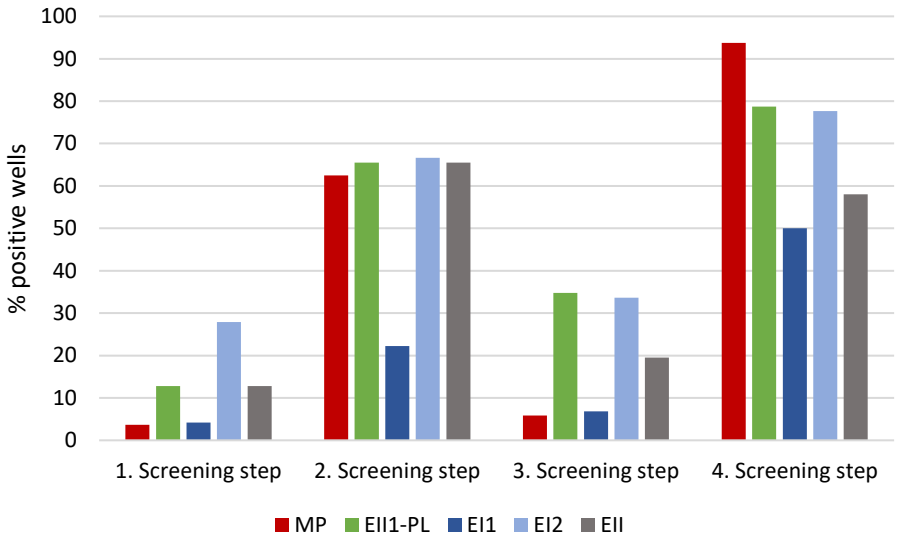

Figure 20 Proportion of positive wells in different screenings for specific mAbs
The mAb screening was performed with supernatant of different cell cultures after cell fusion. The bar heights represent the proportion of positive wells in the four different screenings. The red bars represent the screening for anti-*M. plutonius* mAbs, green bars for anti-*P. larvae* mAbs, dark blue for rat anti-ERIC I and light blue for mouse anti-ERIC I mAbs. Grey bars represent positive wells of anti-ERIC II screening.

After the second screening, the cells of positive wells were diluted to different cell concentrations to separate the mAb producing hybridoma cells of interest. The supernatants of the separated cells were screened in the third screening step. The proportion of positive wells were relatively low with values below 10 % for anti-*M. plutonius* mAbs and rat anti-ERIC I mAbs (EI1). In contrast, the proportion of positives in mouse anti-ERIC I, anti-ERIC II and anti-*P. larvae* mAbs ranged from 20 to 35 %. Three wells with low numbers of cells and high absorbance values, when compared to other positive wells of the same screening, were selected. The selected hybridoma were stored in liquid nitrogen until sub-cloning. One of the three chosen hybridoma was directly sub-cloned and supernatants of the sub-cloned cells were screened in the fourth screening. The highest proportion of positives was detected in the anti-*M. plutonius* mAb screening (93.8 %) resulting in four mAbs (1D3, 3G5, 6F10 and 7D11; 4.3.1). The proportion of positives in anti-*P. larvae* and mouse anti-ERIC I screening was 78.8 % and 77.6 % resulting in four anti-*P. larvae* mAbs (3B3, 5A10, 5B1, 6B8) and three anti-ERIC I mAbs (6D8, 7E12, 8D6), respectively. The rat anti-ERIC I mAb screening resulted in only one mAb (8G3), whereas the anti-ERIC II mAb screening led to four anti-ERIC II mAbs (1A6, 2D12, 4F2, 5B2) (Table 37).

4.3 Monoclonal antibody characterization

The isotypes of the resulting mAbs after screening were characterized to gain more information about their suitability for an LFD approach. The results of mAb characterization are summarized below (Table 37).

Table 37 Produced monoclonal antibodies

mAb ID	target	Antigen size [kDa]	mAb isotype	Light chain	Species	Cross reactivity	% ERIC I strains	% ERIC II strains	% *M. plutonius* strains
1D3	*M. plutonius*	diverse	IgM	κ	mouse	yes	-	-	n.t.
3G5	*M. plutonius*	15	IgG2b	κ	mouse	yes	-	-	n.t.
6F10	*M. plutonius*	60	IgG1	κ	mouse	none	-	-	88
7D11	*M. plutonius*	60	IgG1	κ	mouse	none	-	-	88
3B3	*P. larvae*	60	IgG1	κ	mouse	yes	100	100	-
5A10	*P. larvae*	35	IgG1	κ	mouse	none	87.5	100	-
5B1	*P. larvae*	60	IgG1	κ	mouse	none	100	100	-
6B8	*P. larvae*	60	IgM	κ	mouse	yes	n.t.	n.t.	-
8G3	ERIC I	100	IgG1	κ	rat	none	n.t.	n.t.	-
6D8	ERIC I	20	IgG2b	κ	mouse	yes	n.t.	n.t.	-
7E12	ERIC I	15	IgG1	κ	mouse	none	6.5	0	-
8D6	ERIC I	25	IgG2b	κ	mouse	yes	n.t.	n.t.	-
1A6	ERIC II	130	IgG1	κ	mouse	none	61.3	100	-
2D12	ERIC II	130	IgG1	κ	mouse	none	0	100	-
5B2	ERIC II	130	IgG1	κ	mouse	none	0	100	-
4F2	ERIC II	130	IgG3	κ	mouse	yes	n.t.	n.t.	-

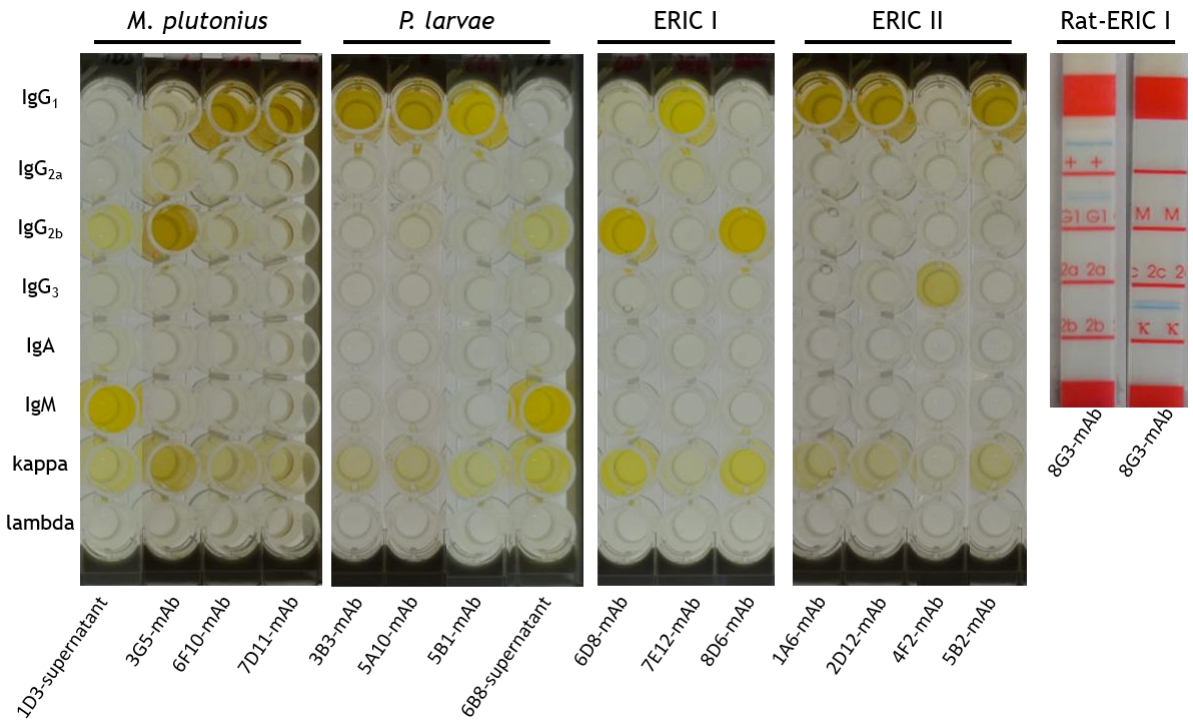

Figure 21 Isotyping of produced mAbs

Mouse antibodies and the rat antibody were isotyped using Test Kits (3.3.1). The strongest yellow coloured wells or blue band (rat mAb) represent a positive reaction for the certain isotype. For isotyping, either diluted purified mAbs (for IgG mAbs) or diluted supernatants (IgM mAbs) were used.

The sixteen antibodies were analysed for their isotype to see if they would be suitable for the use in the LFD. Antibodies of the IgG isotypes are the preferred option for use in the LFD. All antibodies consisted of a kappa light chain and ten of the sixteen mAbs belonged to IgG_1 heavy chain type (Figure 21). Three antibodies (3G5, 6D8, 8D6) belonged to IgG_{2b} isotype, one (4F2) belonged to IgG_3 and two antibodies (1D3, 6B8) belonged to IgM. The mAbs belonging to IgM isotype are not suitable for application in an LFD due to their pentameric structure and other unfavourable properties. Therefore, IgM mAbs were excluded from further analysis (Table 37).

4.3.1 Anti-*M. plutonius* monoclonal antibodies

After final screening of the hybridoma for reactive and specific antibodies, the reactivity of the purified mAbs with suitable isotype was tested using indirect ELISA. This means taht three mAb candidates were tested for *M. plutonius* detection excluding the one mAb belonging to IgM isotype. The optimal concentration of the three mAbs was determined by testing different mAb dilutions against *M. plutonius* as positive control and *E. faecalis* as negative control to find best conditions for distinction between bacteria.

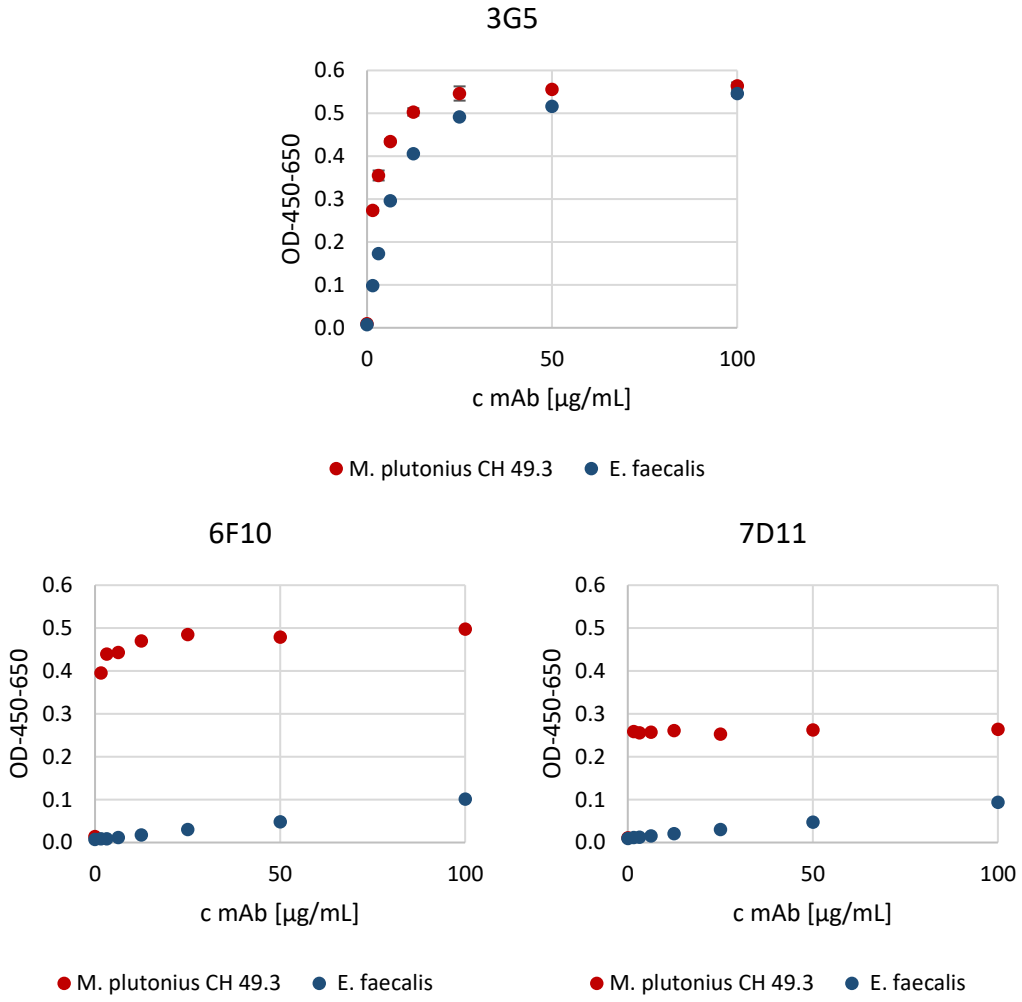

Figure 22 Indirect ELISA: anti-M. plutonius mAb dilution series
The optimal concentrations of the three mAbs (3G5, 6F10 and 7D11) were determined by systematically testing different concentrations (c) in the range from 0 to 100 µg/mL (x-axis). The symbols represent three technical replicates. The red dots represent the positive control (*M. plutonius*) and the blue dots represent the negative control (*E. faecalis*).

Indirect ELISA was performed to find the most suitable working concentration of produced mAbs aiming for a high sensitivity, specificity and economical mAb consumption. One of the four *M. plutonius* strains, which were used for immunization of the mice, was chosen as positive control. The closest phylogenetic relative of the bee-associated bacteria, which is the bacterium *E. faecalis,* was used as negative control. The 3G5 mAb with an IgG_{2b} isotype showed a cross reactivity with *E. faecalis* (Figure 22). The mAb 3G5 was further tested for cross reactivity against other bee-associated bacteria using a concentration of 25 µg/mL (Figure 23). The two IgG_1 mAbs 6F10 and 7D11 distinguished clearly between positive and negative control, whereas 6F10 mAb showed a two times higher signal than 7D11. For both mAbs, a working concentration of 5 µg/mL was used for further testing of mAb cross reactivity using indirect ELISA.

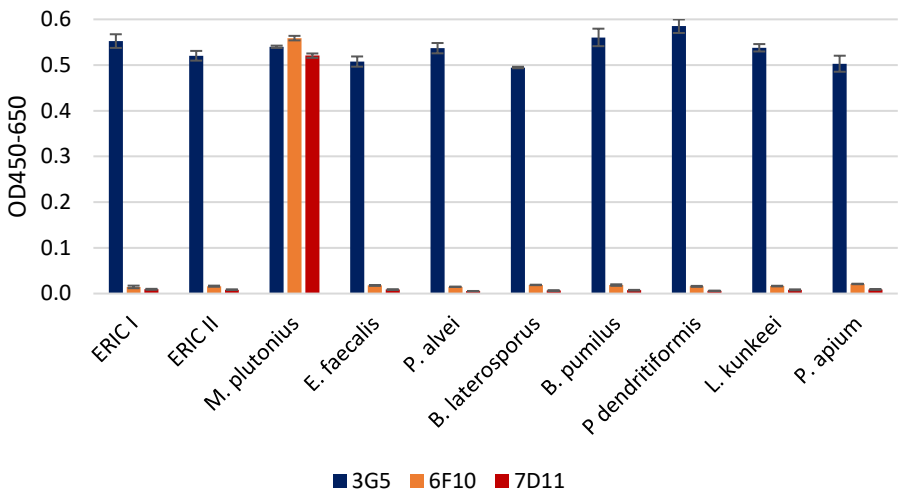

Figure 23 Indirect ELISA: cross reactivity of anti-M. plutonius mAbs

The indirect ELISA was performed with three anti-*M. plutonius* mAbs (6F10 and 7D11: 5 µg/mL and 3G5: 25 µg/mL). The mAbs were tested for cross reactivity against bee-associated bacteria (x-axis). The y-axis depicts the difference of the measured OD values at 450 nm and 650 nm. The bars show the average of three technical replicates. Blue bars represent 3G5, the orange bars 6F10 and the red bars 7D11. The error bars represent the standard deviation of the three technical replicates.

The cross reactivity of the three mAb candidates was checked with strains of ERIC I, ERIC II and bee-associated bacteria to avoid false positive test results of the LFD when used in the field. The 3G5 mAb reacts with all tested bacteria, whereas 6F10 and 7D11 mAbs only show a clear signal for *M. plutonius* and no signal for *P. larvae* or any other of the tested bee-associated bacteria (Figure 23). Concluding, 6F10 and 7D11 mAb could be suitable for LFD usage, if they reliably detect different *M. plutonius* field strains (Figure 24), whereas 3G5 mAb was excluded from further analysis.

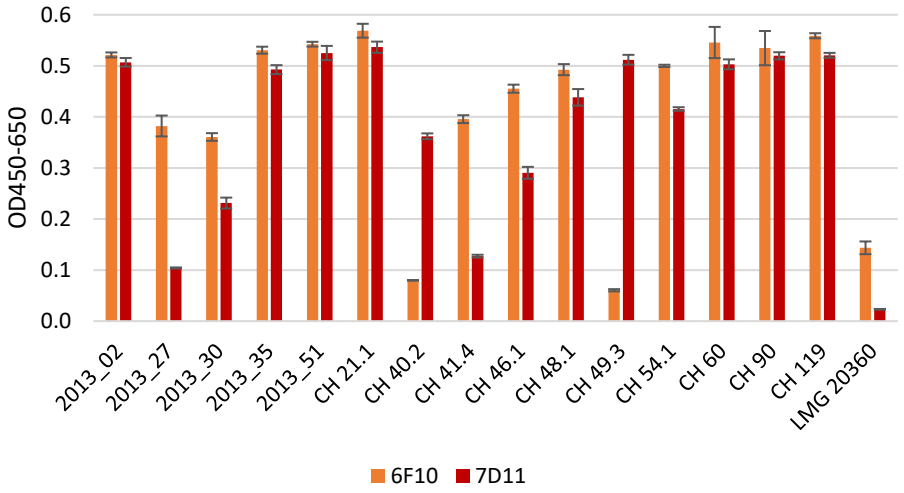

Figure 24 Indirect ELISA: Strain detection of anti-M. plutonius mAbs

The indirect ELISA was performed with the two non-cross reacting anti-*M. plutonius* mAb candidates (6F10 and 7D11: 5 µg/mL). Different *M. plutonius* strains were tested (x-axis). The y-axis depicts the difference of the measured OD values at 450 nm and 650 nm. The bars show the average of three technical replicates. The orange bars are representing 6F10 and the red bars are representing 7D11. The error bars represent the standard deviation of three technical replicates.

The immunization of the mice used for *anti-M. plutonius* mAb production was performed with a mixture of four *M. plutonius* strains (Table 6). For investigation of strain detection coverage, twelve field isolates, which originated from Switzerland, were tested. After calculating the limit of detection (LOD_{OD}) all field strains are defined as positively detected (LOD_{OD}: 6F10: 0.023; 7D11: 0.011). High differences (5 to 100 times higher signals compared to lowest signal) between signal strength of the different field strains are observed (Figure 24).

4.3.2 Anti-*P. larvae* monoclonal antibodies

After exclusion of the IgM isotyped mAb, three remaining mAbs with IgG_1 isotype were tested to determine an appropriate working concentration for *P. larvae* detection in indirect ELISA.

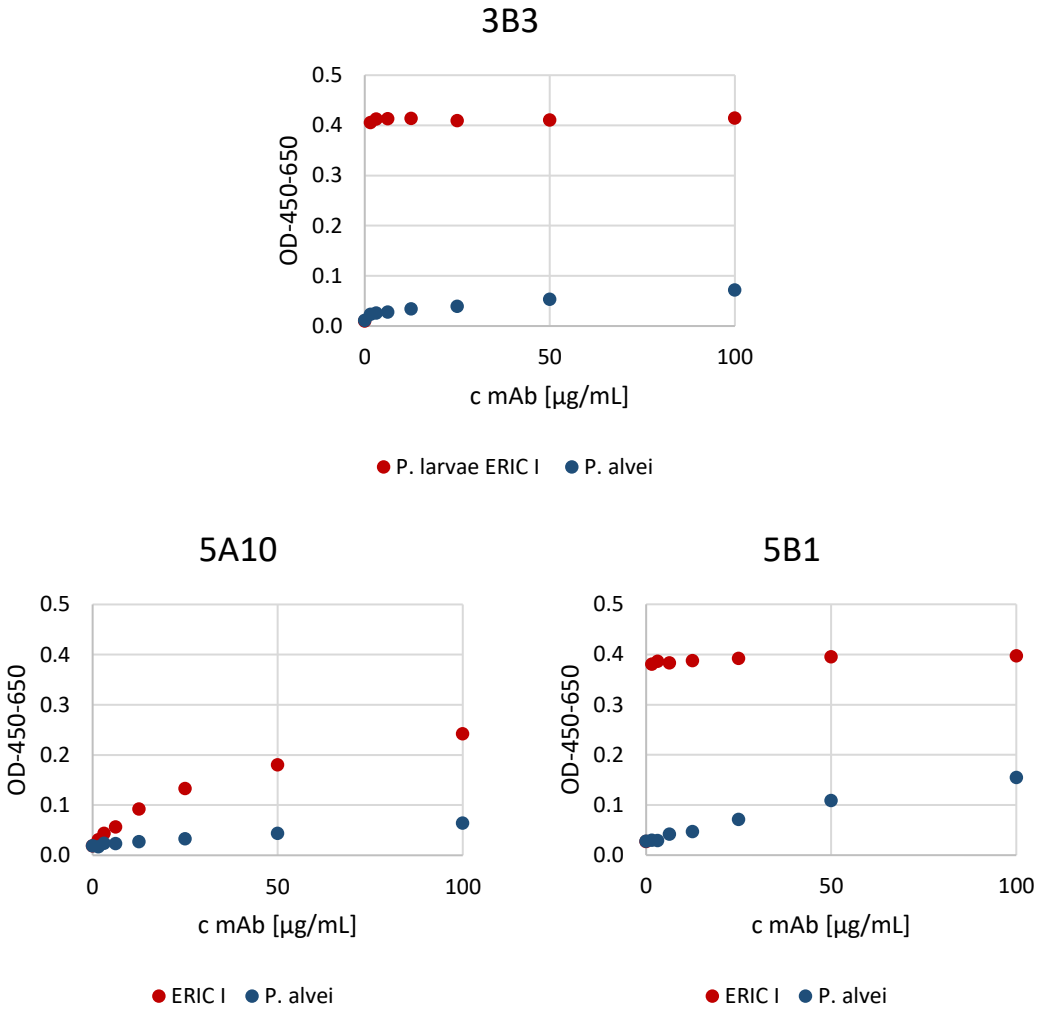

Figure 25 Indirect ELISA: anti-P. larvae mAb dilution series
The optimal concentrations of the three mAbs (3B3, 5A10 and 5B1) were determined by systematically testing different concentrations (c) in the range from 0 to 100 µg/mL (x-axis). The symbols represent three technical replicates. The red dots represent the positive control (*P. larvae*) and the blue dots represent the negative control (*P. alvei*).

To determine a suitable working concentration between positive samples and negative samples a dilution series was performed with a *P. larvae* strain (ERIC I, DSM 25719) for positive reaction and the closely related *P. alvei* for negative control. The 5A10 mAb showed cross reactivity with *P. alvei* with increasing mAb concentration (Figure 25). The mAbs 3B3 and 5B1 showed similar signal heights, when compared to each other ($OD_{450-650}$ = ~0.4). The mAbs 3B3 and 5B1 showed a three to fourfold higher signal when detecting *P. larvae* compared to *P. alvei* but both mAbs showed increasing signal towards *P. larvae* with increasing mAb concentration (Figure 25). Considering that, the aim of this experiment was to determine the optimal concentration for distinction between positive and negative samples, the working concentration of 5 µg/mL was considered to be suitable for 3B3 and 5B1, whereas for 5A10 50 µg/mL was used for further indirect ELISAs.

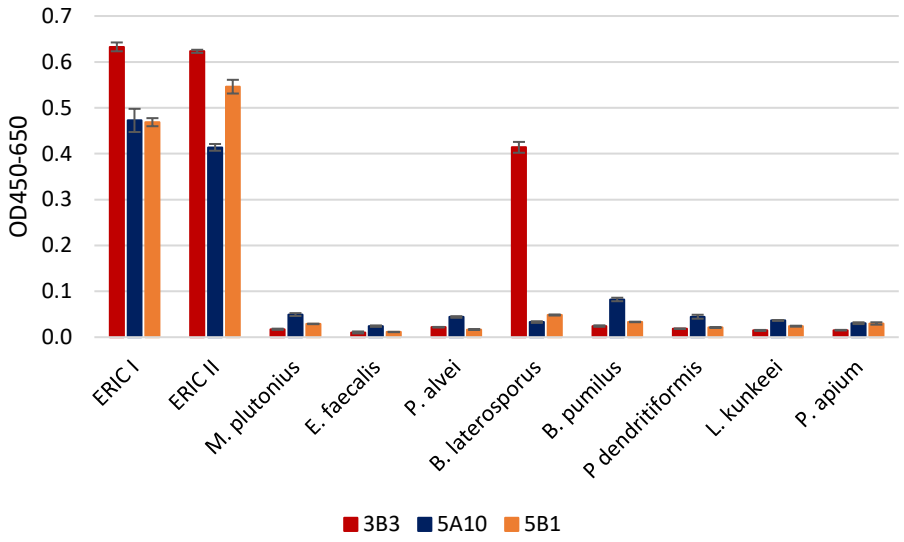

Figure 26 Indirect ELISA: cross reactivity anti-P. larvae mAbs
The indirect ELISA was performed with the three *anti-P. larvae* mAbs (3B3: 5 µg/mL; 5A10: 25 µg/mL; 5B1: 5 µg/mL). The mAbs were tested for cross reactivity against bee-associated bacteria (x-axis). The y-axis depicts the difference of the measured OD values at 450 nm and 650 nm. The bars show the average of three technical replicates. The red bars represent 3B3, blue bars are 5A10 and orange bars show reactivity of 5B1. The error bars represent the standard deviation of the three technical replicates.

The tests for cross reactivity of the suitable *anti-P. larvae* mAb candidates against bee-associated bacteria showed almost no cross reactivity. The 5B1 mAb detected the two main ERIC-genotypes of *P. larvae* and showed no cross reactivity with the tested bacteria (Figure 26). 5A10 and 3B3 also showed a signal against the two main ERIC-genotypes of *P. larvae*. However, 5A10 showed a faint signal, when tested against *B. pumilus*, *P. dendritiformis* and *M. plutonius*. The mAb 3B3 showed cross reactivity with one of the tested bee-associated bacteria, *B. laterosporus*. Only, 5B1 is a highly specific mAb candidate for LFD. But for LFD two antibodies are necessary. In order for the LFD to be specific it is sufficient when only one of the mAb candidates is highly specific. Therefore, all three mAb candidates were tested further for strain detection (Figure 27).

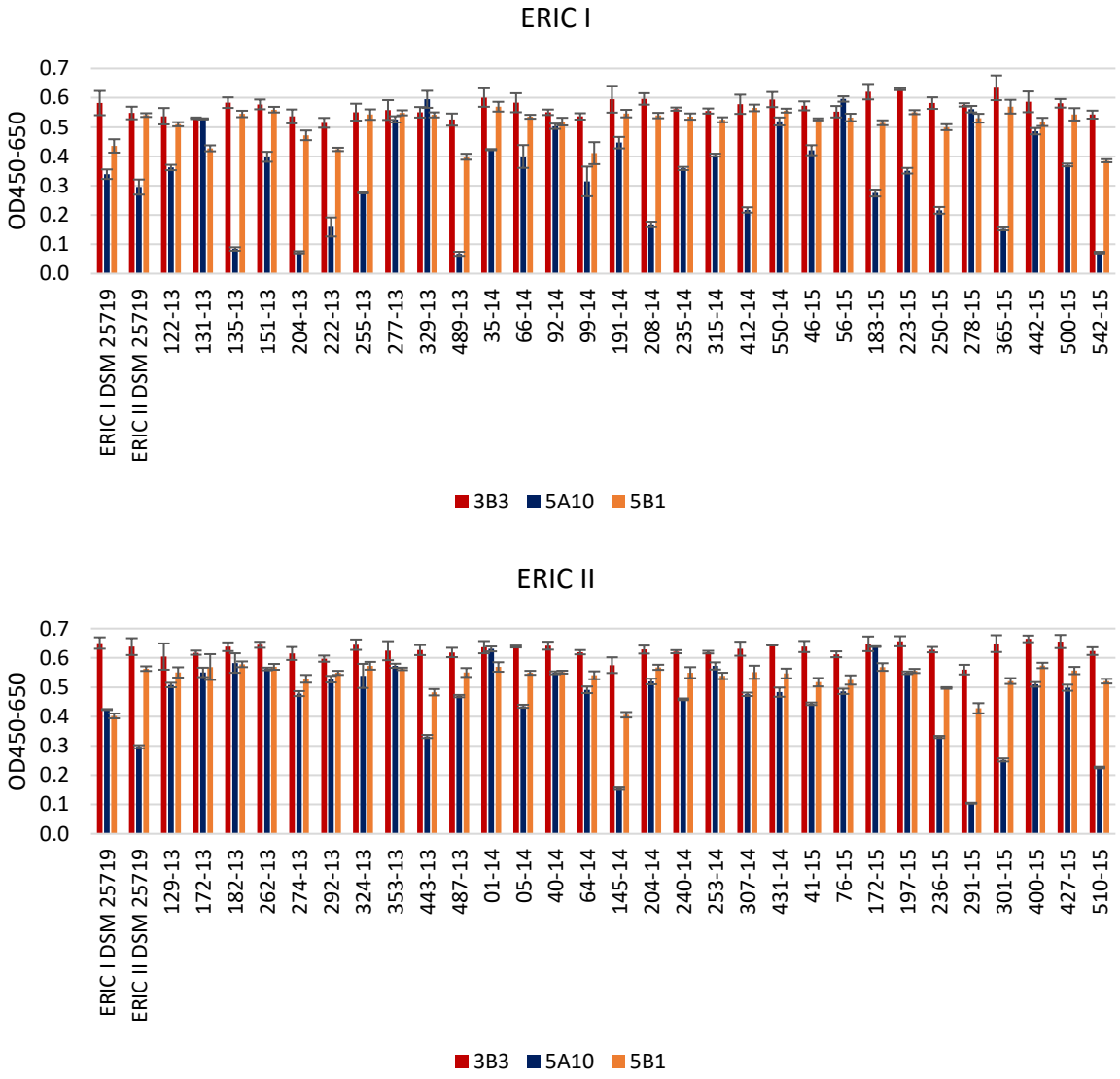

Figure 27 Indirect ELISA: strain detection anti-P. larvae mAbs

The indirect ELISA was performed with three anti-*P. larvae* mAbs (3B3 and 5B1: 5 µg/mL and 5A10: 25 µg/mL). Different ERIC I (30) and ERIC II (30) strains were tested to determine strain detection (x-axis). The y-axis depicts the difference of the measured OD values at 450 nm and 650 nm. The bars show the average of three technical replicates. The red bars are representing 3B3, blue bars are 5A10 and orange bars show reactivity of 5B1. The error bars represent the standard deviation of the three technical replicates.

For strain detection 30 field strains of the two main ERIC-genotypes were tested. The mAbs 3B3 and 5B1 show $OD_{450-650}$ signals ranging from 0.38 to 0.65 (Figure 27) and all of the tested strains are determined as positively detected strains (Figure 27). In contrast, the mAb 5A10 shows a high variance of $OD_{450-650}$ signal height ranging from 0.07 to 0.64, even though the mAb concentration used was higher than for the other anti-*P. larvae* mAbs (5A10: 50 µg/mL). Due to the low signal and high amount of mAb that was necessary for testing 5A10, the suitability of this mAb for LFD development is limited.

4.3.3 Anti-ERIC I monoclonal antibodies

After finding candidates for distinction between the two foulbrood causing agents, *M. plutonius* and *P. larvae*, the focus was on the distinction between the two ERIC-genotypes of *P. larvae*. Therefore, four ERIC I specific mAb candidates were purified and further tested.

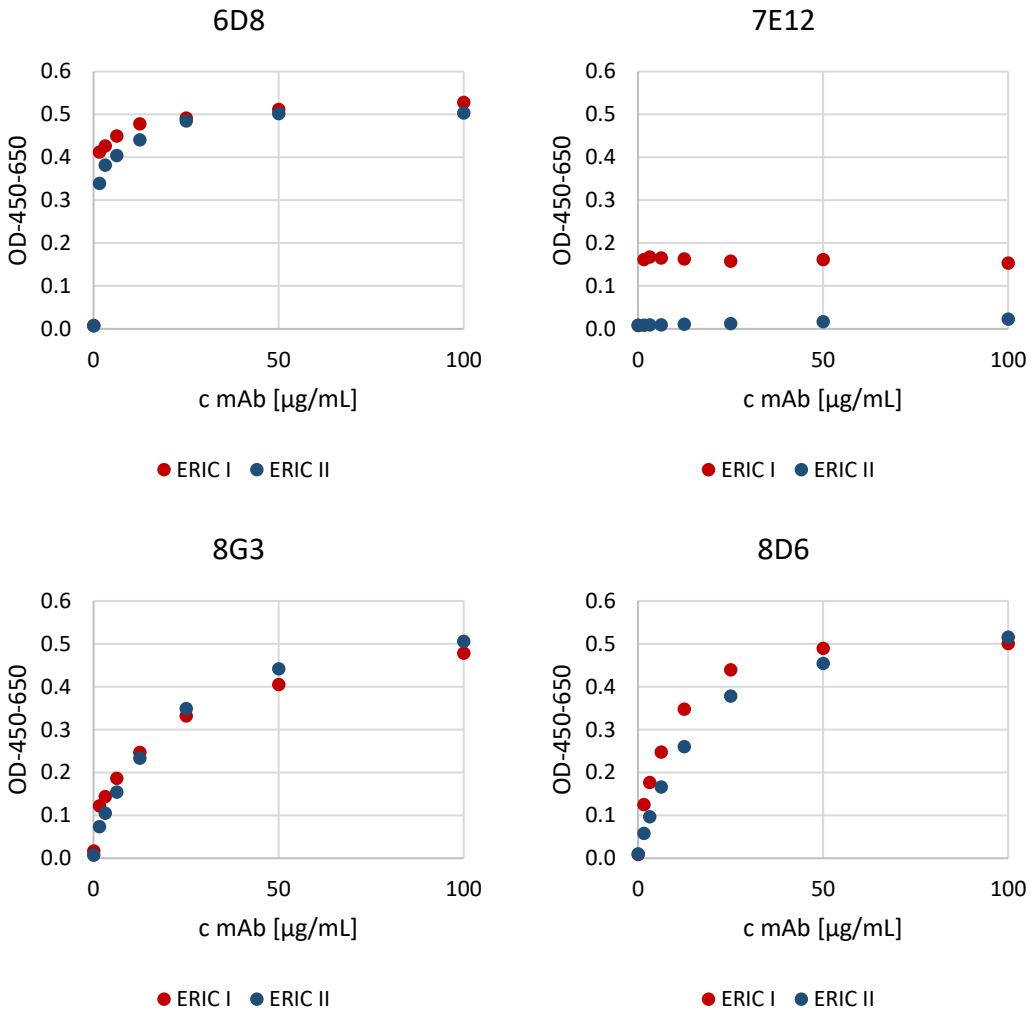

Figure 28 Indirect ELISA: dilution series anti-ERIC I mAbs
The optimal concentrations of the four mAbs (6D8, 7E12, 8G3 and 8D6) were determined by systematically testing different concentrations (c) in the range from 0 to 100 µg/mL (x-axis). The symbols represent three technical replicates. The red dots represent the positive control (ERIC I) and the blue dots represent the negative control (ERIC II).

The dilution series of anti-ERIC I mAbs already showed that three of the four mAbs are not ERIC I specific antibodies (Figure 28). The mAb 8G3 is the only produced rat antibody. The non-ERIC I specific mAbs were further tested against bee-associated bacteria to determine whether or not they were suitable for general *P. larvae* detection (Figure 29). The mAb 7E12 has an at least two times lower signal compared to the other anti-ERIC I mAbs. The produced mAbs were used with the optimal concentration, which was determined based on signal strength and consumption considerations (6D8: 10 µg/mL, 7E12: 5 µg/mL; 8D6: 25 µg/mL; 8G3: 10 µg/mL).

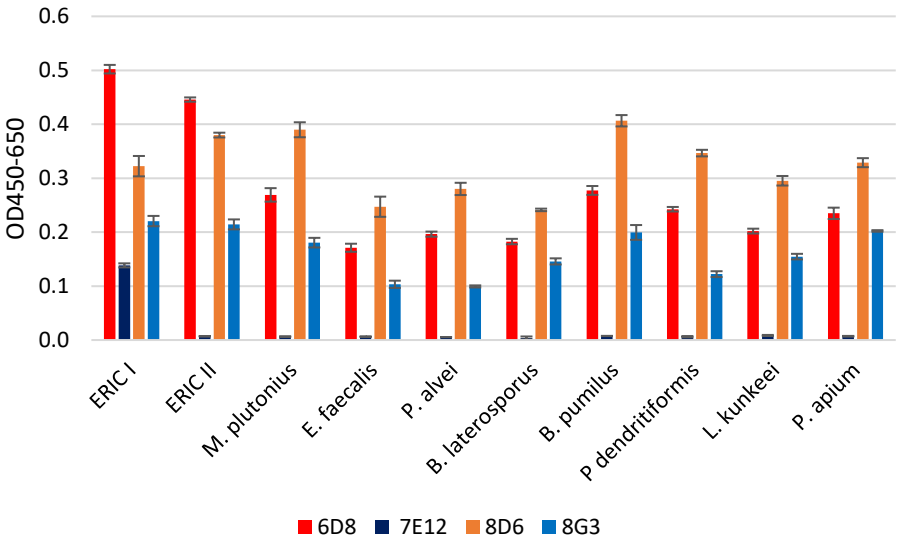

Figure 29 Indirect ELISA: cross reactivity anti-ERIC I mAbs

The indirect ELISA was performed with anti-ERIC I mAbs (6D8: 10 µg/mL, 7E12: 5 µg/mL; 8D6: 25 µg/mL; 8G3: 10 µg/mL). The mAbs were tested for cross reactivity against bee-associated bacteria (x-axis). The y-axis depicts the difference of the measured OD values at 450 nm and 650 nm. The bars show the average of three technical replicates. The red bars represent 6D8, dark blue bars are 7E12, orange bars are 8D6 and light blue bars show reactivity of 8G3. The error bars represent the standard deviation of the three technical replicates.

All the tested anti-ERIC I mAbs except of the mAb 7E12 showed cross reactivity against several bee-associated bacteria. The anti-ERIC I mAb (7E12) showed no cross reactivity with any of the tested bee-associated bacteria but it showed only a weak signal towards the ERIC I strain, with which it was immunized with (Figure 29). Furthermore, the mAb 7E12 was tested against different field strains to get information about the strain detection coverage of this mAb (Figure 30).

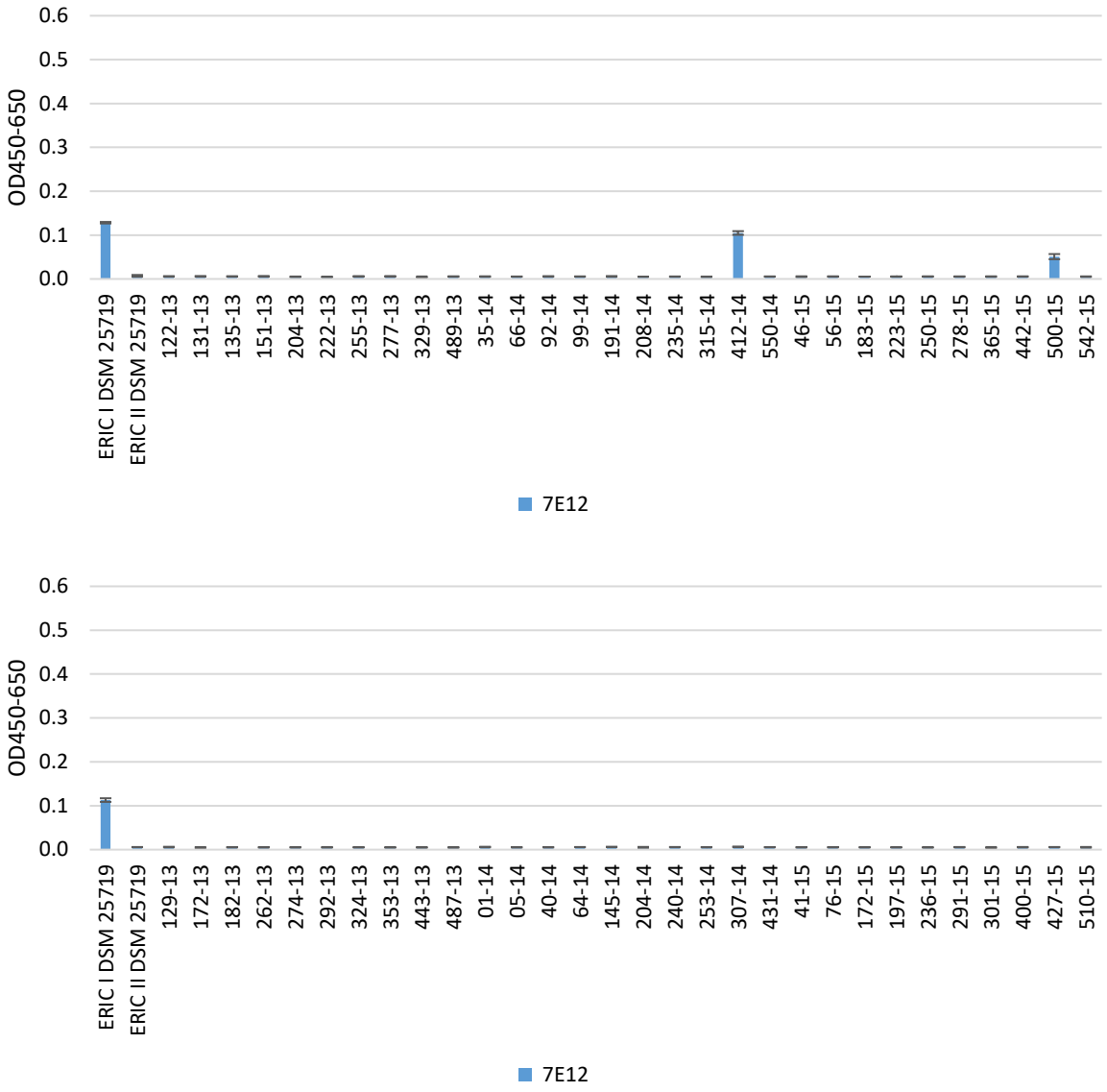

Figure 30 Indirect ELISA: strain detection of anti-ERIC I mAbs

The indirect ELISA was performed with one anti-ERIC I mAb (7E12: 5 µg/mL). Different ERIC I (30) and ERIC II (30) strains were tested to determine strain detection and genotype-specificity (x-axis). The y-axis depicts the difference of the measured OD values at 450 nm and 650 nm. The bars show the average of three technical replicates. The blue bars are representing the mAb 7E12. The error bars represent the standard deviation of the three technical replicates.

The anti-ERIC I mAb (7E12) showed no reactivity with the tested ERIC II field strains but it only reacted with two of the 30 tested ERIC I field strains and is therefore not suitable for application in the LFD (Figure 30). Within the found mAbs so far, there is no ERIC I specific mAb that is suitable for the application in a diagnostic sandwich ELISA or LFD.

4.3.4 Anti-ERIC II monoclonal antibodies

The genotype-specific mAbs are important to distinguish the ERIC-genotypes in the sandwich ELISA and the LFD. Therefore, four ERIC II specific mAb candidates were purified and further tested (Figure 31).

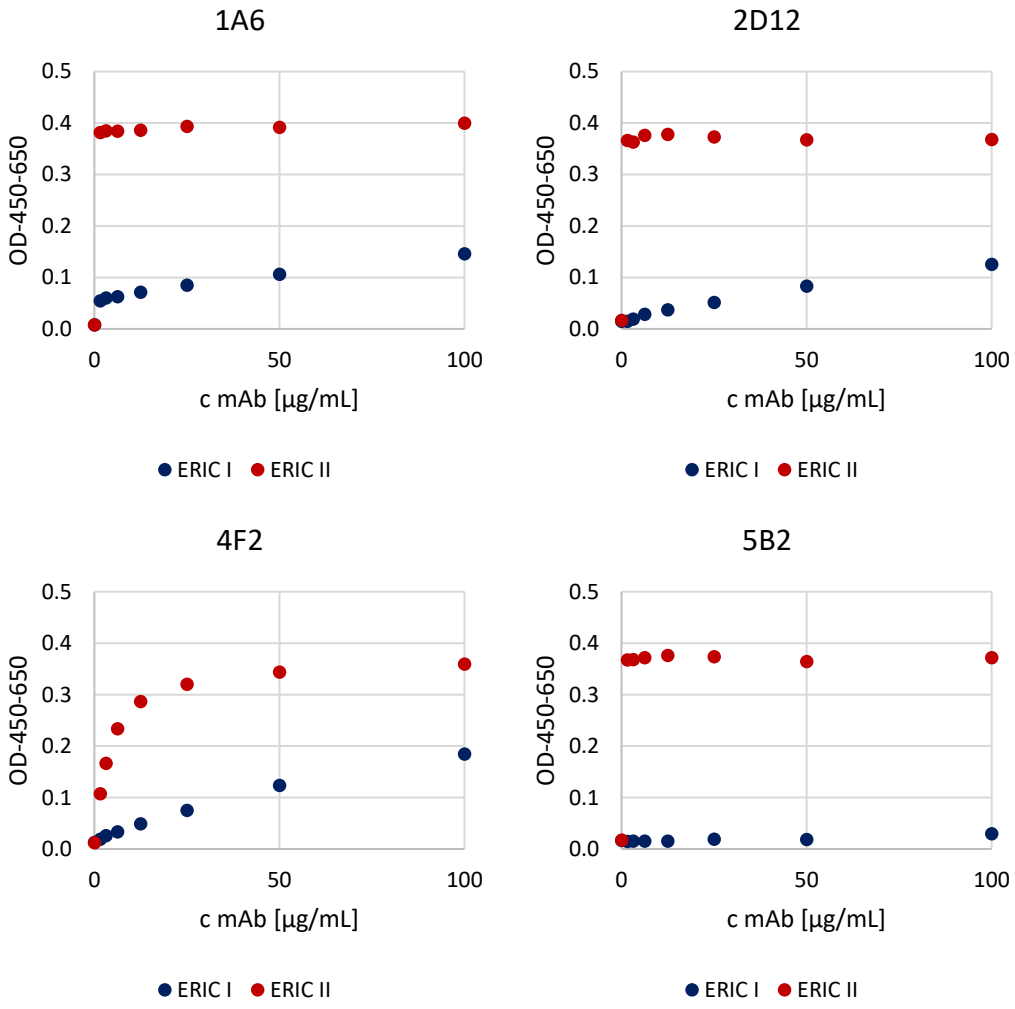

Figure 31 Indirect ELISA: dilution series of anti-ERIC II mAbs
The optimal concentrations of the four mAbs (1A6, 2D12, 4F2 and 5B2) were determined by systematically testing different concentrations (c) in the range from 0 to 100 µg/mL (x-axis). The symbols represent three technical replicates. The red dots represent the positive control (ERIC II) and the blue dots represent the negative control (ERIC I).

In order to determine the best working concentration between positive samples and negative samples the dilution series was performed with ERIC II for positive reaction and with ERIC I for negative control to verify specificity of the mAbs. All four tested mAbs have similar signal heights, when tested against ERIC II, with an $OD_{450-650}$ of ~0.4 (Figure 31). The mAbs 1A6, 2D12 and 4F2 show an increasing signal to ERIC I with increasing mAb concentration. In contrast, the signal of 5B2 against ERIC I is not increasing with mAb concentration. One of the four tested mAbs (4F2) has an IgG_3 isotype and shows a different signal height-to-concentration curve compared to the other tested mAbs (Figure 31). Considering the

signal strength and distinction between positive and negative samples the working concentration of 5 µg/mL was used for 1A6, 2D12 and 5B2, whereas for 4F2 25 µg/mL was used for further indirect ELISAs. All four mAbs were used for further investigations of their cross reactivity against bee-associated bacteria.

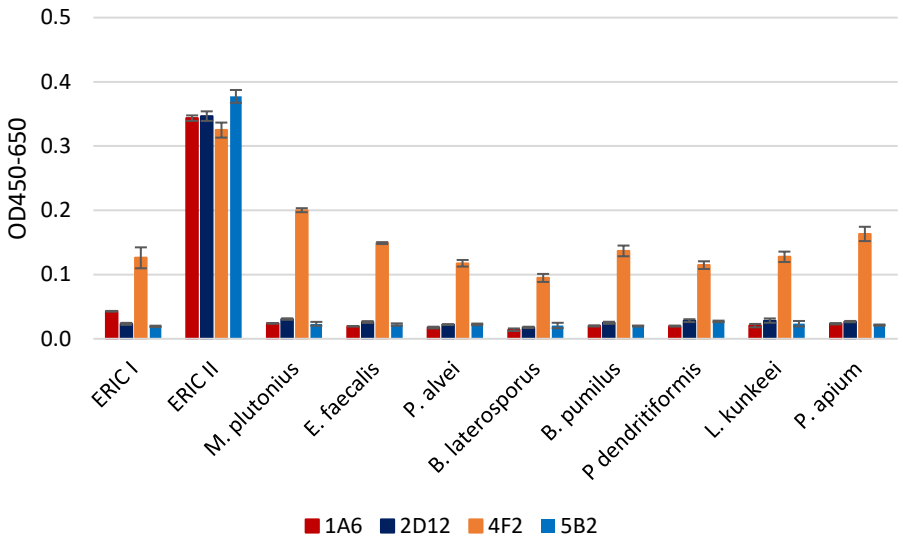

Figure 32 Indirect ELISA: cross reactivity of anti-ERIC II mAbs
The indirect ELISA was performed with four anti-ERIC II mAbs (1A6, 2D12 and 5B2: 5 µg/mL and 4F2: 25 µg/mL) The mAbs were tested for cross reactivity against bee-associated bacteria (x-axis). The y-axis depicts the difference of the measured OD values at 450 nm and 650 nm. The bars show the average of three technical replicates. The red bars are representing 1A6, dark blue bars are 2D12, orange bars are 4F2 and light blue bars show reactivity of 5B2. The error bars represent the standard deviation of the three technical replicates.

The cross reactivity of the suitable anti-ERIC II mAbs was tested against the bee-associated bacteria. All of the four tested mAbs showed similar signal strength against ERIC II. However, the mAb 4F2 showed cross reactivity with all of the tested bee-associated bacteria and also ERIC I. The mAb 1A6 showed a slight increased signal towards ERIC I but did not show any cross reactivity with bee-associated bacteria. Summarizing the results of the cross reactivity testing, the mAbs 2D12 and 5B2 are both ERIC II specific mAbs that could be used in combination in sandwich ELISA and LFD, whereas 1A6 seems to have a limited suitability. The mAb 4F2 was excluded for further analysis of strain detection coverage due to its high cross reactivity.

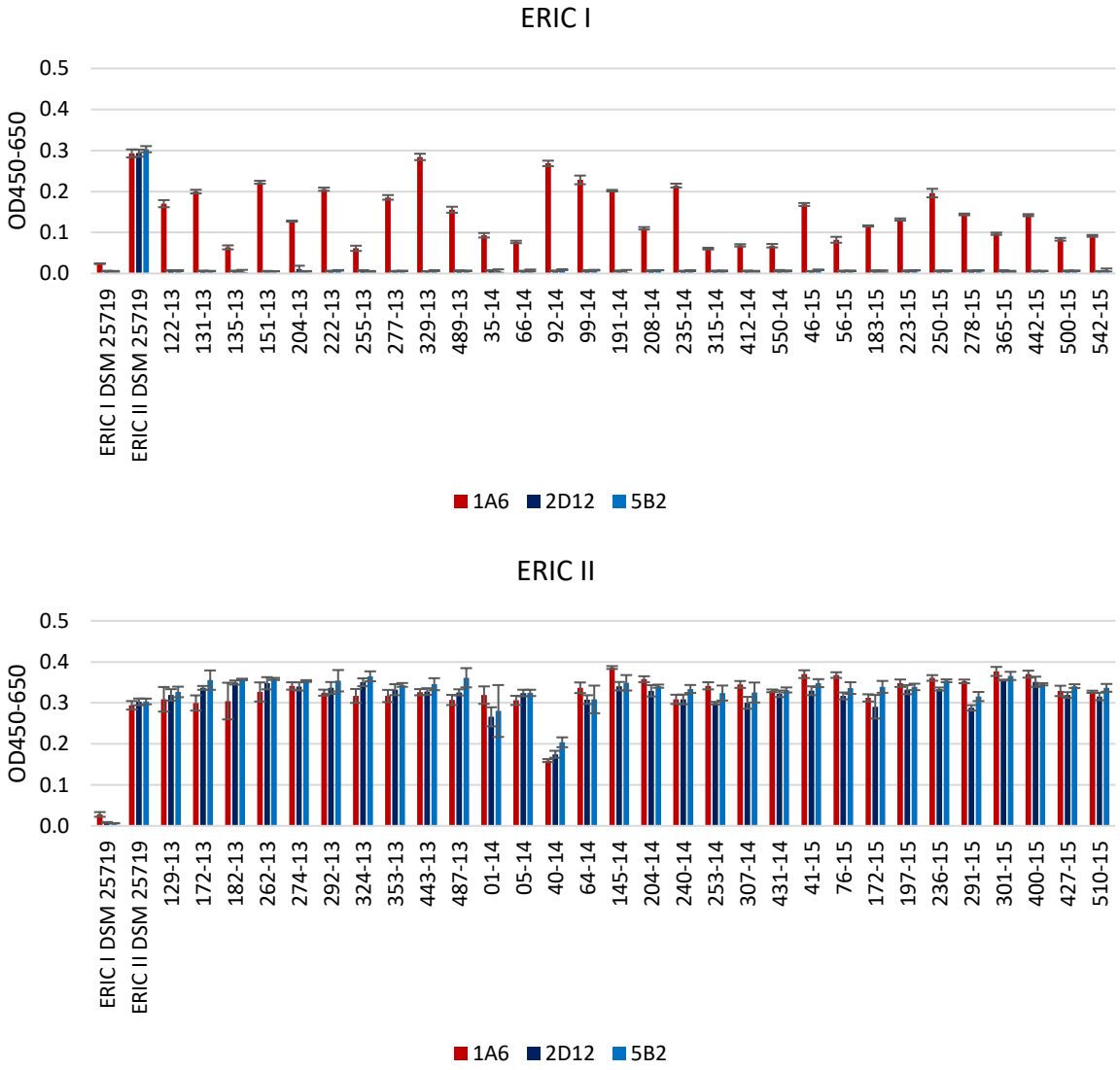

Figure 33 Indirect ELISA: strain detection of anti-ERIC II mAbs

The indirect ELISA was performed with three anti-ERIC II mAbs (1A6, 2D12 and 5B2: 5 µg/mL). Different ERIC I (30) and ERIC II (30) strains were tested to determine strain detection and genotype-specificity (x-axis). The y-axis depicts the difference of the measured OD values at 450 nm and 650 nm. The bars show the average of three technical replicates. The red bars are representing 1A6, dark blue bars are 2D12 and light blue bars show reactivity of 5B2. The error bars represent the standard deviation of the three technical replicates.

To investigate strain detection coverage, 30 field strains of the two ERIC-genotypes (ERIC I and ERIC II) were tested. The focus of this testing lies on the reliable distinction between the two genotypes and the detection of as many ERIC II strains as possible. The three tested mAbs show a relative similar signal strength against the different ERIC II field strains (Figure 33). Having a closer look on the ERIC I field strains, 2D12 and 5B2 are not showing any cross reactivity. In contrast, 1A6 reacts with several ERIC I genotyped field strains (61.3 %). These results support that 2D12 and 5B2 are more specific than 1A6 and are thus the favored mAb candidates for LFD, whereas 1A6 is not finally excluded due to the fact that just one highly specific antibody is already sufficient for LFD application in the field.

4.4 Antigen characterization

4.4.1 Western Blot

4.4.1.1 *Melissococcus plutonius* antigen

The sizes of the antigens detected by the four anti-*M. plutonius* mAbs were determined by WB using protein lysate of M. *plutonius*.

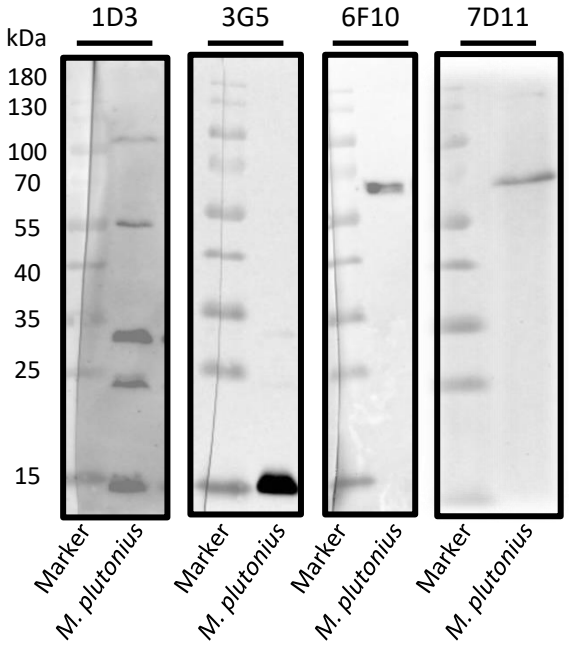

Figure 34 Western Blot of anti-M. plutonius mAbs
The anti-*M. plutonius* mAbs were used either as supernatant (1D3) or as purified mAb (3G5: 1:1000; 6F10: 1:1000; 7D11: 1:500 in 5 % milk-TBST) against *M. plutonius* protein lysate.

The IgM antibody 1D3 detected various antigens (five different ones) of different sizes, whereas the other mAbs only detected one antigen (Figure 34). The mAb 3G5 detected a small protein with a size of 15 kDa, while 6F10 and 7D11 each detected a protein with a size of 60 kDa. Thus, indicating that 6F10 and 7D11 potentially bind the same antigen and therefore might be suitable candidates for the application in sandwich approaches. In order to clarify whether or not 6F10 and 7D11 truly bind the same antigen, IP was performed with the two mAb candidates 6F10 and 7D11 (4.4.2) followed by mass spectrometry of the purified antigens.

4.4.1.2 *Paenibacillus larvae* antigen

The sizes of the antigens detected by the four anti-*P. larvae* mAbs were determined by WB using a protein lysate of *P. larvae*.

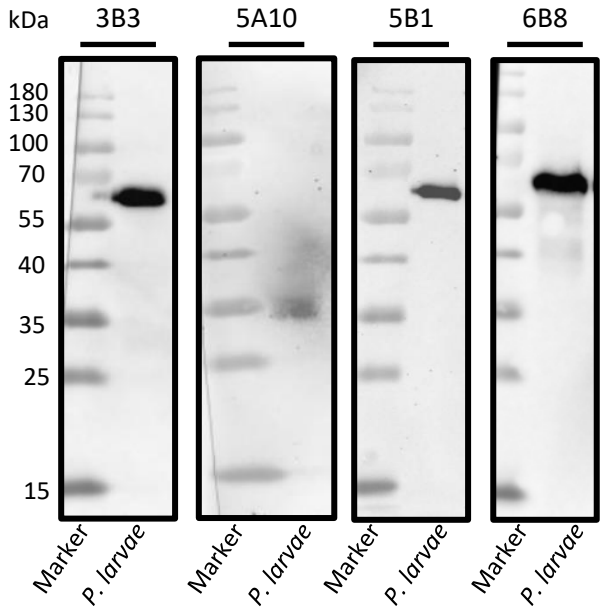

Figure 35 Western Blot of anti-P. larvae mAbs
The anti-*P. larvae* mAbs were used either as supernatant (6B8) or as purified mAb (3B3: 1:5000; 5A10: 1:2500; 5B1: 1:1000 in 5 % milk-TBST) against *P. larvae* protein lysate.

The four general anti-*P. larvae* mAbs detected at least two different antigens. 5A10 detected a 35 kDa protein, while 3B3, 5B1 and 6B8 (IgM) all bound a protein with the size of ~60 kDa (Figure 35). Including the results from the isotyping (4.3) and indirect ELISA (4.3.2), the mAbs 3B3 and 5B1 are potential candidates for LFD. After purification of the antigens using IP, the antigens were identified using mass spectrometry.

4.4.1.3 ERIC I antigen

The sizes of the antigens detected by the four anti-ERIC I mAbs were determined by WB using a protein lysate of *P. larvae* ERIC I (DSM 25719).

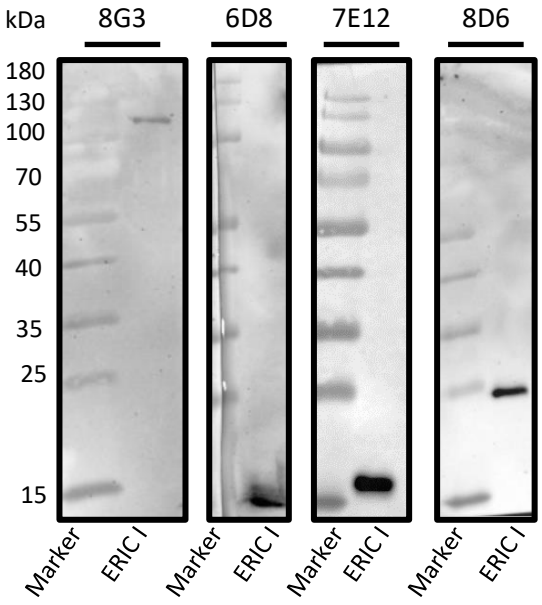

Figure 36 Western Blot of anti-ERIC I mAbs
The anti-ERIC I mAbs were used as purified mAbs (8G3: 1:1000; 6D8: 1:1000; 7E12: 1:1000; 8D6: 1:500 in 5 % milk-TBST) against *P. larvae* ERIC I protein lysate.

All anti-ERIC I mAbs detected the native and the denatured form of their antigens. Three different sized proteins are detected by the four tested anti-ERIC I mAbs. The rat mAb 8G3 detected an ~100 kDa sized protein, while 6D8 and 7E12 detected small ~15 kDa proteins and 8D6 detected ~25 kDa sized antigen.

Comparing these results with the WBs for verification of the immune reaction (4.2.1.2), one can see that antigens with ~15 kDa were also detected in the rabbit serum. The ~20-25 kDa antigens were visible for the mouse (Figure 18) and the rat anti-ERIC I sera (Figure 19). The 100 kDa antigen, which was detected by the mAb 8G3 was not visible as specific band in the WB, when tested with the rat anti- ERIC I serum.

4.4.1.4 ERIC II antigen

The sizes of the antigens detected by the four anti-ERIC II mAbs were determined by WB using a protein lysate of *P. larvae* ERIC II (DSM 25430).

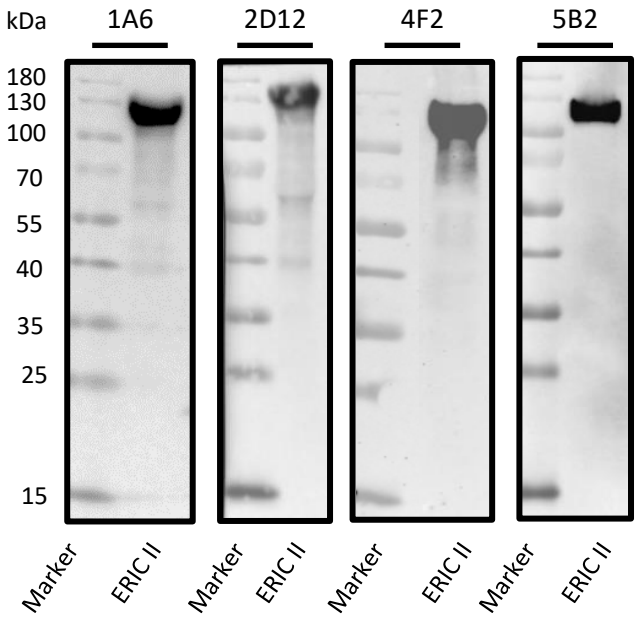

Figure 37 Western Blot of anti-ERIC II mAbs
The anti-ERIC II mAbs were used as purified mAbs (1A6: 1:5000; 2D12: 1:5000; 4F2: 1:2500; 5B2: 1:500 in 5 % milk-TBST) against *P. larvae* ERIC II protein lysate.

All of the four tested anti-ERIC II mAbs also bound the denatured antigen. The antigens bound by these four mAbs all showed roughly the same size of 130 kDa, but the intensity of the occurring bands differed between the different mAbs (Figure 37). The 130 kDa ERIC II-specific antigen was also visible in all anti-ERIC II animal sera (Figure 17; Figure 18; Figure 19). The antigen identification via mass spectrometry was performed for one mAb (2D12).

4.4.2 Identification of antigens

For identification of the specific antigens, IP was performed to purify the antigens with the help of the produced mAbs. The successful antigen purification was verified by SDS-PAGE (Figure 38) and the purified antigens were analysed with mass spectrometry.

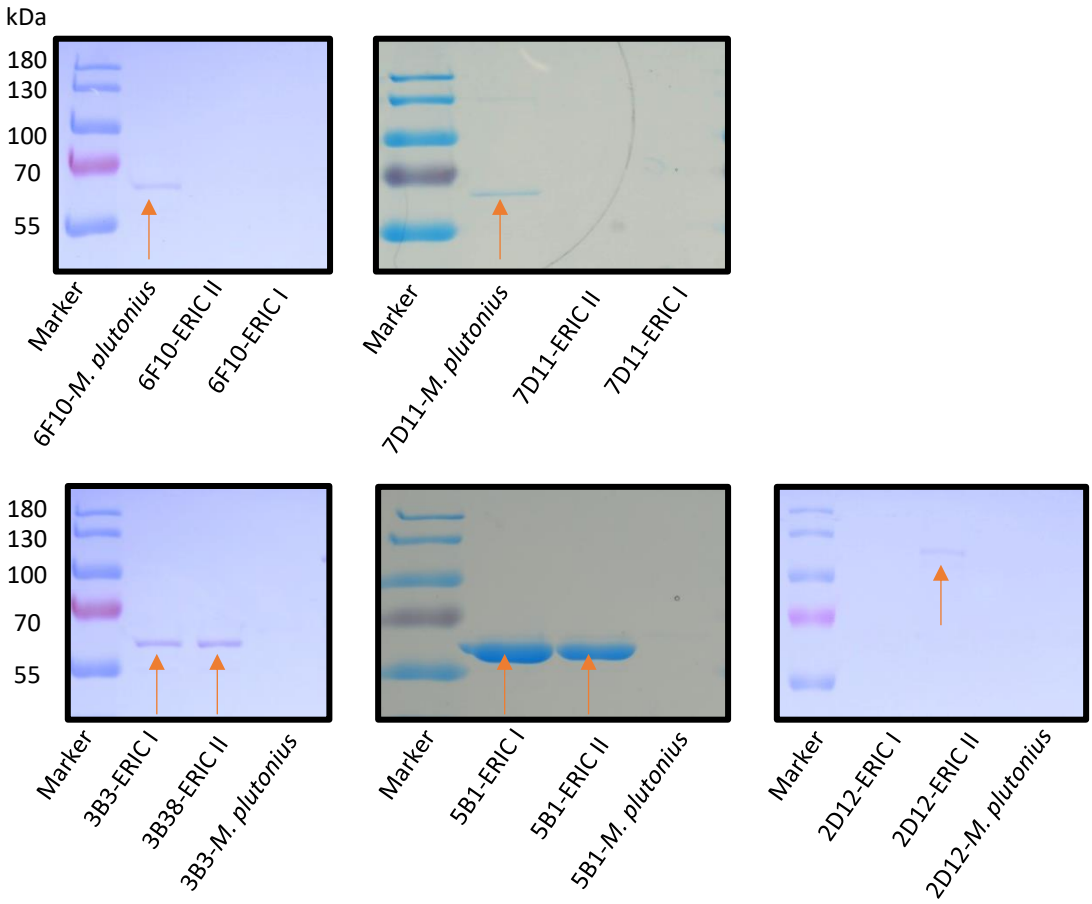

Figure 38 SDS-PAGE after immunoprecipitation

IP was performed as described in 3.4.2. The success of the IP was verified by SDS-PAGE followed by Coomassie staining. The arrows indicate the positively detected protein bands after successful IP reaction. The upper gel pictures show the IP results of the two anti-*M. plutonius* mAb candidates (6F10 and 7D11) detecting a ~60 kDa antigen. The lower gels show the IP results of the two anti-*P. larvae* mAb candidates (3B3 and 5B1) detecting ~60 kDa antigen. The lower gel on the right shows the IP result of one of the anti-ERIC II (2D12) mAb candidates detecting a ~130 kDa antigen.

The SDS-PAGE results showed the success of the IP with the different specific mAbs (Figure 38). All IPs resulted in clear single bands. This also verified the specificity of the mAbs. The IPs with anti-*M. plutonius* mAbs and the anti-ERIC II mAb resulted in relative weak bands compared to the IPs conducted with the anti-*P. larvae* mAbs (Figure 38). The stronger bands indicated a better binding of the antibody to the antigen. The protein bands were cut out and prepared for mass spectrometry to identify the antigens (Table 38).

Table 38 Identification of antigens by mass spectrometry

mAb used for IP	Organism of antigen	Antigen (kDa)	Antigen	Gene ID
6F10	*M. plutonius*	60	chaperonin	BBD17195
7D11	*M. plutonius*	60	chaperonin	BBD17195
3B3	*P. larvae*	60	chaperonin	WP_023482503
5B1	*P. larvae*	60	chaperonin	WP_023482503
2D12	*P. larvae*	130	S-layer	AHD03965

The anti-*M. plutonius* mAbs 6F10 and 7D11 both bind the same chaperonin also known as heat shock protein (HSP60) (Lund, 2009). The same protein type is bound by the *anti-P. larvae* mAbs 3B3 and 5B1. These findings showed that the species-specific mAb combinations are suitable candidates for application in sandwich ELISA and LFD for *M. plutonius* or *P. larvae* detection respectively. Chaperonins are commonly used as housekeeping genes and play an important role in protein folding (Thirumalai & Lorimer, 2001; Lin *et al.*, 2008; Lund, 2009).

The analysis of the ERIC II specific antigen bound by 2D12 showed that the antigen with ~130 kDa size is a Surface-layer (S-layer) protein. In bacteria, S-layers are responsible for protection against harmful environmental factors, adhesion to surfaces, evading of the host immune system and can serve as carriers for virulence factors (Thompson, 2002; Ryan *et al.*, 2011; Settem *et al.*, 2013; Gerbino *et al.*, 2015).

4.4.3 Recombinant antigen expression and verification of antigen identity

For the verification of the antigen identity, the DNA-sequences of the target antigens were cloned into a vector for recombinant protein expression. The recombinantly produced proteins were tested with the generated mAbs. After the successful cloning of the gene of interest into a vector using restriction enzymes (Table 31), recombinant protein expression was induced. The induction of protein expression was performed with IPTG addition and was confirmed by SDS-PAGE (Figure 39) and WB (Figure 40).

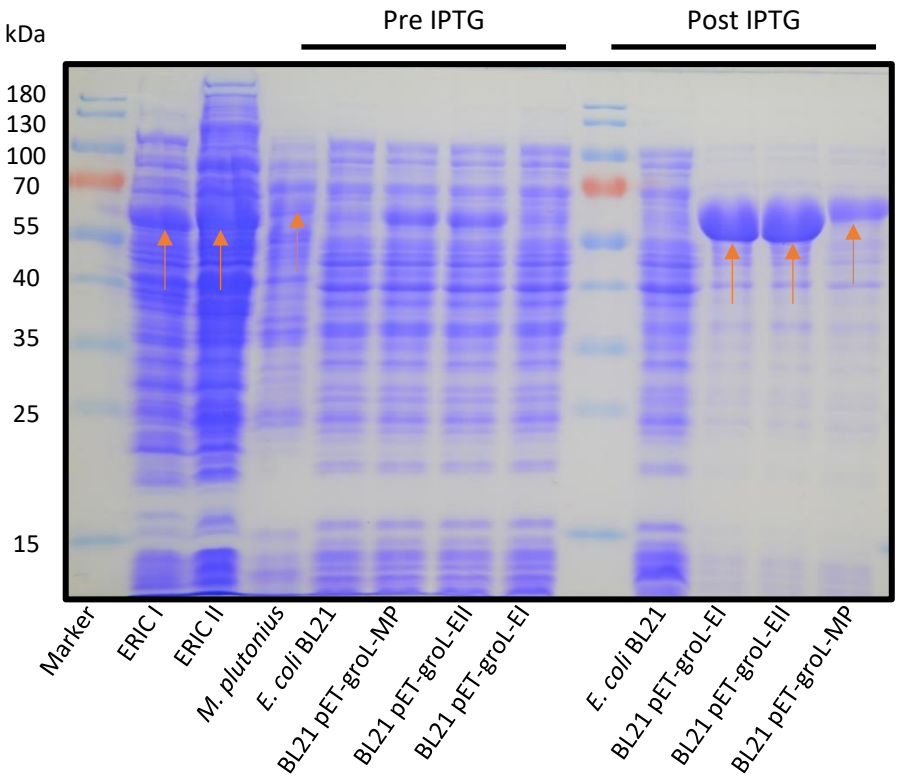

Figure 39 SDS-PAGE for verification of chaperonin expression

The SDS-PAGE followed by Coomassie staining was performed using bacteria lysates from *P. larvae, M. plutonius* and *E. coli.* The *E. coli* lysates were used before and after the induction of the recombinant protein expression. Protein expression was induced after verification of correct plasmid DNA via sequence analysis. IPTG was applied as described in 3.4.3. The SDS-PAGE shows genetically modified *E. coli* before (Pre IPTG) and after induction of protein expression (Post IPTG). The orange arrows mark bands representing the chaperonin of *P. larvae* and the black arrows represent the chaperonins of *M. plutonius*.

The overexpression of the *P. larvae* chaperonin is visible in Figure 39 and showed strong bands at 60 kDa that did not occur in *E. coli* BL21 without the vector and were weaker before induction of recombinant protein expression. For the *M. plutonius* chaperonin also an overexpression of protein was observed. For verification of the mAb recognition of the recombinant chaperonins of the different bacteria species a WB was performed (Figure 40).

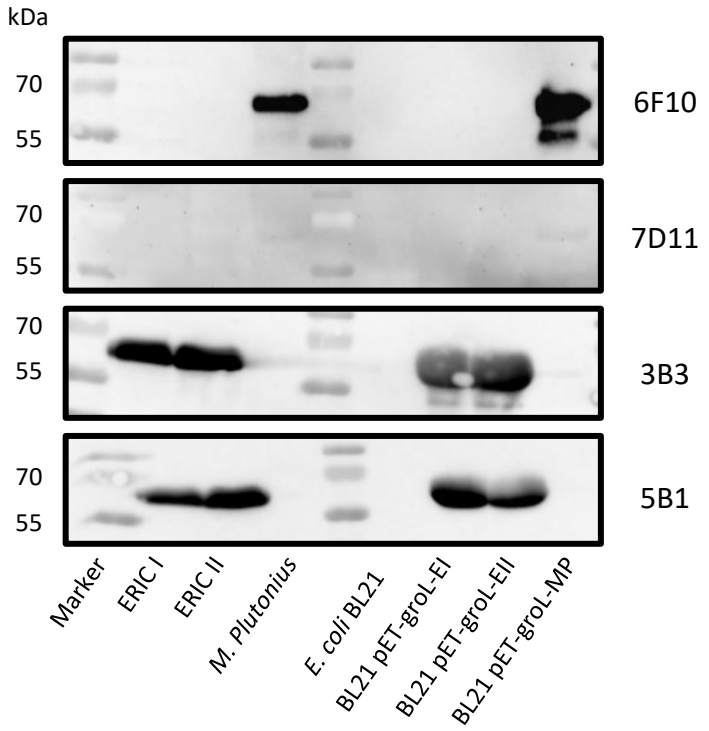

Figure 40 WB: verification of chaperonin expression and detection by mAbs
The identities of the antigens determine by mass spectrometry was verified with WB analysis using the overexpressed recombinant chaperonins and the produced mAbs. The upper two boxes show *anti-M. plutonius* mAbs (6F10, 7D11) applied to samples containing recombinant chaperonins. The lower two boxes show *anti-P. larvae* mAbs (3B3 and 5B1) reacting with recombinant *P. larvae* chaperonins.

The anti-*M. plutonius* mAb 6F10 bound to the chaperonin in *M. plutonius* and the recombinantly expressed *M. plutonius* chaperonin (Figure 40). However, the mAb 6F10 did not detect the *P. larvae* chaperonin expressed by *P. larvae* nor the recombinantly expressed *P. larvae* chaperonin by *E. coli*. The anti-*M. plutonius* mAb 7D11 showed only weak binding to *M. plutonius* and the recombinantly expressed *M. plutonius* chaperonin. No reactivity of 7D11 with *P. larvae* chaperonin was detected. The anti-*P. larvae* mAbs 3B3 and 5B1 bound to the ERIC I, ERIC II and the recombinantly expressed *P. larvae* chaperonins. Both anti-*P. larvae* mAbs showed no binding of *M. plutonius* chaperonin (Figure 40). These findings support the indirect ELISA results that the species-specific mAbs do not have any cross reactivity with the other foulbrood causing bacteria.

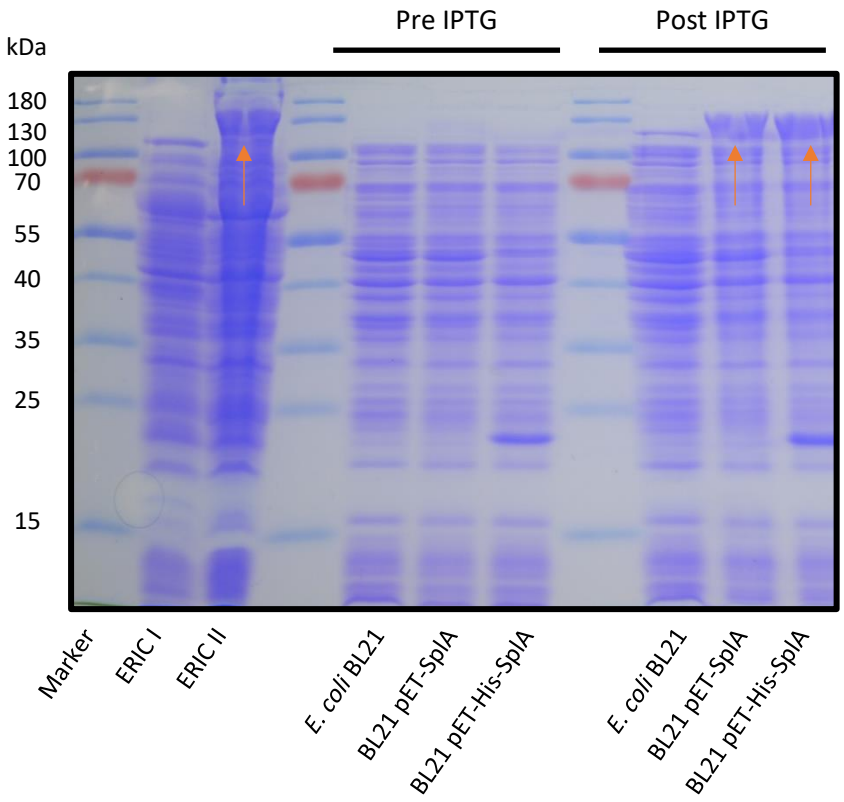

Figure 41 SDS-PAGE for verification of S-layer expression

The SDS-PAGE followed by Coomassie staining was performed using bacteria lysates from *P. larvae* and *E. coli*. Protein expression was induced after verification of the correct plasmid DNA via sequence analysis. IPTG was applied as described in 3.4.3. SDS-PAGE shows genetically modified *E. coli* before induction of protein expression (Pre IPTG) and after induction of protein expression (Post IPTG). The orange arrows mark the band that represents the S-layer protein.

For the ERIC II specific antigen, the S-layer protein was cloned into a vector, without any tags and with a 6x His-tag at the N-terminus of the recombinant protein. The overexpression of the protein was verified by SDS-PAGE (Figure 41) followed by the verification of the mAb detection in the WB (Figure 42). The *E. coli* bacteria containing the plasmid with S-layer gene showed a prominent band at 130 kDa that was not present in *E. coli* without the vector (Figure 41).

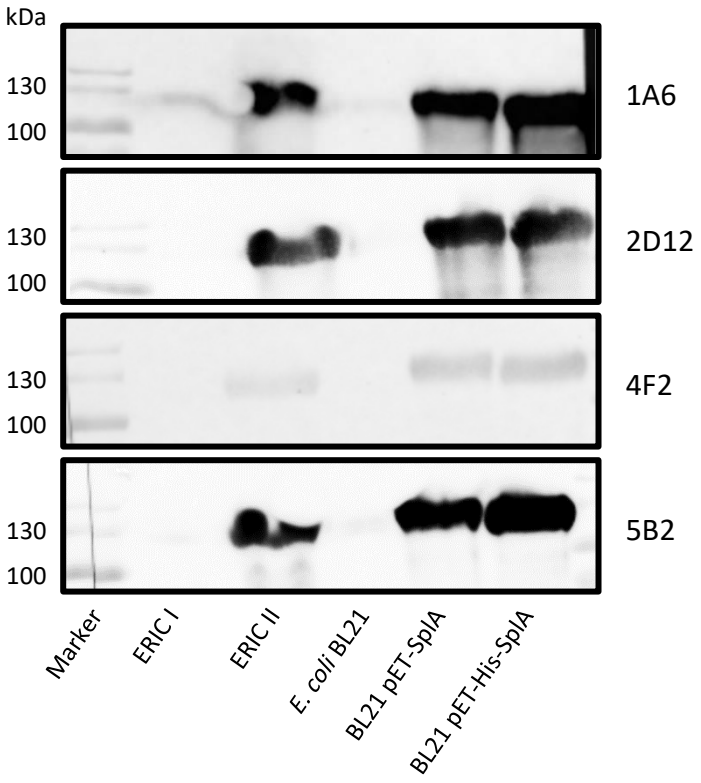

Figure 42 WB: verification of S-layer expression and detection by mAbs
The identities of the antigens determine by mass spectrometry was verified with WB analysis using the overexpressed recombinant chaperonins and the produced mAbs. For verification that all of the four anti-ERIC II mAbs detect the S-layer protein, all anti-ERIC II mAbs (1A6, 2D12, 4F2 and 5B2) were used in the WB. The overexpressed recombinant S-layer in *E. coli* was produced with and without a His-tag.

For verification of the mAb binding, the WB was performed with all four anti-ERIC II mAbs because all of the four mAbs detected a 130 kDa antigen (Figure 37). All of the four mAbs also detected the recombinant produced S-layer protein (Figure 42). The 4F2 mAb showed a weaker band than the other mAbs. Overall, the identity of the antigens was verified and it was shown that all mAb combinations suggested after the indirect ELISA testing were suitable candidates for the sandwich approaches (4.3.4).

4.4.3.1 IMAC of the recombinant His-S-layer

Immobilized metal affinity chromatography was performed with the recombinant His-S-layer protein to purify the protein (3.4.3). The success of the IMAC was verified with SDS-PAGE followed by Coomassie staining (Figure 43).

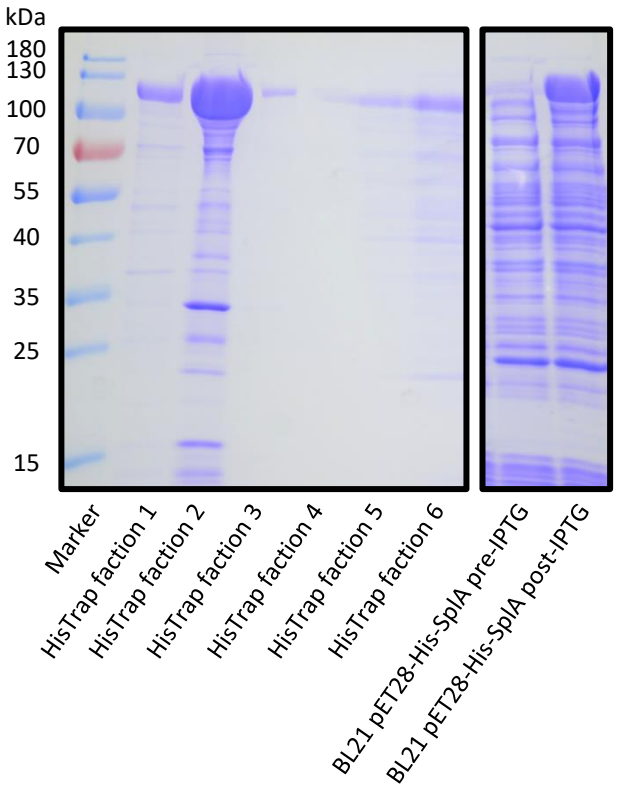

Figure 43 SDS-PAGE of IMAC fractions of recombinant His-S-layer

SDS-PAGE for verification of IMAC purification success of recombinant His-S-layer. Bands of IMAC fractions are compared to protein bands occurring in whole bacteria lysate of transformed *E. coli* with His-S-layer plasmid before and after induction of protein expression.

The SDS-PAGE showed the different elution fractions of IMAC in comparison to whole bacteria lysates before and after induction of recombinant protein expression. The bacteria lysates showed additional bands besides the 130 kDa band of the S-layer protein (Figure 43). The strongest band in the IMAC fractions (HisTrap fractions=) were visible in the second IMAC fraction followed by fraction 1 and 3. In the IMAC fraction 1 and 2 additional smaller protein bands could be observed. To test if the remaining bands were caused by small parts of recombinant His-S-layer protein or by impurities a WB analysis was performed (Figure 44).

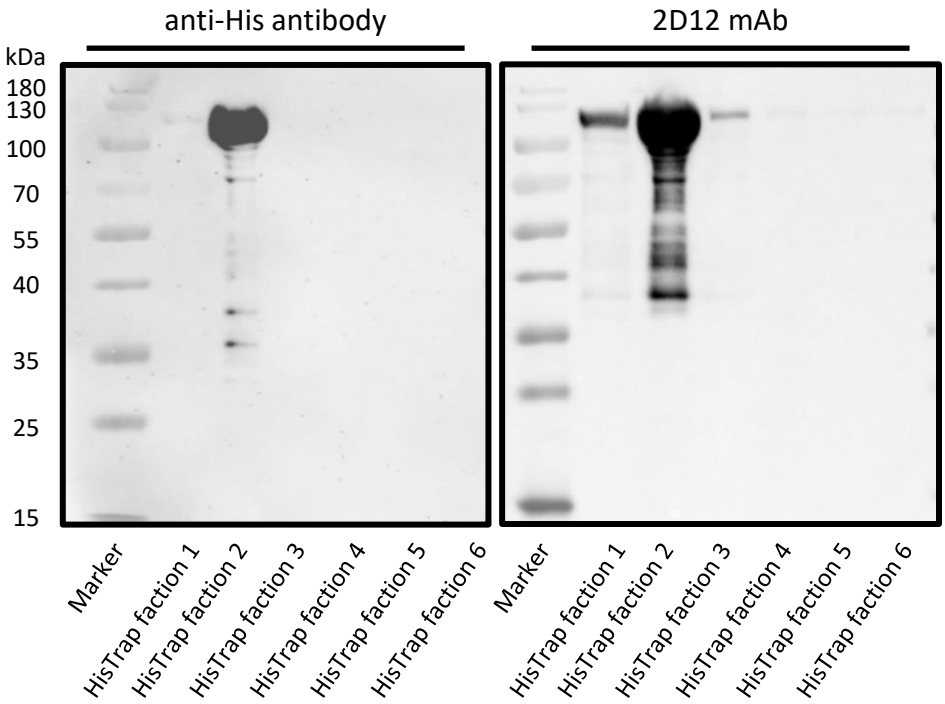

Figure 44 WB of IMAC fractions of recombinant His-S-layer
Identification of the small bands that occurred in SDS-PAGE (Figure 43) using two antibodies in the WB. The anti-His antibody (1:3000 in 5 % milk-TBST) showed that small bands have poly histidine (left site) that is well in line with the bands occurring when anti-ERIC II mAb (2D12 1:500 in 5 % milk-TBST) was applied to IMAC fractions (right site).

The WB was performed with a commercially available antibody against His-Tag and the anti-ERIC II mAb 2D12. Both applied antibodies also bound the smaller bands, indicating that the smaller bands were partial S-layer proteins that were either not expressed completely or degraded during the purification process. The WB signals were mainly occurring for the IMAC fraction 2 followed by fraction 1 and 3 for the anti-ERIC II mAb 2D12. The purified S-layer protein of fraction 2 was send to the project partner Senova for ERIC II ELISA optimization.

4.4.4 Target antigens in the atypical *P. larvae* strains

The presence of the target antigens in the atypical *P. larvae* strains was investigated using the produced anti-*P. larvae* and anti-ERIC II mAbs in the indirect ELISA and WB (Figure 45 and Figure 46).

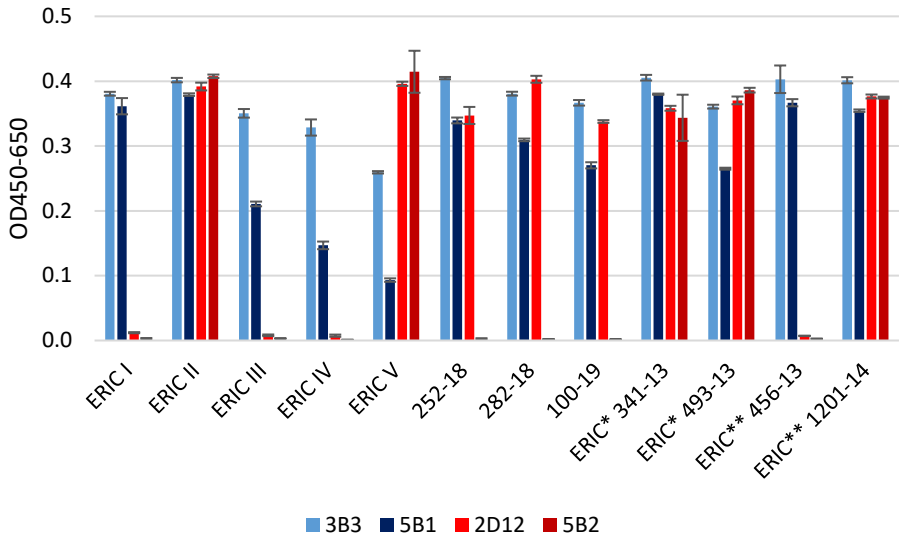

Figure 45 Indirect ELISA for characterization of atypical P. larvae strains

The indirect ELISA was performed using different representatives of the ERIC-genotypes of *P. larvae.* Bacteria were immobilized on ELISA plates (x-axis). The anti-*P. larvae* mAbs (light blue: 3B3 and dark blue: 5B1) and the anti-ERIC II mAbs (light red: 2D12 and dark red: 5B2) were applied for detection of the different *P. larvae* strains. The y-axis depicts the difference of the measured OD values at 450 nm and 650 nm. The bars represent the average of three technical replicates and the error bars show the standard deviation.

The indirect ELISA was performed to investigate whether the anti-*P. larvae* mAbs would confirm the identity of the atypical strains as *P. larvae* (Figure 45). All of the tested strains were detected by the two anti-*P. larvae* mAbs 3B3 and 5B1, confirming their identity as *P. larvae*. Interesting differences were observed when the two anti-ERIC II mAbs (2D12 and 5B2) were tested against the different genotypes and the atypical strains from Latin America. Both anti-ERIC II mAbs detect the reference strain of ERIC II as well ERIC V. The two strains that belong to ERIC * (341-13 and 493-13) and one of the ERIC ** strains (1201-14) were also detected by the anti-ERIC II mAbs. As indicated by the SDS-PAGE analysis (Figure 13), the ERIC ** strain 456-13 did not show any signal in the indirect ELISA. The atypical strains from Latin America were only detected by the mAb 2D12 but not by 5B2. This observation indicates that the S-layer might be differently organized in the atypical Latin American strains compared to the ones of the ERIC II and ERIC V strains.

In order to find out more about the differences of the S-layer proteins in the atypical strains, a WB analysis was performed with the produced anti-ERIC II mAbs (1A6, 2D12 and 5B2).

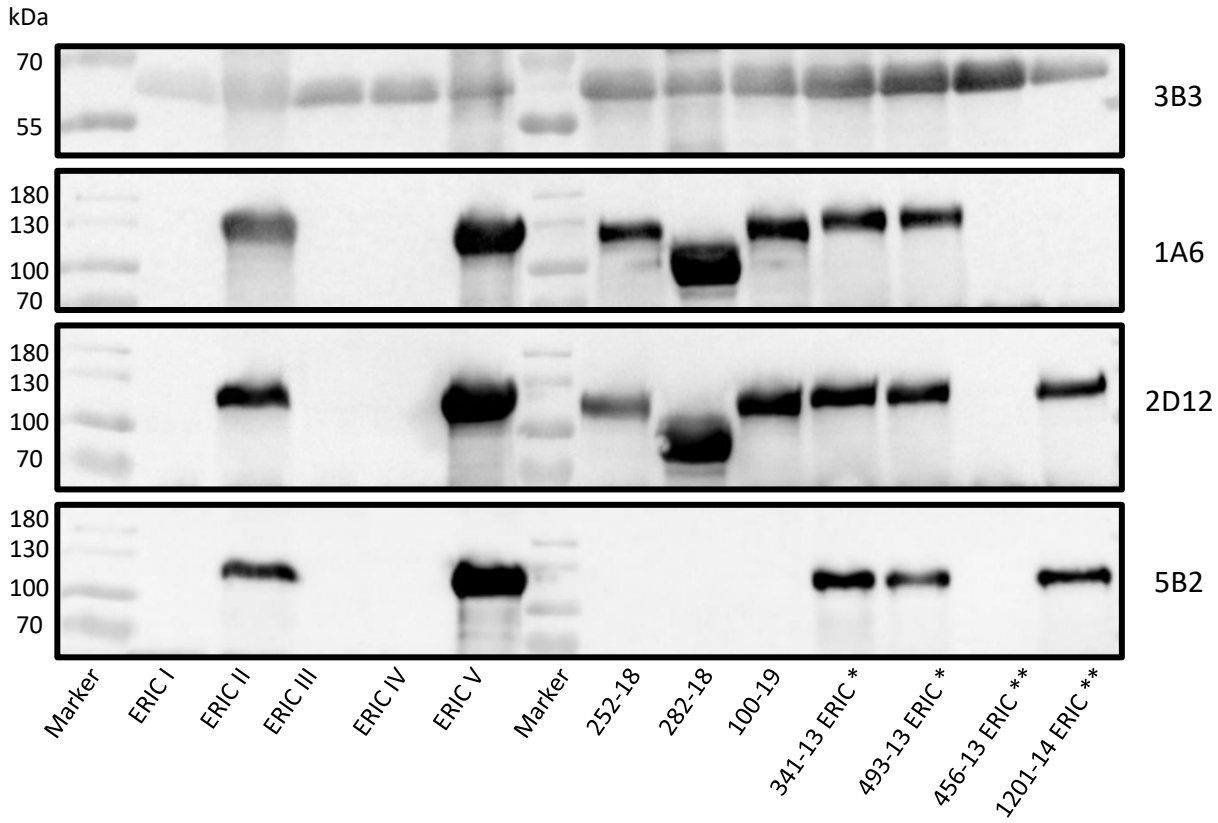

Figure 46 WB: atypical P. larvae strains analysed with anti-ERIC II mAbs
The protein lysates of the strains belonging to the different ERIC-genotypes and the atypical Latin American genotypes (252-18; 282-19 and 100-19) were tested with the three anti-ERIC II mAbs (1A6, 2D12, 5B2) and the anti-*P. larvae* mAb 3B3, which was the loading control of the protein lysates.

The analysis with the anti-*P. larvae* mAb confirmed the existence of *P. larvae* chaperonin in all tested strains. The WB analysis unravelled that ERIC I, III and IV and the ERIC ** strain 456-13 do not have a band that is recognized by the anti-ERIC II mAbs at 130 kDa, whereas ERIC II, ERIC V and ERIC * showed a band at 130 kDa, which was detected by all of the used anti-ERIC II mAbs (Figure 46).

The mAb 2D12 bound to the ERIC II specific antigen in all of the atypical strains from Latin America, as it was the case in the indirect ELISA (Figure 45). Interestingly the mAb 1A6 did not detect the S-layer protein of the strain 1201-14, which belonged to ERIC **. However, 2D12 and 5B2 detected the S-layer protein of the strain 1201-14. The mAb 5B2 did not bind the S-layer from the Latin American strains (252-18, 282-18 and 100-19) while 1A6 and 2D12 do.

Summarizing, the presence of the *P. larvae* specific antigen could be verified in all tested atypical strains using the generated anti-*P. larvae* mAbs. All of the ERIC *, ERIC ** and the Latin American atypical strains, except for the strain 456-13, express a protein that was detected by the anti-ERIC II mAbs.

To further investigate the relations of the different *P. larvae* strains, the groEL gene of each strain was either extracted from the NCBI database (ERIC I to V) or sequenced after PCR using the DNA of the ERIC *, ERIC ** and the atypical Latin American strains. The genetic distances were analysed and a phylogenetic tree was calculated using geneious (Figure 47). Interestingly, the ERIC-genotypes I, II and V clustered with the strains belonging to ERIC * and ERIC **. The ERIC II strain (DSM 25430) showed sequence identity of 100 % when compared to the two ERIC * and one ERIC ** strain (1201-14). The other ERIC ** strain (456-13) showed 100 % sequence identity with ERIC V. The strains of ERIC III and ERIC IV showed more similarities with the atypical Latin American strains (252-18; 282-18; 100-19) than the other strains, which are belonging to the genotypes ERIC I, II and V (Figure 47).

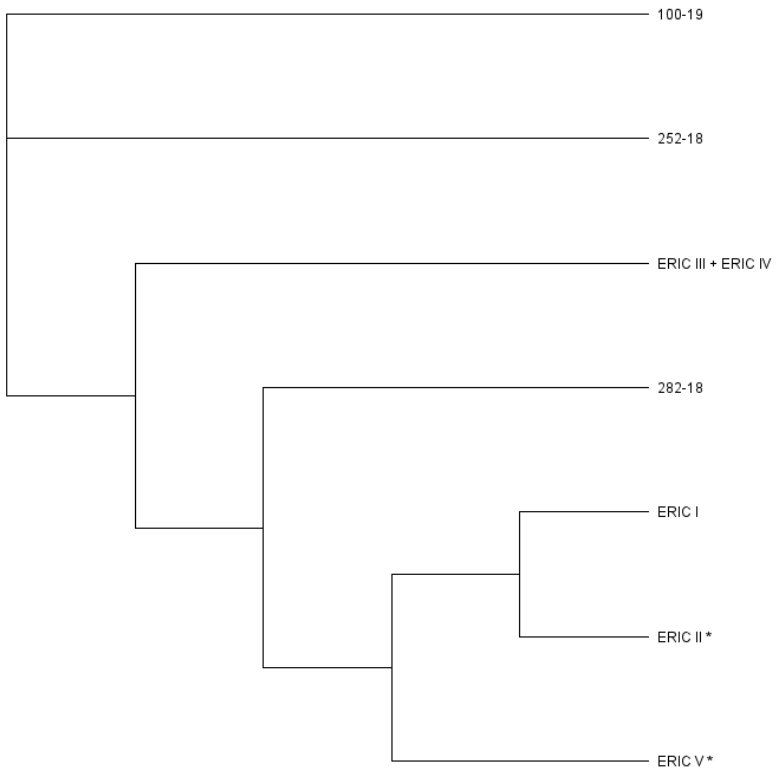

Figure 47 Phylogeny of P. larvae strains
Sequences of the groEL gene of the representatives of ERIC I to V were extracted from the NCBI database. The groEL gene of the atypical strains was sequenced after PCR was performed, just like it was done for the confirmation of the genes after cloning (3.4.3.3). Phylogeny is depicted by the neighbour-joining method. For this purpose, pairwise genetic distances were calculated using the Tamura-Nei genetic distance model. For building the phylogenetic tree, the program geneious was used. ERIC II* represents sequences that have 100 % identity with ERIC II including the atypical strains belonging to ERIC * and one ERIC ** strain (341-13, 493-13 and 1201-14). ERIC V* represents sequence of ERIC V and the ERIC ** sequence of 456-13 that showed 100 % DNA sequence identity.

The nucleotide sequences of the groEL gene showed only single nucleotide exchanges. In the most cases, these exchanges did not lead to a change in the amino acid (AA) sequence. One amino acid exchange was detected in the groEL gene (nucleotide (nt) position: 134; AA change from serine to isoleucine) of ERIC II (including the strains 341-13, 493-13 and 1201-14). The Argentinian strain 252-18 showed three AA changes (1. nt position: 1276; AA change from alanine to serine; 2. nt position: 1289;

AA change from glutamic acid to glycine; 3. nt position: 1432; AA change from alanine to serine). These changes in the amino acid sequence did not lead to lower signals when detecting the antigen with the anti-*P. larvae* mAbs that are targeting the groEL protein (Figure 45 and Figure 46).

4.5 Application of mAbs in sandwich ELISA

The suitable mAbs were tested to ensure that the two antibodies bind to two different epitopes of the antigen. In order to further verify the results of the indirect ELISA, the same bacteria strains were tested in the sandwich ELISA. The reactivity with different concentrated bacteria samples were tested for the different mAb combinations (Figure 48, Figure 51 and Figure 52).

4.5.1 Sandwich ELISA: *M. plutonius*

For *M. plutonius* sandwich ELISA, two different mAb combinations were tested. The combination of 6F10 and 7D11 was tested. The other mAb combination that was tested, was performed the combination of the rabbit anti-*M. plutonius* pAb and the 6F10 mAb. For both combinations, the mAb 6F10 was conjugated with biotin to serve as the detector antibody (Figure 48).

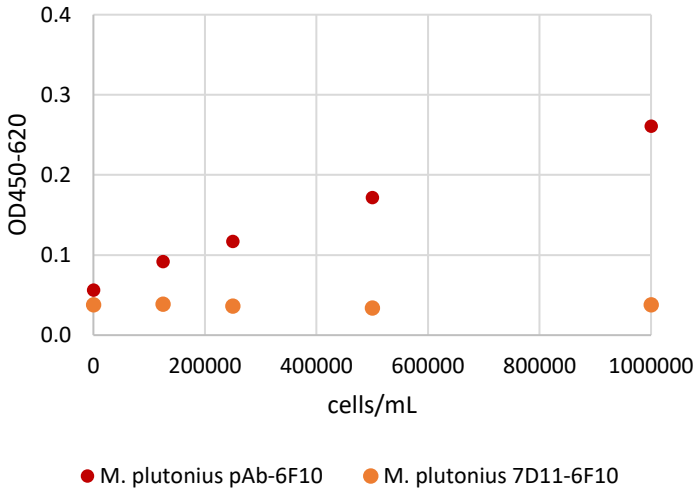

Figure 48 Sandwich ELISA: anti-M. plutonius mAb dilution series
Investigating the optimal sample (antigen) concentration in the *M. plutonius* sandwich ELISA two antibody combinations were tested with different sample dilutions using *M. plutonius* strain CH 49.3. Blue symbols represent three technical replicates of the sandwich ELISA with anti-*M. plutonius* rabbit pAb as capture antibody and 6F10 mAb conjugated with biotin as detector antibody. The orange symbols represent three technical replicates of the sandwich ELISA with 7D11 mAb as capture antibody and 6F10 mAb conjugated with biotin as detector antibody.

The mAb combination with 6F10 and 7D11 was not leading to any signal in the assay. The testing with differently concentrated bacteria samples showed that the signal increase is not stronger in the reactions with bacteria samples than in the buffer control. The combination with mAb candidate 6F10

and the rabbit pAb resulted in a clear signal development. The signal increased with increasing bacteria concentration (Figure 48). However, the general signal strength is relatively low compared to the *P. larvae* sandwich ELISA (4.5.2). A linear regression including all tested bacteria concentrations was performed for determination of LODs of the *M. plutonius* sandwich ELISA. This led to following equation $LOD_{cells/mL}$ calculation: y = 2*10-7 x -0.056 (R^2 = 0.988). After inserting the LOD_{OD} of 0.067 into the equation, the $LOD_{cells/mL}$ of ~$6x10^4$ cells/mL was determined for the *M. plutonius* sandwich ELISA pAb-mAb-6F10 combination. For further analysis, the antibody combination with the rabbit pAb and the 6F10 mAb was used, applying the bacteria concentration of $5x10^5$ cells/mL.

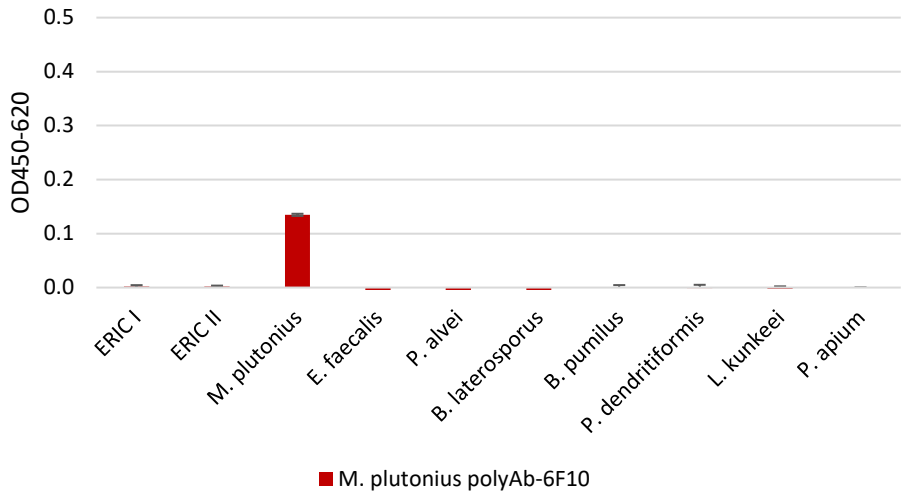

Figure 49 Sandwich ELISA: cross reactivity of anti-M. plutonius mAbs
The anti-*M. plutonius* pAb-mAb combination was tested for cross reactivity in a sandwich ELISA. The bars represent the mean of three technical replicates that was normalized to the buffer control. The error bars are representing the standard deviation of the three technical replicates.

The 6F10 mAb combination with the rabbit anti-*M. plutonius* pAb showed no cross reactivity with the tested bee-associated bacteria (Figure 49). The specificity of the pAb-mAb combination in sandwich ELISA was as good as the specificity of the mAb 6F10 tested in the indirect ELISA (Figure 23). For investigation of the strain detection of the sandwich ELISA, sixteen *M. plutonius* strains were tested (Figure 50).

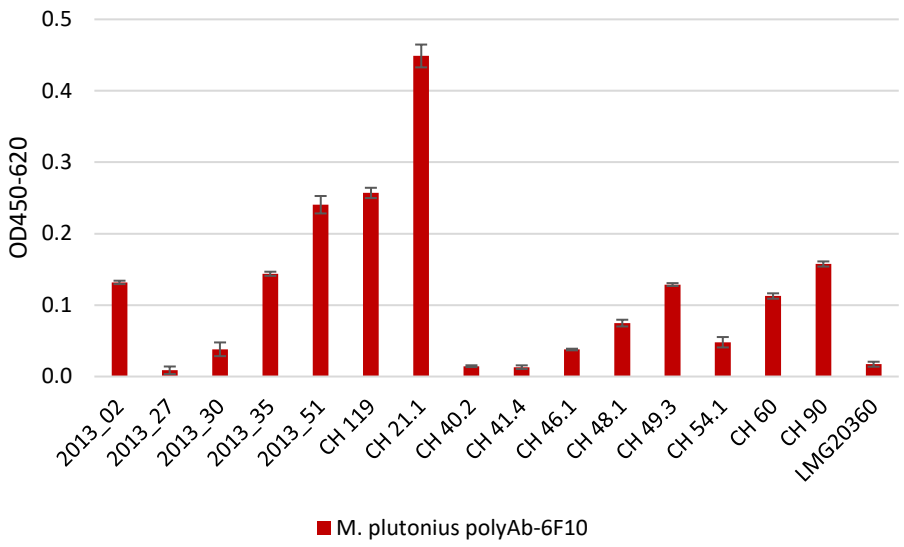

Figure 50 Sandwich ELISA: strain detection of anti-M. plutonius mAbs
The anti-*M. plutonius* pAb-mAb combination was tested for strain detection in a sandwich ELISA. The bars represent the mean of three technical replicates that was normalized to the buffer control. The error bars are representing the standard deviation of the three technical replicates.

Considering the limit of detection of the sandwich ELISA (LOD_{OD} = 0.067) 75 % of the 16 tested *M. plutonius* strains were detected successfully. The general signal strength of the sandwich ELISA is low compared to the *P. larvae* sandwich ELISA (see 4.5.2).

4.5.2 Sandwich ELISA: *P. larvae* and ERIC II distinction

For *P. larvae* detection, the two suitable mAb candidates 3B3 and 5B1 were tested in the sandwich ELISA. In this assay, 3B3 was used as capture antibody and 5B1 was used as the detector antibody that was conjugated with biotin. The sensitivity of the assay was tested with a dilution series of ERIC I and ERIC II bacteria (Figure 51).

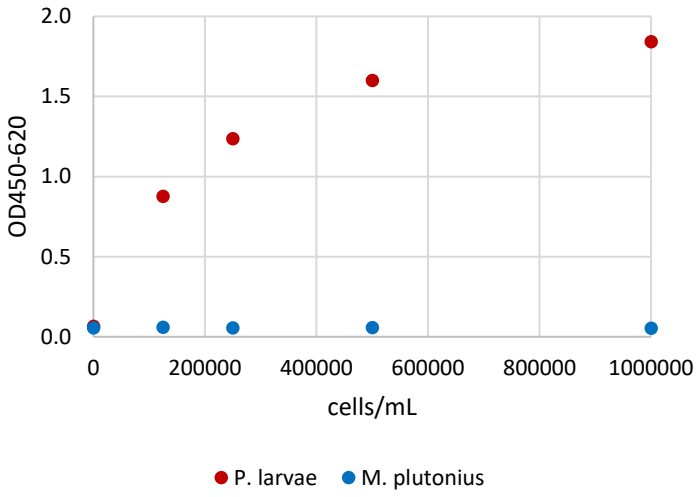

Figure 51 Sandwich ELISA: anti-P. larvae mAb dilution series
Investigating suitable sample (antigen) concentration in the *P. larvae* sandwich ELISA, the following antibody combination was used to test different sample dilutions using ERIC I (DSM 25719) reference strain and *M. plutonius* (CH 49.3) as negative control. The mAb 5B1 was used as capture antibody and the mAb 3B3 was used as biotin-conjugated detector antibody. The blue symbols represent the mean of three technical replicates of the ERIC I sample tested. The red symbols represent the mean of three technical replicates of *P. larvae* ERIC I sample tested.

The signal strength of the *P. larvae* sandwich ELISA is stronger compared to the signal of the *M. plutonius* assay. The signal strength increases with bacteria number. A Linear regression of the *P. larvae* ELISA was performed with the three lowest bacteria concentrations (0; 125 000; 250 000 cells/mL). This led to the following equation $LOD_{cells/mL}$ calculation: y = 5*10- 6 x - 0.074 (R^2 = 0.945). After inserting the LOD_{OD} of 0.087 into the equation the $LOD_{cells/mL-PL}$ of ~$3x10^3$ cells/mL was determined for the *P. larvae* sandwich ELISA. For further analysis of the assay, the bacteria concentration of $5x10^5$ cell/mL was used.

For the ERIC II detection, the mAb candidates 2D12 and 5B2 were used. The capture antibody was 5B2 and as detector antibody, 2D12 was conjugated with biotin. The dilution series was performed with the two reference strains of the ERIC-genotypes to get an impression whether or not genotype differentiation is possible.

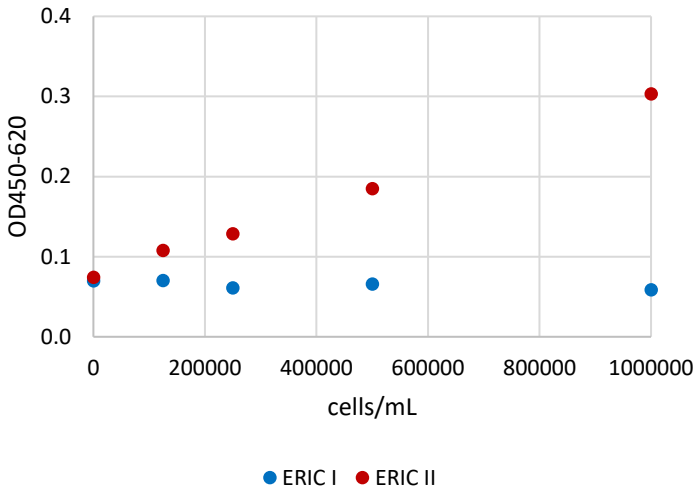

Figure 52 Sandwich ELISA: anti-ERIC II mAb dilution series

Investigating suitable sample (antigen) concentration in the ERIC II sandwich ELISA, the following antibody combination was used to test different sample dilutions using ERIC I (DSM 25719) and ERIC II (DSM 25430) reference strains. The mAb 5B2 was used as capture antibody and the mAb 2D12 was used as biotin-conjugated detector antibody. The blue symbols represent the mean of three technical replicates of ERIC I sample tested. The red symbols represent the mean of three technical replicates of ERIC II sample tested.

The signal of the ERIC II sandwich ELISA increased with increasing bacteria concentration of ERIC II. However, the signal does not increase with increasing ERIC I bacteria concentration. The general signal strength of the ERIC II sandwich ELISA is lower compared to the *P. larvae* sandwich ELISA. A linear regression analysis of the ERIC II ELISA was performed with all tested bacteria concentrations. This led to the following equation for ERIC II $LOD_{cells/mL} = 2*10\text{-}76\ x - 0.074$ ($R^2 = 0.999$). After inserting the LOD_{OD} of 0.093 into the equation the $LOD_{cells/mL\text{-}EII}$ of ~$1x10^5$ cells/mL was calculated. The $LOD_{cells/mL\text{-}EII}$ is higher than for the *P. larvae* sandwich ELISA and for *M. plutonius* sandwich ELISA. For further analysis, bacteria concentration of $5x10^5$ cell/mL was used in the ERIC II sandwich ELISA.

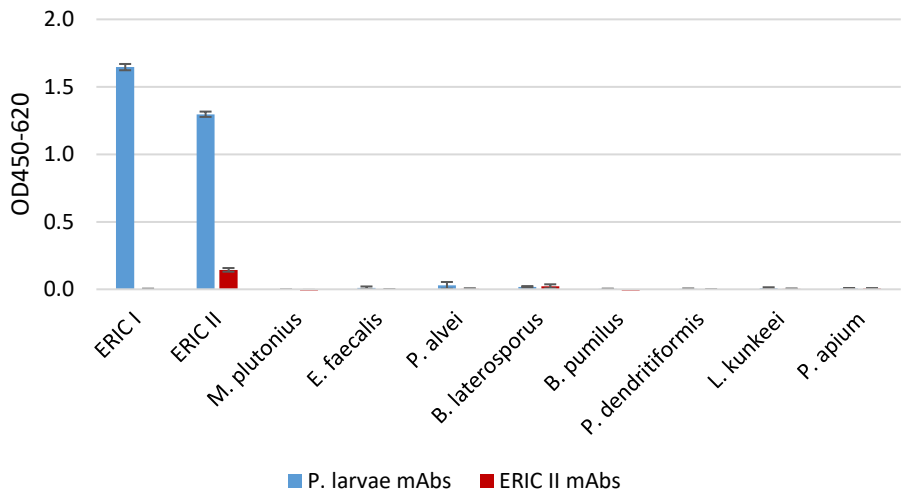

Figure 53 Sandwich ELISA: cross reactivity of P. larvae and ERIC II

The anti-*P. larvae* and anti-ERIC II mAbs were tested for cross reactivity in a sandwich ELISA. For the *P. larvae* sandwich ELISA (blue bars) 5B1 was used as capture antibody and for detector antibody biotin-conjugated 3B3 mAb was used. For the ERIC II sandwich ELISA (red bars), 5B2 was used as capture antibody and as detector antibody biotin-conjugated 2D12 mAb was used. The bars represent three technical replicates that were normalized to the buffer control. The error bars represent the standard deviation of the three technical replicates.

The testing the bee-associated bacteria showed in no cross reactivity in the *P. larvae* sandwich ELISA nor in the ERIC II sandwich ELISA. A huge difference in signal strength was observed between the *P. larvae* assay and the ERIC II assay.

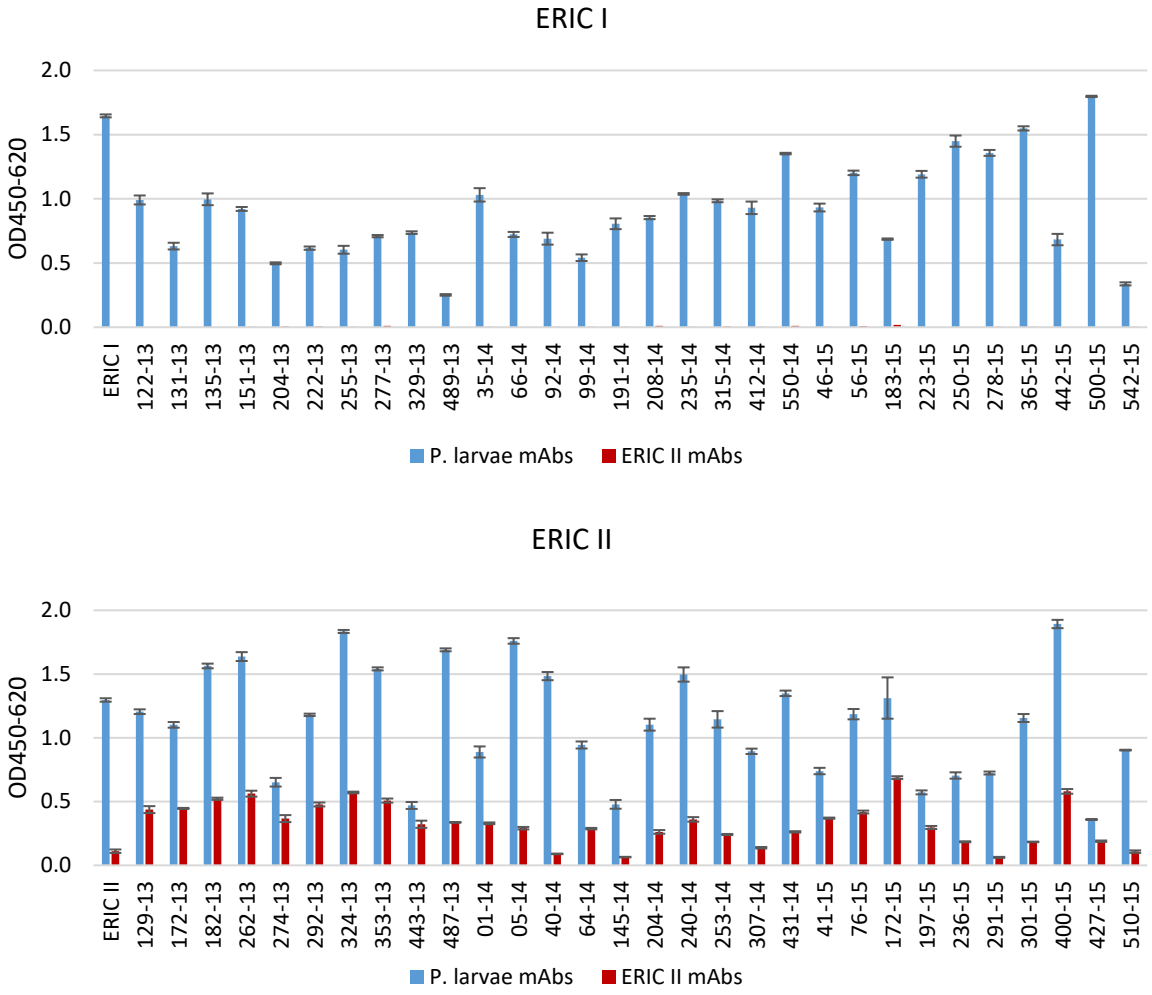

Figure 54 Sandwich ELISA: strain detection of anti-P. larvae and anti-ERIC II mAbs

The anti-*P. larvae* and anti-ERIC II mAbs were tested for strain detection in a sandwich ELISA. The same 30 ERIC I and 30 ERIC II field strains, which are used for indirect ELISA, were tested in sandwich ELISA. For the *P. larvae* sandwich ELISA (blue bars) 5B1 was used as capture antibody and for detector antibody, biotin-conjugated 3B3 mAb was used. For the ERIC II sandwich ELISA 5B2 was used as capture antibody and as detector antibody biotin-conjugated 2D12 mAb was used. The bars represent three technical replicates that were normalized to the buffer control. The error bars represent the standard deviation of the three technical replicates.

Considering the limit of detection for the *P. larvae* assay (LOD_{OD} = 0.087), 100 % of the 60 tested *P. larvae* field strains were positively detected. The ERIC II assay (LOD_{OD} = 0.093), detected 100 % of the 30 tested ERIC II field strains. None of the 30 tested ERIC I strains showed a positive signal in the ERIC II sandwich ELISA (Figure 54). This proves a good genotype differentiation of the ERIC II sandwich ELISA.

Sandwich ELISAs for the detection of *M. plutonius*, *P. larvae* and ERIC II were established. The *P. larvae* sandwich ELISA worked very well, giving strong and reliable signals. The produced and characterized mAbs used for sandwich ELISA were sent to the project partners Senova for the LFD development.

4.6 Validation of EFB & AFB lateral flow devices

The project partner Senova (Industriestraße 8, 99427 Weimar) produced the LFDs for the *M. plutonius* and *P. larvae* detection separately with the mAbs that were characterized before (4.3). The EFB-LFD detected the tested *M. plutonius* strain (Figure 55). The AFB-LFD successfully detected the strains belonging to *P. larvae* ERIC I and ERIC II. Though the ERIC II detection resulted in a weak band that is barely visible (Figure 55).

Figure 55 EFB- and AFB-EII-LFD results
LFDs were tested with their target bacteria (*P. larvae*: 5x106 cells/mL and *M. plutonius*: 1x107 cells/mL). The EFB-LFD was tested with *M. plutonius* strain (CH 21.1) and the AFB-LFD was tested with the reference strains of ERIC I (DSM 25719) and ERIC II (DSM 25430). For better visualization picture was taken after 1 h of incubation. The blue arrow shows the positive band in the EFB-LFD. The orange arrows indicate positive LFDs for AFB in general and the green arrow represent positive results for ERIC II.

The application of *M. plutonius* sample to both LFDs resulted in well detectable signals for the two highest concentrated *M. plutonius* samples ($1x10^7$ and $5x10^6$ cells/mL) in the EFB-LFD (Table S 7). *Melissococcus plutonius* showed no cross reactivity in the AFB-EII-LFD with a bacteria concentration of $1x10^7$ cells/mL (Table S 7). Thus, a detection limit of $5x10^5$ cells of *M. plutonius* per EFB-LFD was determined. The dilution of *P. larvae* samples was performed with ERIC I and ERIC II to investigate whether the genotype differentiation is possible using the AFB-EII-LFD. For general AFB detection a bacteria concentration of $1x10^5$ cells/mL showed a weak band, whereas the sample containing $5x10^4$ cells/mL did not show any signals at all, indicating a limit of detection of $1x10^5$ cells/mL. Thus, the AFB-LFD at the general *P. larvae* position was able to detect $1x10^4$ *P. larvae* cells. For genotype

differentiation, the detection of ERIC II is decisive in this assay. The detection of the ERIC II strain showed a generally weak signal and a high limit of detection. For the development of a noticeable signal, at least 100 µL with a concentration of $5x10^6$ cells/mL (so a total number of $5x10^5$ cells) have to be applied (Figure 55).

The EFB-LFDs and the AFB-LFDs showed no cross reactivity with bee-associated bacteria (Table S 6). Different strains of *M. plutonius* were tested in the EFB-LFD to determine strain detection. The same *M. plutonius* strains, which were used for the ELISAs, were tested in a final concentration of $1x10^7$ cells/mL in the LFDs. All tested strains showed a weak positive band in the EFB-LFD (Table S 7). This leads to a strain detection of 100 % of the EFB-LFD, but high numbers of cells are needed for successful *M. plutonius* detection. Different field strains of *P. larvae* were tested in the AFB-LFD to determine strain detection for the AFB-LFD. The field strains were tested for *P. larvae* only, not for ERIC II differentiation because only the first prototype of AFB-LFD without the ant-ERIC II mAbs was tested. The field strains of *P. larvae* were detected with a final concentration of $5x10^5$ cells/mL, which was found to be sufficient for *P. larvae* detection. All of the tested *P. larvae* strains including all before mentioned ERIC-genotypes were successfully detected by the AFB-LFD (Table S 8).

In order to compare the developed AFB-LFD to the already available LFD from Vita (Vita Europe Ltd., Basingstoke, UK), strains belonging to different ERIC-genotypes I to IV were tested. In a former PhD thesis from Saville (2011) it was declared that the current available test kit is not detecting the ERIC-genotypes II, III and IV.

Figure 56 LFD comparison of commercially available AFB-LFD (Vita) and developed AFB-LFD (Senova)
For comparison of the existing AFB-LFD from Vita and the new developed AFB-LFD from Senova, ERIC I (DSM 25719), ERIC II (DSM 25430), ERIC III (DSM 8443) and ERIC IV (DSM 3615) were with the Vita-LFD. For ERIC I and II detection with Senova LFD see Figure 55. A) Vita-AFB-LFD tested with ERIC I, B) Vita AFB-LFD tested with ERIC II, C) Vita-AFB-LFD tested with ERIC III, D) Vita-AFB-LFD tested with ERIC IV, E) Senova-AFB-LFD tested with ERIC III, F) Senova-AFB-LFD tested with ERIC IV. The orange arrows represent positive LFD results showing the occurring bands.

The commercially available test kit detected strains that belong to ERIC I and ERIC II genotypes (Figure 56). However, the commercially available test kit did not detect the bacteria that belonged to ERIC III and ERIC IV. In contrast, the developed LFD provided by Senova showed a clear signal, when testing strains of ERIC III and ERIC IV (Figure 56).

5. Discussion

The aim of this study was the development of a sandwich ELISA and a lateral flow device (LFD) for detection and differentiation of EFB and AFB including the differentiation of the two main genotypes of *P. larvae* (ERIC I and ERIC II). Prior to antibody production, different field strains of *P. larvae* were analysed based on their genetic variance using ERIC-genotyping and MLVA to get an impression of the variance of the available field isolates and to later on be able to draw conclusions about the ability of the produced mAbs to detect various strains. Atypical strains were identified and further characterized on genetic and protein level.

Specific mAbs are necessary for immunological diagnostic tools, such as ELISA and LFD. Therefore, mAbs were selected from mice, after they had been immunized with *M. plutonius* and *P. larvae* strains belonging to either ERC I or ERIC II. The generated mAbs were characterized focusing on their specificity towards the target bacterium and cross reactivity towards other bee-associated bacteria. Two specific mAbs for *M. plutonius* (6F10 and 7D11), two for *P. larvae* (3B3 and 5B1) and two for ERIC II (2D12 and 5B2) detection were found to be most suitable candidates for sandwich ELISA and LFD. Furthermore, the antigens of the mAbs used in sandwich ELISA and the LFD were identified as chaperonins for the species-specific mAbs and as S-layer for the anti-ERIC II mAbs. The generated anti-*P. larvae* mAbs were also able to detect the atypical *P. larvae* strains. This indicates that the mAbs may well be capable of detecting other atypical strains and new emerging strains as well. The technical implementation of the sandwich ELISA and the LFD was performed in cooperation with the company Senova (Weimar, Germany). Both assays were tested for strain detection of the target pathogen and cross reactivity with bee-associated bacteria showing no cross reactivity and high specificity towards target bacteria.

5.1 Bacteria characterization

In total 16 *M. plutonius* strains and 72 *P. larvae* strains including the reference strains were used in this study. The differences in the number of used field strains occurred due to the difficult availability of *M. plutonius* strains as no cases of EFB have been reported in Germany in the last decades. Furthermore, some difficulties in *M. plutonius* cultivation were experienced in this study. Three of the provided field isolates from Switzerland had to be excluded from further analyses as the bacteria failed to grow on the chosen cultivation medium. These difficulties are well in line with previous observations, where *M. plutonius* was considered to be difficult in *in vitro* cultivation (White, 1906; Forsgren, 2010).

For the assessment of the strain detection ability of the developed diagnostic tools under real life conditions, it is important to consider the genetic variance of the tested strains. Six of the 16 analysed *M. plutonius* field isolates were characterized in previous studies using MLST (Djukic *et al.*, 2018; Grossar *et al.*, 2020). These six genotyped strains were grouped into five different STs, which are belonging to two clonal complexes, CC3 or CC13 (Haynes *et al.*, 2013; Budge *et al.*, 2014; Djukic *et al.*, 2018; Grossar *et al.*, 2020). Strains belonging to the clonal complex CC12 are considered to be atypical and relatively rare in comparison to the other CCs (Budge *et al.*, 2014; Nakamura *et al.*, 2016). From this, the lack of testing strains belonging to CC12 might not influence the strain detection in Germany. In general, the lower diversity of the tested *M. plutonius* strains is well in line with previous studies; where a low genetic diversity of *M. plutonius* strains was described (Budge *et al.*, 2014). The lower number of tested *M. plutonius* field strains might not influence the reliability of the testing due to the general lower diversity of *M. plutonius strains* (Budge *et al.*, 2014)

The ERIC-genotyping unravelled the existence of the five previously uncharacterized ERIC-genotypes in addition to the five described ones (Genersch *et al.*, 2006; Schäfer *et al.*, 2016; Beims *et al.*, 2020). The ERIC-genotyping and SDS-PAGE clarified that the German strains belonging to ERIC * and ERIC ** show high similarities in DNA and protein band patterns compared to ERIC II. These results are well in line with previous findings using MALDI-TOF (Schäfer *et al.*, 2016). The band patterns of the atypical strains from Latin America differed more from ERIC II than the ERIC */**. This leads to the conclusion that ERIC * and ERIC ** might be closely related to the common ERIC I and ERIC II strains. These findings are well in line with the phylogenetic analysis of the groEL gene, where the ERIC */** clustered with ERIC I, II and V and the atypical Latin American strains showed more similarities with the historical strains ERIC III and IV. These finding are well in line with previous description that ERIC I, II and V cluster together and ERIC III and IV are closer related to each other (Genersch *et al.*, 2006; Beims *et al.*, 2020). The identity and the right classification into *P. larvae* species of the Latin American and ERIC */** strains has still to be confirmed using genomic analyses and *in vitro* infection experiments in the same way as recently done for ERIC V recently (Beims *et al.*, 2020).

The MLVA-typing of the used *P. larvae* strains supports the unpublished findings of new MLVA-types (Schäfer, M., personal communication) and unravelled additional MLVA-types. The MLVA-type variance of ERIC I is higher (15 different MLVA-types) than in the tested ERIC II strains (8 MLVA-types). These findings are equivalent to the previous findings where 17 MLVA-types in ERIC I and six MLVA types in ERIC II strains were reported (Descamps *et al.*, 2016). Furthermore, the results from the MLVA-typing showed that the ERIC I reference strain DSM 25719 belongs to a new MLVA-type that is relatively rare compared to other MLVA-types. Consequently, it becomes clear, that this non-typical strain might not be a good representative of ERIC I strains in general and it therefore might be

reasonable to determine a new more typical reference strain. The tested *P. larvae* strains show a higher diversity compared to the *M. plutonius* strains representing a more realistic situation of strain diversity in the field.

The identity of all used bee-associated bacteria was successfully confirmed by sequencing the 16S rRNA gene. The close phylogenetic relations of bacteria species indicate a higher similarity in the protein content of the bacteria, which might in turn indicate a higher chance for cross reactivity in the developed assays.

5.2 Immune reaction and potential specific antigens

The immune reaction of different animal species differed in signal height in sandwich ELISA and in detected band patterns in the WB. These findings are well in line with previous descriptions that different animal species are reacting to different immunogenic proteins (Groves & Morris, 2000). Differences between the immunized animal species could also be detected in the screening for specific mAbs. In the mAb screening with the rat hybridoma a lower number of surviving hybridoma in each screening step was observed in comparison to the mouse hybridoma. The reason for this might be the interspecific fusions made for the rat hybridoma. Generally, interspecific fusions are less successful than intraspecific fusions due to the rejection of lymphocyte chromosomes during cultivation (Groves & Morris, 2000). For successful rat mAb generation a rat derived myeloma cell line might be more suitable than the used mouse myeloma cell line. Differences in signal heights and detected antigens in the different individuals of the same species, which were immunized with the same bacteria, could be observed. The strong variance in the production of serum derived pAbs (Grubb, 1973) makes reproducibility of the pAb composition for assay implementations difficult. Therefore, pAbs are not the best choice for the development of diagnostic tools.

In general, the pAbs of the animals, immunized with *M. plutonius* showed lower signals in the indirect ELISA and lower number of immunogenic proteins compared to the pAbs of the animals immunized with *P. larvae*, independent of the species of the immunized animal. These findings are well in line with previously described low signals in an indirect ELISA using pAbs generated against *M. plutonius* (Pinnock & Featherstone, 1984) underlining the low immunogenicity of *M. plutonius*. The low immunogenicity of *M. plutonius* was also reflected in the screening for specific mouse mAbs, where the hybridoma supernatants showed lower signal strength and a lower proportion of anti-*M. plutonius* mAb producing hybridoma was detected. The low signals in screening of anti-M. plutonius mAb might be due to the low number of immunogenic proteins in *M. plutonius* and/or the poor accessibility and/or low amount of these proteins.

The anti-ERIC I and anti-ERIC II pAbs identified high numbers of shared immunogenic proteins in the WB analysis. Only two potentially specific proteins were detectable for ERIC I and only one prominent antigen for ERIC II was observed. The low number of potential genotype-specific proteins underlines the difficulties in the use of pAbs for distinction between the ERIC-genotypes, while simultaneously demonstrating that genotype-specific antigens do exist. The potential genotype-specific antigens were not clearly identified before mAb screening.

The whole cells of the target bacteria were used for immunization to find the most promising antigens for differentiation of the target pathogens and the two ERIC-genotypes. This promising strategy was previously already implemented successfully (Tomkies *et al.*, 2009) and proved to be successful within this study. The immunization with bacteria cells led to successful production of species-specific mAbs and specific anti-ERIC II mAbs. However, no specific anti-ERIC I mAb was found. This indicates that the chosen strategy might not be the most suitable one for the differentiation of closely related bacteria/genotypes. Theoretically another possible explanation could be that there simply is no ERIC I specific antigen. This, however is rather unlikely and would also contradict previous findings of genotype-specific differences in protein composition (Fünfhaus & Genersch, 2012).

5.3 Monoclonal antibody characterization

The generation of mAbs resulted in four possible candidates for each pathogen strain used for immunization, including anti-*M. plutonius*, anti-*P. larvae*, anti-ERIC I and anti-ERIC II mAbs. Former studies that described mAb generation for EFB and AFB detection reported the successful generation of only one mAb per disease (Olsen *et al.*, 1990; Tomkies *et al.*, 2009). An increase of the number of selected wells/hybridoma after the first screening or additional testing for specificity during the first screening could potentially lead to a further increase of the final number of specific mAbs but this may be difficult due to capacity limitations.

Isotyping of the generated mAbs unravelled that unexpectedly, two IgM antibodies were generated, even though an anti-mouse IgG (H+L) antibody was used as secondary detector. This implies that this detector antibody shows a non-specific binding of IgM antibodies. In general, the isotype proportion of the generated mAbs is roughly in line with the concentrations of antibody isotypes occurring in antiserum (Klein-Schneegans *et al.*, 1989). The most prominent isotype in antiserum and the produced mAbs is IgG_1.

While testing the generated mAbs for cross reactivity, some mAbs showed seemingly contradictory results. Five mAbs showed cross reactivity with bee-associated bacteria or the other pathogenic

bacteria. This cross reactivity was not detected in the second screening when testing against *P. larvae* and *M. plutonius*. This unexpected effect could potentially be explained by the differences in mAb concentration during the screening steps compared to the final purified and concentrated mAb. This explanation in supported by the absorbance heights of tested supernatants, which were lower in the screening steps compared to the purified mAb. Furthermore, the tested hybridoma supernatant in the second screening consists of several thousand hybridoma cells that all might produce different antibodies. The prominent antibody-producing hybridoma detected in a screening might have been lost during the different screening steps.

To avoid false positive results in the field the mAbs with no to low cross reactivity against bee-associated bacteria were chosen. This study investigated extensively the potential bacteria that might cause cross reactivity of the mAbs in the field including EFB-associated bacteria (*B. laterosporus*, *B. pumilus*, *E. faecalis*, *P. alvei* and *P. dendritiformis*) (Forsgren, 2010) and bacteria that may occur in healthy colonies (*P. apium* and *L. kunkeei*) (Corby-Harris *et al.*, 2016; Erban *et al.*, 2017). Previous studies that developed antibody-based assays for EFB detection only tested for cross reactivity with *P. larvae*, *P. alvei*, *E. faecalis* and *B. laterosporus* (Tomkies *et al.*, 2009; Poláchová *et al.*, 2019). In previous studies about the development of assays for AFB detection, the cross reactivity with *M. plutonius*, *P. alvei*, *B. laterosporus* and different *Bacillus* species was tested (Olsen *et al.*, 1990; Pastucha *et al.*, 2021). Since the cross-reactivity of these previously developed antibody-based assays for AFB and EFB detection was only tested against a small number of different bee-associated bacteria, these assays could potentially suffer from a high false positive rate. This could significantly affect the reliability of these assays. In conclusion, based on the extensive focus on the exclusion of cross reactivity with bee associated bacteria for the newly developed assay within this study, it is likely that the newly developed assay has a smaller false positive rate than the assays developed in those previous works (Olsen *et al.*, 1990; Tomkies *et al.*, 2009; Poláchová *et al.*, 2019; Pastucha *et al.*, 2021).

A reliable diagnostic test has to detect several different strains of the target pathogen. Therefore, a number of different *P. larvae* and *M. plutonius* field strains was used to test the developed assays. Due to the limited availability of *M. plutonius* field strains less *M. plutonius* field strains were tested. However, as *M. plutonius* is considered to show a lower strain diversity than *P. larvae,* the lower strain number of field strains might still be sufficient for representative results (Bailey & Gibbs, 1962; Allen & Ball, 1993; Djordjevic *et al.*, 1999). Testing different pathogen field strains with the generated mAbs resulted in large differences in signal strength for the different field isolates when tested with some mAbs (5A10, 6F10 and 7D11). The observed behaviour could possibly be explained either by differences in the expression of the antigen between the different field strains or by differences in the

amino acid sequence at the epitopes of the target antigen. However, the antigens of the anti-*M. plutonius* mAb (6F10 and 7D11) were identified as chaperonins, which are known to be constantly present in the bacteria cell (Lund, 2009). The potential differences in expression of the target antigen in the different field strains could be investigated using a quantitative real-time PCR that is detecting the mRNA of the target antigen. Testing different strains is important when mAbs are used in the diagnostic assay because mAbs only detect one specific antigen, whereas pAbs are detecting several antigens of the target pathogen. The previous studies that developed assays with mAbs for EFB and AFB detection tested 3 to 91 field strains or field sample to validate the final assay (Olsen *et al.*, 1990; Tomkies *et al.*, 2009). To avoid later false negative results of the developed assays in this study the mAbs were tested for strain detection prior to the LFD production. False negative results with different *P. larvae* genotypes were already reported for the AFB-LFD from Vita (Fünfhaus *et al.*, 2018b), for more details see chapter 4.6 and 5.6.

5.4 Antigen characterization

For sandwich ELISA two different mAbs binding the same antigen are necessary. Therefore, only sets of two mAbs that bind to same sized antigens are possible candidates, since two mAbs that bind to differently sized antigens bind to different antigens. The detection of one specific protein band indicates monoclonality of the mAb producing hybridoma. The WBs using the generated mAbs showed that all mAbs detected single bands except for one anti-*M. plutonius* IgM mAb that detected five different sized protein bands (Figure 34). The anti-*M. plutonius* IgM mAb might be not monoclonal. The different sized antigen bands in the WB of the anti-*M. plutonius* IgM mAb could either occur due to an unspecific binding of the mAb or because the recognized epitope is present in several proteins (Nezlin, 1998).

The generated mAbs unravelled the existence of species-specific antigens and an ERIC II specific antigen. The antigens of the most suitable species-specific mAbs (anti-*M. plutonius* and anti-*P. larvae*) are species-specific chaperonins. The chaperonins, also known as heat shock proteins (HSP), are interesting targets for antibodies since they are highly conserved proteins among different organisms (plants, mammals, bacteria) that are involved in protein folding. Due to this function chaperonins are present in a large amount and in almost all stages of bacteria growth (Kumar *et al.*, 2015). The presence in all life stages of bacteria is an important property of the target antigen for maintaining high sensitivity of the diagnostic assay since the disease-causing agents can be detected in several pathogen phases. The amount of the target antigen also plays a big role in the sensitivity of the assay. Chaperonin expression is induced by heat and other treatments that lead to high amounts of unfolded proteins in

the cell (Völker *et al.*, 1994; Rince *et al.*, 2000; Teixera-Gomes *et al.*, 2000; Lund, 2009; Kumar *et al.*, 2015). Stress could also be induced in the bacteria after invasion of a host or other factors in the host environment that could lead to a high amount of chaperonins. In a previous study, it was shown that the antimicrobial activity of the larval food, mainly royal jelly, leads to a stress response of *M. plutonius,* including increased chaperonin expression (Takamatsu *et al.*, 2020). These findings indicate that chaperonins are good candidates for a target antigen because they could be higher expressed in the bacteria when the bacteria are invading the larvae. However, multiple genes for chaperonins (HSP60) have been reported in 30 % of the sequenced bacteria (Lund, 2009). This might cause difficulties in mAb-detection of the different pathogen strains, when the target chaperonin is not present at all or only in low quantities. Chaperonins are also good target because of the correlation of chaperonin expression and bacteria growth detected in *P. larvae* (Descamps *et al.*, 2017). The detection of fast-growing bacteria might be of special interest due to their potential of faster spread. Furthermore, the correlation between chaperonin expression and bacteria growth might be an interesting target for treatment against the pathogens.

Chaperonins are also interesting target for further research to understand pathogenesis and the host-pathogen interaction. Therefore, the generated mAbs may be a good tool for labelling and/or isolation of the chaperonins. The influence of chaperonins on virulence is supported by the fact that *P. larvae* secrets the groEL derived chaperonin (HSP60) as it is known to be the case for other pathogenic bacteria such as *Chlamydia trachomatis, Chlamydia pneumoniae* and *Salmonella enterica* (Buchmeier & Heffron, 1990; Sanchez-Campillo *et al.*, 1999; Henderson & Jensen, 2006; Antunez *et al.*, 2010). Furthermore, chaperonins are involved in pathogen recognition of the host's innate immunity. Chaperonins can be recognized by toll-like receptor 2 (TLR2), a receptor of the innate immune system (Tsan & Gao, 2009). A homologous TLR2 is also present in honey bees and it is involved in the toll-pathway (Aronstein & Saldivar, 2005; Evans *et al.*, 2006). So far, it was not functionally investigated if TLR2 of the honey bee binds the bacterial chaperonin of *P. larvae* and/or *M. plutonius*. This shows that the chaperonins are interesting targets to understand pathogenesis and host-pathogen interactions in addition to their suitability for pathogen detection using mAbs.

The anti-ERIC II mAbs are detecting S-layer proteins that are also an interesting target for antibody based diagnostic methods due their high expression and accessibility for antibodies because of their location outside of the cell (Sleytr *et al.*, 2001). Difficulties in accessibility for antibodies could occur due to the paracrystalline bidimensional structure and membrane association of the S-layer proteins, which makes the solubilization of these proteins challenging (Sleytr *et al.*, 2001). S-layer proteins occur in several pathogenic and non-pathogenic bacteria species, for example in *L. kunkeei*, *E. faecalis*, *B. laterosporus*, *P. alvei* and *P. larvae* (Zarschler *et al.*, 2009; Fünfhaus & Genersch, 2012; Theodore *et*

al., 2014; Maeno *et al.*, 2016; Igbinosa & Beshiru, 2019) but show a relatively low sequence similarity (Gerbino *et al.*, 2015). The low sequence similarity of S-layers between different bacteria species makes this protein an interesting target for accurate diagnostic detection with a low possibility for cross reactivity with S-layer proteins of other species.

S-layer proteins are also interesting targets for further research, in which the specific mAbs can be included for labelling and extraction purposes. The function of S-layer proteins in *P. larvae* is described as an important virulence factor, especially in the first phase of bacteria invasion, and it is involved in cell shape maintenance of bacteria and colony formation (Poppinga *et al.*, 2012). Furthermore, the role in virulence is supported by the fact that parts of S-layer (67 kDa) are secreted by *P. larvae* around the bacteria cell (Antunez *et al.*, 2010). In general, the secretion of S-layer protein when *P. larvae* invades honey bee larvae, opens the potential for good accessibility of the S-layer protein by antibody detection. However, whether or not the generated mAbs are capable of detecting the secreted S-layer protein was not yet explicitly tested and therefore this has to be investigated further before a final conclusion can be drawn. S-layer proteins are also interesting targets for further research about host-pathogen interaction since S-layer proteins can also be detected by the host immune system using Toll-like receptor 2 (TLR2) and 4 (TLR4) (Ryan *et al.*, 2011). However, only the gene for TLR2, not for TLR4, was described in the honey bee genome indicating that the same immune pathway is induced when chaperonins are recognized by the immune system of the honey bee (Evans *et al.*, 2006). If the immune response of honey bee larvae is induced by the recognition of S-layer proteins needs to be further investigated.

The S-layer described in *P. larvae* (SplA) exclusively occurs in ERIC II and ERIC V genotyped strains (Fünfhaus & Genersch, 2012; Beims *et al.*, 2020). Therefore, the genotype specific detection of ERIC II using the developed anti-ERIC II mAbs will also detect ERIC V strains. So far, only one finding of ERIC V in Spain was described. Therefore, the differentiation between ERIC I and ERIC II based on the occurrence of SplA should be sufficiently precise when testing samples from Germany. A contrary description of the occurrence of SplA was made by Erban *et al* (2019), who performed a proteomic analysis of reference strains belonging to different ERIC-genotypes (ERIC I to IV). It was found that the SplA is present in the ERIC I (DSM 7030) reference strain (Erban *et al.*, 2019) that was not used in this study. However, the presence of SplA in the ERIC I reference strain (DSM 7030) could not be confirmed by testing this reference strain with the generated anti-ERIC II mAbs (Figure S 1). In strains (DSM 7030 and DSM 25429) belonging to ERIC I the SplA gene has a frame shift at the position 894 due to the addition of an adenine (Poppinga *et al.*, 2012) that leads to a stop codon after 912 bp of the S-layer gene. Therefore, protein translation stops prematurely (Poppinga *et al.*, 2012). It could be that Erban *et al* (2019) detected the first part of the protein if it is expressed. Furthermore, the mAb 1A6, which

was not used for sandwich ELISA, detected a few ERIC I field strains as well (4.3.4, Figure 27). It may be that the mAb 1A6 detects the first AA sequence of the SplA before the stop codon and this part may be expressed in a few strains belonging to ERIC I. In conclusion, the existence of SplA remains controversial in the different ERIC I strains and needs to be further investigated.

The identified antigens of the produced mAbs (chaperonins and S-layer) are promising candidates for further investigation of the pathogenesis and host-pathogen interaction in EFB and AFB. The availability of specific antibodies makes detection of these important proteins *in vitro* and *in vivo* easy.

Additionally, the presence of the antigens (groEL and SplA) was investigated in the atypical Latin American strains and the strains belonging to ERIC */**. All of the tested atypical strains showed the presence of the chaperonin that was detected by the anti-*P. larvae* mAbs. The sequence analysis unravelled only a few AA sequence changes due to mutations in the different strains. These mutations seem relatively rare, what makes chaperonins a stable target for pathogen detection. The calculated phylogeny based on the chaperonin DNA sequences did not correlate with the presence of the S-layer protein in the strains belonging to different genotypes. The different anti-ERIC II mAbs (1A6, 2D12 and 5B2) showed differences in the detection of the S-layer proteins in the atypical strain from Latin America and the ERIC */** strain. A possible explanation might be that the different anti-ERIC II mAbs bind at different epitopes of the S-layer protein. Furthermore, there might be AA exchanges at the different epitopes of the S-layer proteins of the different strains. There might be a higher number of mutations in the S-layer protein compared to the chaperonins. Interestingly, the S-layer proteins have been detected in all of the tested atypical Latin American and ERIC */** strains, except of one ERIC ** strain (456-13) using the mAb 2D12. This is indicating that the mAb 2D12 might bind at conserved regions of the S-layer proteins. Using the other anti-ERIC II mAbs, 1A6 and 5B2, against the atypical strains unravelled differences in detection of the S-layer compared to 2D12. The Latin American strains seem not to harbour the epitope, which is detected by 5B2. The epitope, which is detected by 1A6 is present in the atypical Latin American strains but lacks in one ERIC ** strain (1201-14). For understanding the differences in S-layer proteins of *P. larvae* further investigations of the DNA-sequences, resulting structural and functional properties of the different proteins and their influence on the pathogenesis of the different *P. larvae* strains are needed.

Testing the anti-*P. larvae* mAbs against the atypical *P. larvae* strains showed that the anti-*P. larvae* mAbs are able to detect reliably more distantly related *P. larvae* strains, making the use of the mAbs in future assays a reliable tool for detection of new emerging strains. Furthermore, the existence of S-layer protein in several strains in addition to the strains belonging to ERIC II and ERIC V, was

demonstrated. The atypical Latin American strains and the ERIC */** strains are relatively rare strains that should not strongly influence the genotyping of ERIC I and ERIC II with the LFD in the field.

5.5 Application of mAbs in sandwich ELISA

The establishment of the sandwich ELISA is a big step towards the diagnostics with an LFD in the field. The combination of the anti-*M. plutonius* mAbs did not lead to any signal in sandwich ELISA when testing the *M. plutonius* strains. However, separately in indirect ELISA both mAbs showed signals against most of the tested *M. plutonius* strains. A possible explanation for this discrepancy is that either the two mAbs bind the same epitope or the epitopes of the mAbs are overlapping/close to each other and therefore inhibit the binding of one another. To validate this explanation further antibody-antigen binding studies, would be necessary. This could be performed for example by investigating the effect of partial deletions of the target antigens on the reactivity of the antibodies.

In the developed sandwich ELISA 75 % of the tested *M. plutonius* strains were successfully detected. This relative low strain detection was not expected based on previously described high morphological, physiological, genetical and immunological homogeneity of *M. plutonius* strains (Bailey & Gibbs, 1962; Allen & Ball, 1993; Djordjevic *et al.*, 1999; Arai *et al.*, 2012; Budge *et al.*, 2014). Therefore, the low strain detection might rather be a result of the generally low signals of the *M. plutonius* assays than a result of differences of the target antigen between the strains.

The LOD in sandwich ELISAs detecting bacteria usually ranges from 10^4 to 10^6 colony forming units (CFU) per mL (Poláchová *et al.*, 2019). In previous studies that established sandwich ELISAs, different LODs of *M. plutonius* detection have been estimated. For a sandwich ELISA using pAbs in combination to each other, a LOD of $1.4x10^5$ CFU/mL was estimated, whereas for a sandwich ELISA with a mAb-pAb combination a LOD of 10^5 cells/mL was identified (Pinnock & Featherstone, 1984; Poláchová *et al.*, 2019). In this study, the developed *M. plutonius* sandwich ELISA showed a LOD of ~$6x10^4$ cells/mL. Comparing the LOD of the sandwich ELISA established in this study to Pinnock & Featherstone (1984), who used the double amount of sample (200 µL instead of 100 µL) in the sandwich ELISA, the LOD of the sandwich ELISA of this study was approximately three times lower. Similar differences in LODs can be detected, when comparing to the sandwich ELISA established by Polachová *et al.* (2019). However, the LODs are difficult to compare to the ELISA with the pAb combination because the method used to determine the number of bacteria cells and the formulas used to calculate the LOD were different (Poláchová *et al.*, 2019). Polachová *et al.* (2019) used a photometer to evaluate the number of cells, whereas in this study cells were counted under the microscope. The number of *M. plutonius* cells per bee in symptomatic diseased colonies have been reported to be around ~$5x10^4$ CFU per bee (Roetschi

et al., 2008). Therefore, it could be concluded that the established sandwich ELISA is not able to detect the EFB-causing agent of one diseased bee but a pool of bees would lead to successful detection. However, the comparison of the LOD of the established sandwich ELISA to the number of *M. plutonius* cells detected in a bee is difficult due to the comparison of a concentration to an absolute number of bacteria cells.

The mAb combination in the sandwich ELISA for *P. larvae* detection shows higher signals compared to the *M. plutonius* ELISA. The *P. larvae* sandwich ELISA successfully detected 100 % of the tested strains of the genotypes ERIC I and ERIC II. The ERIC II specific sandwich ELISA also showed 100 % detection of ERIC II strains with no cross reactivity against ERIC I strains and other bee-associated bacteria. However, the general signal height of the ERIC II sandwich ELISA is lower compared to the *P. larvae* sandwich ELISA signal heights. Low signal heights in ERIC II sandwich ELISA could occur because of low affinity of the anti-ERIC II mAbs towards the target antigen or due to poor accessibility of the target antigen. The S-layer is known to be able to self-assemble forming paracrystalline structures and it is associated with the bacteria membrane (Poppinga *et al.*, 2012; Sleytr *et al.*, 2014), which have to be broken so that antibodies have access to their epitope. For improving the accessibility of the epitope, a prior lysis step of the bacteria could potentially lead to higher signals in sandwich ELISA.

The previously described *P. larvae* sandwich ELISA had a LOD of 6.5×10^4 CFU/mL and used a pAb from rabbit (Pastucha *et al.*, 2021). Because no ERIC II sandwich ELISA was established so far, the LOD values were compared to already existing *P. larvae* ELISAs. In this study, the LOD of the *P. larvae* sandwich ELISA was ~3×10^3 cells/mL and the LOD of the ERIC II ELISA was ~1×10^5 cells/mL. When comparing the LOD of the general *P. larvae* ELISA, it shows a 20 times higher sensitivity than the previous developed one, whereas the ERIC II sandwich ELISA shows a two times lower sensitivity than the previously developed *P. larvae* sandwich ELISA. As described before, a direct comparison to the developed sandwich ELISA in this study is difficult due to the differences in CFU determination. The study by Pastucha *et al.* (2021) used a photometer to evaluate the number of cells, whereas in this study the cells were counted under the microscope.

In conclusion, the *P. larvae* sandwich ELISA is a great and sensitive tool for detection of *P. larvae*. As the differentiation between ERIC I and ERIC II can be performed on the basis of an elimination process using the developed ERIC II sandwich ELISA in combination with the *P. larvae* sandwich ELISA, there is no need for an additional ERIC I specific sandwich ELISA for the differentiation between the two genotypes. However, the signal strength of the *M. plutonius* and ERIC II sandwich ELISA have to be improved for reliable use in diagnostics.

5.6 Validation of EFB and AFB lateral flow devices

The developed LFDs showed no cross reactivity with the tested bee-associated bacteria and the tested respective other foulbrood causing agent. All tested field strains of the pathogens were detected either by EFB- or AFB-LFD. These results are well in line with the results from the indirect ELISAs where the mAbs were characterized. There is no information about the LODs of the already existing EFB-LFD and AFB-LFD (Tomkies *et al.*, 2009). The LODs of other bacteria detecting LFDs depend on the specific device in general and the tested organism. The reported LODs ranged from 10^4 cells/mL to 10^9 cells/mL using LFDs for detection of *Yersinia pestis*, *Francisella tularensis* and *Bacillus anthracis* (Ziegler *et al.*, 2021). The developed AFB-ERIC II-LFD and EFB-LFD fit in this LOD range and are closer to the lower LODs (EFB: $5x10^6$ cells/mL; AFB: $1x10^5$ cells/mL; ERIC II: $5x10^6$ cells/mL). The AFB-LFD developed in this study successfully detects $1x10^4$ *P. larvae* cells that are applied to LFD, which is a more than ten times lower number of cells than the number of cells needed for *M. plutonius* detection in the developed EFB-LFD ($5x10^5$ *M. plutonius* cells). The detection limit of *M. plutonius* is above the observed number of *M. plutonius* cells (~$5x10^4$ CFU) per bee in symptomatic diseased colonies (Roetschi *et al.*, 2008) and the band strength of positive EFB-LFD was weak and needed higher number of bacteria cells compared to AFB-LFD. a weak band occurring in the EFB- and ERIC II-LFD is well in line with the previous results showing low signals in the sandwich ELISAs. This is underlining that the affinity of the mAbs towards the antigen might not be strong enough or the amount might be low or the accessibility of the antigen might be poor. The EFB- and ERIC II-LFDs have to be optimized. Either better mAbs have to be found or the conditions of the LFD have to be changed. A two-mAb combination for the EFB-LFD would be more suitable for reproducibility of the assay, when a new batch of antibodies is needed for LFD production and may increase sensitivity.

The commercially available AFB-LFD from Vita (Basingstoke, UK) was reported to be incapable of detecting *P. larvae* strains that are belonging to ERIC II, ERIC III and ERIC IV (Saville, 2011; Fünfhaus *et al.*, 2018b). Therefore, the Vita-LFD and the developed AFB-LFD were tested with one strain of each ERIC-genotype of ERIC I to IV. While the Vita-LFD detected only the tested strains belonging to ERIC I and ERIC II, the newly developed AFB-LFD was able to detect all of the tested *P. larvae* strains including ERIC I to IV. The detection of ERIC II by the Vita-LFD is well in line with the findings in the literature, as the *P. larvae* strain used to test the Vita-LFD was originally falsely classified as ERIC II and later on was reclassified as ERIC IV (Saville, 2011; Morrissey *et al.*, 2015). These results indicate that the commercially available AFB-LFD would very likely also work with other ERIC II strains. Comparing the developed AFB-LFD to that from Vita unravelled that the AFB-LFD from Senova is detecting a larger range of different *P. larvae* genotypes than the Vita-LFD.

The developed LFDs of this study are prototypes that have so far only been tested preliminary. In principle, the produced mAbs are capable of detecting the target bacterium. However, only the AFB-LFD has a sufficiently good sensitivity, whereas the EFB-LFD and the ERIC II-LFD show a low sensitivity for reliable detection. Therefore, the LFDs have to be further optimized using different lysis strategies and/or more suitable conditions in LFD production. Possibly, changes in LFD production could be adjusting the size of conjugated nanoparticles, antibody concentration in nanoparticle conjugation, pH of the conjugation reaction and membrane properties (Safenkova *et al.*, 2012). These properties can only be adjusted in the production process of the LFDs and have to be optimized by the project partner Senova before the use of the LFDs in the field. After successful technical optimizations, a fast, reliable, cheap and easy to use diagnostic tool for EFB, AFB and genotype differentiation will be available.

6. Conclusions and Outlook

In this study, specific mAbs for AFB and EFB detection were produced. Furthermore, anti-ERIC II mAbs for genotyping the *P. larvae* strains were also characterized for further diagnostic use. Several mAb candidates were characterized determining their isotype, specificity and cross reactivity. The most promising mAb candidates were used for the establishment of a sandwich ELISA testing the mAb-suitability for the LFD production. Finally, the LFDs were produced by Senova for EFB, AFB detection and the ERIC-genotype differentiation using the suitable mAb combinations determined in the sandwich ELISA.

The antigens of the mAbs, which were used for sandwich ELISA and LFD, were identified as chaperonins for species-specific mAbs and as S-layer (SplA) for ERIC II specific mAbs. These proteins might be an interesting topic for future research about the host-pathogen interaction and the pathogenesis to unravel the mechanistic role of the S-layer and chaperonins in pathogenesis with the use of the generated mAbs.

The used *P. larvae* strains were characterized to gain information about the variance of tested strains. The characteristics of atypical strains was further investigated and the produced mAbs for AFB and ERIC II detection were used for a fast characterization of the atypical strains. The differences in the S-layer detection by the mAbs in the atypical strains imply differences in the S-layer proteins that might influence also the function of these proteins. Whether or not the differences in the S-layer proteins influence the virulence of the strains needs to be investigated. The successful application of the anti-*P. larvae* mAbs against the atypical strains confirms the reliability of the mAbs for detecting a high variance of *P. larvae* strains, therefore, giving the LFD a good future perspective for detecting various *P. larvae* strains.

Summarizing the study, two easy applicable, cheap and reliable methods for EFB and AFB detection and ERIC-genotyping have been established in the laboratory. However, before field use, the sandwich ELISA and the LFDs have to be further optimized and validated comparing them to already used methods in accordance to sensitivity, reliability and applicability with different hive products. After validation and optimization of the two assays, all in one LFDs for the detection of EFB and AFB and ERIC-genotyping will be produced resulting in a great tool for diagnostic purposes in the field without the need for expensive equipment or advanced expertise.

7. References

Alippi, A. M. (2014). Bacterial diseases of honey bees. In R. W (Ed.), *Bee Health and Veterinarians* (pp. 117-124): OIE.

Allen, M. F., & Ball, B. V. (1993). The cultural characteristics and serological relationships of M.pluton isolates. *Journal of Apicultural Research*, 80-88.

Antunez, K., Anido, M., Evans, J. D., & Zunino, P. (2010). Secreted and immunogenic proteins produced by the honeybee bacterial pathogen, Paenibacillus larvae. *Veterinary Microbiology, 141*, 5. doi:10.1016/j.vetmic.2009.09.006

Arai, R., Miyoshi-Akiyama, T., Okumura, K., Morinaga, Y., Wu, M., Sugimura, Y., . . . Takamatsu, D. (2013). Development of duplex PCR assay for detection and differentiation of typical and atypical M plutonius strains. *The Journal of Veterinary Medical Science*, 30.

Arai, R., Tominaga, K., Wu, M., Okura, M., Ito, K., Okamura, N., . . . Takamatsu, D. (2012). Diversity of Melissococcus plutonius from honeybee larvae in Japan and experimental reproduction of European foulbrood with cultured atypical isolates. *PLoS ONE, 7*(3), e33708. doi:10.1371/journal.pone.0033708

Arnemann. (2019). *Lexikon der Medizinischen Laboratoriumsdiagnostik (Chapter_Snellius-Brechungsgesetz)*.

Aronstein, K., & Saldivar, E. (2005). Characterization of a honey bee Toll related receptor gene *Am18w* and its potential involvement in antimicrobial immune defense. *Apidologie, 36*(1), 3-14. doi:10.1051/apido:2004062

Ash, C., Priest, F. G., & Collins, M. D. (1993). Molecular identification of rRNA group 3 bacilli (Ash, FArrow, Wallbanks and Collins) using a PCR probe test *Antonie van Leeuwenhoek, 64*, 253-260.

Aupperle-Lellbach, H., Müller, L., Fünfhaus, A., & Genersch, E. (2018). EFB in honey bees (Apis mellifera): Histological insights into the pathogenesis of larval infections with the low virulent strain LMG20360 belonging to the clonal complex 13. *Berliner und Munchener Tierarztliche Wochenschrift*. doi:10.2376/0005-9366-18062

Bahadır, E. B., & Sezgintürk, M. K. (2016). Lateral flow assays: Principles, designs and labels. *TrAC Trends in Analytical Chemistry, 82*, 286-306. doi:10.1016/j.trac.2016.06.006

Bailey, L. (1957). The cause of European Foul Brood. *Bee World, 38*(4), 85-89.

Bailey, L. (1983). *Melissococcus pluton,* the cause of European foulbrood of honey bees (*Apis* ssp.). *Journal of Applied Bacteriology, 55*, 65-69.

Bailey, L., & Ball, B. V. (1991). Honey Bee Pathology. 196.

Bailey, L., & Gibbs, A. J. (1962). Cultural characters of Streptococcus pluton and its differentiation from associated enterococci. *Journal of General Microbiology, 28*, 385-391. doi:10.1099/00221287-28-3-385

Bamrick, J. F. (1967). Resistance to American foulbrood in honey bees VI. Spore germination in larvae of different ages. *Journal of Invertebrate Pathology, 9*, 30-34.

Bamrick, J. F., & Rothenbuhler, W. C. (1961). Resistance to American foulbrood in honey bees. IV the relationship between larval age at inoculation and mortality in a resistant and in a susceptible line. *Journal of Insect Pathology, 3*, 381-390.

Beims, H., Bunk, B., Erler, S., Mohr, K. I., Sproer, C., Pradella, S., . . . Steinert, M. (2020). Discovery of Paenibacillus larvae ERIC V: Phenotypic and genomic comparison to genotypes ERIC I-IV reveal different inventories of virulence factors which correlate with epidemiological prevalences of American Foulbrood. *International Journal of Medical Microbiology, 310*(2), 11. doi:10.1016/j.ijmm.2020.151394

Beims, H., Janke, M., Von der Ohe, W., & Steinert, M. (2020). Rapid identification and genotyping of the honeybee pathogen P. larvae by combining culturing and multiplex qPCR. *Open Veterinary Journal, 10*(1), 6. doi:10.4314/ovj.v10i1.9

Biova, J., Charriere, J. D., Dostalkova, S., Skrabisova, M., Petrivalsky, M., Bzdil, J., & Danihlik, J. (2021). Melissococcus plutonius Can Be Effectively and Economically Detected Using Hive Debris and Conventional PCR. *Insects, 12*(2), 12. doi:10.3390/insects12020150

BLE. (2021). Weltbienentag am 20. Mai – Neue Forschungsprojekte gestartet. Retrieved from https://www.ble.de/SharedDocs/Meldungen/DE/2021/210514_Weltbienentag.html

Brodsgaard, C. J., Ritter, W., & Hansen, H. (1998). Response of in vitro reared honey bee larvae to various doses of *Paenibacillus larvae* larvae spores. *Apidologie, 29*, 569-578.

Buchmeier, N. A., & Heffron, F. (1990). Induction of Salmonella Stress Proteins upon Infection of Macrophages. *Science, 248*.

Budge, G. E., Barrett, B., Jones, B., Pietravalle, S., Marris, G., Chantawannakul, P., . . . Brown, M. A. (2010). The occurrence of *Melissococcus plutonius* in healthy colonies of Apis mellifera and the efficacy of European foulbrood control measures. *Journal of Invertebrate Pathology, 105*(2), 164-170. doi:10.1016/j.jip.2010.06.004

Budge, G. E., Shirley, M. D., Jones, B., Quill, E., Tomkies, V., Feil, E. J., . . . Haynes, E. G. (2014). Molecular epidemiology and population structure of the honey bee brood pathogen Melissococcus plutonius. *ISME J, 8*(8), 1588-1597. doi:10.1038/ismej.2014.20

Burnside, C. E. (1934). Studies on the bacteria associated with EFB. *Journal of Economic Entomology, 27*.

Bussmann, B. M., Reiche, S., Jacob, L. H., Braun, J. M., & Jassoy, C. (2006). Antigenic and cellular localisation analysis of the severe acute respiratory syndrome coronavirus nucleocapsid protein using monoclonal antibodies. *Virus Research, 122*(1-2), 8. doi:10.1016/j.virusres.2006.07.005

Chandrasekhar, K., Dileep, A., Lebonah, D. E., & Kumari, J. P. (2014). A Short Review on Proteomics and its Applications. *International Letters of Natural Sciences, 17*, 8. doi:10.18052/www.scipress.com/ILNS.17.77

Chantawannakul, P., & Dancer, B. N. (2001). American foulbrood in honey bees. *Bee World, 82*(4), 168-180.

Cheshire, F. R., & Cheyne, W. W. (1885). The pathogenic history and history under cultivation of a new Bacillus. *Journal of the Royal Microscopical Society, 5*(4), 581-601.

Coordinators, N. R. (2018). Database resources of the National Center for Biotechnology Information. *Nucleic Acids Research, 46*(D1), D8-D13. doi:10.1093/nar/gkx1095

Corby-Harris, V., Snyder, L., Meador, C. A., Naldo, R., Mott, B., & Anderson, K. E. (2016). Parasaccharibacter apium, gen. nov., sp. nov., Improves Honey Bee (Hymenoptera: Apidae) Resistance to Nosema. *Journal of Economic Entomology*. doi:10.1093/jee/tow012

Corby-Harris, V., Snyder, L. A., Schwan, M. R., Maes, P., McFrederick, Q. S., & Anderson, K. E. (2014). Origin and effect of alpha 2.2 *Acetobacteraceae* in honey bee larvae and discription of *Parasaccharibacter apium* gen. nov., sp. nov. *Applied and Environmental Microbiology, 80*(24), 7460-7472.

Crowther, J. R. (2009). *The ELISA Guidebook* (2 ed.).

Dainat, B., Grossar, D., Ecoffey, B., & Haldemann, C. (2018). Triplex real-time PCR method for the qualitative detection of European and American foulbrood in honeybee. *Journal of Microbiological Methods, 146*, 61-63. doi:10.1016/j.mimet.2018.01.018

De Graaf, D. C., Alippi, A. M., Antunez, K., Aronstein, K., Budge, G., de Koker, D., . . . Genersch, E. (2013). Standard methods for American foulbrood research. *Journal of Apicultural Research, 52*(1), 1-28. doi:10.3896/IBRA.1.52.1.11

de Graaf, D. C., Alippi, A. M., Brown, M., Evans, J. D., Feldlaufer, M., Gregorc, A., . . . Ritter, W. (2006). Diagnosis of American foulbrood in honey bees: a synthesis and proposed analytical protocols. *Letters in Applied Microbiology, 43*(6), 583-590. doi:10.1111/j.1472-765X.2006.02057.x

Descamps, T., De Smet, L., De Vos, P., & de Graaf, D. C. (2017). Unbiased random mutagenesis contributes to a better understanding of the virulent behaviour of *Paenibacillus larvae*. *Journal of Applied Microbiology*. doi:10.1111/jam.13611

Descamps, T., De Smet, L., Stragier, P., De Vos, P., & de Graaf, D. C. (2016). Multiple Locus Variable number of tandem repeat Analysis: A molecular genotyping tool for *Paenibacillus larvae*. *Microb Biotechnol, 9*(6), 772-781. doi:10.1111/1751-7915.12375

Djordjevic, S. P., Noone, K., Smith, L., & Hornitzky, M. (1998). Development of a hemi-nested PCR assay for the specific detection of *Melissococcus pluton*. *Journal of Apicultural Research, 37*(3), 165-174.

Djordjevic, S. P., Smith, L. A., Forbes, W. A., & Hornitzky, M. A. (1999). Geographically diverse Australian isolates of Melissococcus pluton exhibit minimal genotypic diversity by restriction endonuclease analysis. *FEMS Microbiology Letters, 173*, 311-318.

Djukic, M., Brzuszkiewicz, E., Funfhaus, A., Voss, J., Gollnow, K., Poppinga, L., . . . Daniel, R. (2014). How to kill the honey bee larva: genomic potential and virulence mechanisms of Paenibacillus larvae. *PLoS ONE, 9*(3), e90914. doi:10.1371/journal.pone.0090914

Djukic, M., Erler, S., Leimbach, A., Grossar, D., Charriere, J. D., Gauthier, L., . . . Poehlein, A. (2018). Comparative Genomics and Description of Putative Virulence Factors of Melissococcus plutonius, the Causative Agent of European Foulbrood Disease in Honey Bees. *Genes (Basel), 9*(8), 419. doi:10.3390/genes9080419

Drobníková, V., V, R., Häusler, J., & Pytelová, I. (1994). Characterization of Bacillus larvae and related bacilli by chromatography of cell fatty acids. *Journal of Apicultural Research, 33*(2), 69-74.

Ebeling, J., Funfhaus, A., Knispel, H., Krska, D., Ravulapalli, R., Heney, K. A., . . . Genersch, E. (2017). Characterization of the toxin Plx2A, a RhoA-targeting ADP-ribosyltransferase produced by the honey bee pathogen Paenibacillus larvae. *Environmental Microbiology, 19*(12), 5100-5116. doi:10.1111/1462-2920.13989

Ebeling, J., Knispel, H., Funfhaus, A., & Genersch, E. (2019). The biological role of the enigmatic C3larvinAB toxin of the honey bee pathogenic bacterium Paenibacillus larvae. *Environmental Microbiology*. doi:10.1111/1462-2920.14709

Engel, P., James, R. R., Koga, R., Kwong, W. K., McFrederick, Q. S., & Moran, N. A. (2013). Standard methods for research on *Apis mellifera* gut symbionts. *Journal of Apicultural Research, 52*(4), 1-24. doi:10.3896/IBRA.1.52.4.07

Erban, T., Ledvinka, O., Kamler, M., Hortova, B., Nesvorna, M., Tyl, J., . . . Hubert, J. (2017). Bacterial community associated with worker honeybees (*Apis mellifera*) affected by European foulbrood. *PeerJ, 5*, e3816. doi:10.7717/peerj.3816

Erban, T., Zitek, J., Bodrinova, M., Talacko, P., Bartos, M., & Hrabak, J. (2019). Comprehensive proteomic analysis of exoproteins expressed by ERIC I, II, III and IV Paenibacillus larvae genotypes reveals a wide range of virulence factors. *Virulence, 10*(1), 363-375. doi:10.1080/21505594.2019.1603133

Erler, S., Lewkowski, O., Poehlein, A., & Forsgren, E. (2017). The Curious Case of Achromobacter eurydice, a Gram-Variable Pleomorphic Bacterium Associated with European Foulbrood Disease in Honeybees. *Microbial Ecology*. doi:10.1007/s00248-017-1007-x

Evans, J. D., Aronstein, K., Chen, Y. P., Hetru, C., Imler, J. L., Jiang, H., . . . Hultmark, D. (2006). Immune pathways and defence mechanisms in honey bees *Apis mellifera*. *Insect Molecular Biology, 15*(5), 645-656.

Molecular diagnosis and characterization of honey bee pathogens, (2009).

Forsgren, E. (2010). European foulbrood in honey bees. *Journal of Invertebrate Pathology, 103 Suppl 1*, S5-9. doi:10.1016/j.jip.2009.06.016

Forsgren, E., Budge, G., Charriere, J., & Hornitzky, M. (2013). Standard methods for European foulbrood research. *Journal of Apicultural Research, 52*(1), 1-14. doi:10.3896/IBRA.1.52.1.12

Forsgren, E., Locke, B., Sircoulomb, F., & Schäfer, M. O. (2018). Bacterial Diseases in Honeybees. *Current Clinical Microbiology Reports*. doi:10.1007/s40588-018-0083-0

Fünfhaus, A., Ashiralieva, A., Borriss, R., & Genersch, E. (2009). Use of suppression subtractive hybridization to identify genetic differences between differentially virulent genotypes of *Paenibacillus larvae*, the etiological agent of American foulbrood of honeybees. *Environmental Microbiology Reports, 1*(4), 240-250. doi:10.1111/j.1758-2229.2009.00039.x

Fünfhaus, A., Ebeling, J., & Genersch, E. (2018a). Bacterial pathogens of bees. *Current Opinion in Insect Science, 26*, 89-96. doi:10.1016/j.cois.2018.02.008

Fünfhaus, A., & Genersch, E. (2012). Proteome analysis of Paenibacillus larvae reveals the existence of a putative S-layer protein. *Environmental Microbiology Reports, 4*(2), 194-202. doi:10.1111/j.1758-2229.2011.00320.x

Fünfhaus, A., Göbel, J., Ebeling, J., Knispel, H., & Genersch, E. (2018b). Questions, problems and solutions in the diagnosis of AFB - a German perspective. *Berliner und Munchener Tierarztliche Wochenschrift*, 9. doi:10.2376/0005-9366-18023

Fünfhaus, A., Poppinga, L., & Genersch, E. (2013). Identification and characterization of two novel toxins expressed by the lethal honey bee pathogen Paenibacillus larvae, the causative agent of American foulbrood. *Environmental Microbiology*. doi:10.1111/1462-2920.12229

Genersch, E. (2010). American foulbrood in honeybees and its causative agent, *Paenibacillus larvae*. *Journal of Invertebrate Pathology, 103 Suppl 1*, S10-19. doi:10.1016/j.jip.2009.06.015

Genersch, E., Forsgren, E., Pentikainen, J., Ashiralieva, A., Rauch, S., Kilwinski, J., & Fries, I. (2006). Reclassification of Paenibacillus larvae subsp. pulvifaciens and Paenibacillus larvae subsp. larvae as Paenibacillus larvae without subspecies differentiation. *International Journal of Systematic and Evolutionary Microbiology, 56*(Pt 3), 501-511. doi:10.1099/ijs.0.63928-0

Genersch, E., & Otten, C. (2003). The use of repetitive element PCR fingerprinting (rep-PCR) for genetic subtyping of German field isolates of *Paenibacillus larvae* subsp. larvae. *Apidologie, 34*(3), 195-206. doi:10.1051/apido:2003025

Gerbino, E., Carasi, P., Mobili, P., Serradell, M. A., & Gomez-Zavaglia, A. (2015). Role of S-layer proteins in bacteria. *World Journal of Microbiology & Biotechnology, 31*(12), 1877-1887. doi:10.1007/s11274-015-1952-9

Govan, V. A., Brözel, V., Allsopp, M. H., & Davison, S. (1998). A PCR detection method for rapid identification of *Melissococcus pluton* in honeybee Larvae. *Applied and Environmental Microbiology, 64*(5), 1983-1985.

Graham, J. (1992). The hive and the honey bee,. *Dadant and Sons, Hamilton, Ill.*

Grossar, D., Kilchenmann, V., Forsgren, E., Charriere, J. D., Gauthier, L., Chapuisat, M., & Dietemann, V. (2020). Putative determinants of virulence in Melissococcus plutonius, the bacterial agent causing European foulbrood in honey bees. *Virulence, 11*(1), 15. doi:10.1080/21505594.2020.1768338

Groves, D. J., & Morris, B. A. (2000). Veterinary Sources of Nonrodent Monoclonal Antibodies: Interspecific and Intraspecific Hybridomas. *Hybridoma, 19*(3).

Grubb, A. (1973). Immunochemical quantitation of IgG: influences of the antiserum and of the antigenic population. *Scandinavian Journal of Clinical and Laboratory Investigation, 31*(4), 465-472. doi:10.3109/00365517309084332

Haseman, L. (1961). How long can spores of American foulbrood live. *American Bee Journal, 101*, 2. doi:-

Haynes, E., Helgason, T., Young, J. P., Thwaites, R., & Budge, G. E. (2013). A typing scheme for the honeybee pathogen *Melissococcus plutonius* allows detection of disease transmission events and a study of the distribution of variants. *Environmental Microbiology Reports, 5*(4), 525-529. doi:10.1111/1758-2229.12057

Henderson, G. P., & Jensen, G. J. (2006). Three-dimensional structure of Mycoplasma pneumoniae's attachment organelle and a model for its role in gliding motility. *Molecular Microbiology, 60*(2), 376-385. doi:10.1111/j.1365-2958.2006.05113.x

Heyndrickx, M., Vandemeulebroecke, K., Hoste, B., Janssen, P., Kersters, K., De Vos, P., . . . Berkeley, R. C. W. (1996). Reclassification of *Paenibacillus* (formerly *Bacillus*) *pulvifaciens* (nakamura 1984) ash et al. 1994, a later subjective synonym of *Paenibacillus* (formerly *Bacillus*) *larvae* (white 1906) ash et al. 1994, as a subspecies of *P. larvae*, with emended descriptions of *P. larvae* subsp. *larvae* and *P. larvae* subsp. *pulvifaciens*. *International Journal of Systhematic Bacteriology, 46*(1), 270-279.

Hornitzky, M., & Smith, L. (1998). Procedures for the culture of *Melissococcus pluton* from dideased brood and bulk honey samples *Journal of Apicultural Research, 37*(4), 293-294.
Hornitzky, M. A. Z., & Djordjevic, S. (1992). Sodium dodecyl sulphate polyacylamide profiles and Western blots of *Bacillus larvae*. *Apicultural Abstracts*, 47-49.
Hristov, P., Shumkova, R., Palova, N., & Neov, B. (2020). Factors Associated with Honey Bee Colony Losses: A Mini-Review. *Vet Sci, 7*(4). doi:10.3390/vetsci7040166
Igbinosa, E. O., & Beshiru, A. (2019). Antimicrobial Resistance, Virulence Determinants, and Biofilm Formation of Enterococcus Species From Ready-to-Eat Seafood. *Frontiers in Microbiology, 10*, 728. doi:10.3389/fmicb.2019.00728
Johnson, J. S., Spakowicz, D. J., Hong, B. Y., Petersen, L. M., Demkowicz, P., Chen, L., . . . Weinstock, G. M. (2019). Evaluation of 16S rRNA gene sequencing for species and strain-level microbiome analysis. *Nat Commun, 10*(1), 5029. doi:10.1038/s41467-019-13036-1
Jolley, K. A., Bray, J. E., & Maiden, M. C. J. (2018). Open-access bacterial population genomics: BIGSdb software, the PubMLST.org website and their applications. *Wellcome Open Res, 3*, 20. doi:10.12688/wellcomeopenres.14826.1
Kanbar, G., Engels, W., Nicholson, G., Hertle, R., & Winkelmann, G. (2005). Corrigendum to: "Tyramine functions as a toxin in honey bee larvae during Varroa-transmitted infection by Melissococcus pluton" [FEMS Microbiol. Lett. 234 (2004) 149-154]. *FEMS Microbiology Letters, 245*(1), 193-193. doi:10.1016/j.femsle.2005.02.021
Kanbar, G., Engels, W., Nicholson, G. J., Hertle, R., & Winkelmann, G. (2004). Tyramine functions as a toxin in honey bee larvae during Varroa-transmitted infection by Melissococcus pluton. *FEMS Microbiology Letters, 234*(1), 149-154. doi:10.1016/j.femsle.2004.03.022
Kasetsirikul, S., Shiddiky, M. J. A., & Nguyen, N.-T. (2020). Challenges and perspectives in the development of paper-based lateral flow assays. *Microfluidics and Nanofluidics, 24*(2). doi:10.1007/s10404-020-2321-z
Katznelson, H. (1950). *Bacillus pulvifaciens* (N. Sp.) an organism associated with powdery scale of honeybee larvae *Journal of Bacteriology, 59*, 153-155.
Klein-Schneegans, A. S., Kuntz, L., Fonteneau, P., & Loor, F. (1989). Serum Concentrations of IgM, IgGl, IgG2b, IgG3 and IgA in C57BL/6 Mice and their Congenics at the Zpr (Lymphoproliferation) Locus. *Journal of Autoimmunity, 2*, 869-875.
Klein, A. M., Vaissiere, B. E., Cane, J. H., Steffan-Dewenter, I., Cunningham, S. A., Kremen, C., & Tscharntke, T. (2007). Importance of pollinators in changing landscapes for world crops. *Proceedings: Biological Sciences, 274*(1608), 303-313. doi:10.1098/rspb.2006.3721
Köhler, G., & Milstein, C. (1975). Continouse cultures of fused cells secreting antibody of predefined specificity. *Nature, 256*, 3. doi:10.1038/256495a0
Kumar, C. M., Mande, S. C., & Mahajan, G. (2015). Multiple chaperonins in bacteria--novel functions and non-canonical behaviors. *Cell Stress & Chaperones, 20*(4), 20. doi:10.1007/s12192-015-0598-8
Lee, L. G., Nordman, E. S., Johnson, M. D., & Oldham, M. F. (2013). A low-cost, high-performance system for fluorescence lateral flow assays. *Biosensors (Basel), 3*(4), 360-373. doi:10.3390/bios3040360
Lewkowski, O., & Erler, S. (2018). Virulence of *Melissococcus plutonius* and secondary invaders associated with European foulbrood disease of the honey bee. *Microbiologyopen*, e00649. doi:10.1002/mbo3.649
Lin, Z., Madan, D., & Rye, H. S. (2008). GroEL stimulates protein folding through forced unfolding. *Nature Structural & Molecular Biology, 15*(3), 303-311. doi:10.1038/nsmb.1394
Lochhead, A. G. (1928). The etiology of EFB of bees. *Science*.
Lund, P. A. (2009). Multiple chaperonins in bacteria--why so many? *FEMS Microbiology Reviews, 33*(4), 785-800. doi:10.1111/j.1574-6976.2009.00178.x
Maassen, A. (1908). Über die unter dem Namen Faulbrut bekannten seuchenhaften Bruterkrankungen den Honigbiene. *Springer-Verlag Berlin Heidelberg*.

Maeno, S., Tanizawa, Y., Kanesaki, Y., Kubota, E., Kumar, H., Dicks, L., . . . Endo, A. (2016). Genomic characterization of a fructophilic bee symbiont Lactobacillus kunkeei reveals its niche-specific adaptation. *Systematic and Applied Microbiology, 39*(8), 516-526. doi:10.1016/j.syapm.2016.09.006

Matsuda, E. M., de Campos, I. B., de Oliveira, I. P., Colpas, D. R., Carmo, A., & Brigido, L. F. M. (2021). Field evaluation of COVID-19 antigen tests versus RNA based detection: Potential lower sensitivity compensated by immediate results, technical simplicity, and low cost. *Journal of Medical Virology, 93*(7), 4405-4410. doi:10.1002/jmv.26985

McKee, B. A., Djordjevic, S. P., Goodman, R. D., & Hornitzky, M. (2003). The detection of *Melissococcus pluton* in honey bees (*Apis mellifera*) and their products using a hemi-nested PCR. *Apidologie, 34*, 19-27. doi:10.1051/apido:2002047

McKee, B. A., Goodman, R. D., & Hornitzky, M. A. (2004). The transmission of European foulbrood (*melissococcus plutonius*) to artificially reared honey bee larvae (*Apis mellifera*). *Journal of Apicultural Research, 43*(3), 93-100.

Mikušová, Z., Farka, Z., Pastucha, M., Poláchová, V., Obořilová, R., & Skládal, P. (2019). Amperometric Immunosensor for Rapid Detection of Honeybee Pathogen Melissococcus Plutonius. *Electroanalysis, 31*(10), 1969-1976. doi:10.1002/elan.201900252

Mohan Rao, K., Rana, B. S., Chakravart, S. K., Sapna, K., & Sharma, A. (2011). Characterization of *Melissococcus pluton* from European honey bee (*Apis mellifera* L.) of north-west Himalayas. *International Journal of Science and Nature, 2*(3), 632-638.

Morrissey, B. J., Helgason, T., Poppinga, L., Funfhaus, A., Genersch, E., & Budge, G. E. (2015). Biogeography of *Paenibacillus larvae,* the causative agent of American foulbrood, using a new multilocus sequence typing scheme. *Environmental Microbiology, 17*(4), 1414-1424. doi:10.1111/1462-2920.12625

Nakamura, K., Okumura, K., Harada, M., Okamoto, M., Okura, M., & Takamatsu, D. (2021). Peritrophic matrix-degrading proteins are dispensable virulence factors in a virulent Melissococcus plutonius strain. *Scientific Reports, 11*(1), 8798. doi:10.1038/s41598-021-88302-8

Nakamura, K., Yamazaki, Y., Shiraishi, A., Kobayashi, S., Harada, M., Yoshiyama, M., . . . Takamatsu, D. (2016). Virulence Differences among Melissococcus plutonius Strains with Different Genetic Backgrounds in Apis mellifera Larvae under an Improved Experimental Condition. *Scientific Reports, 6*, 33329. doi:10.1038/srep33329

Nezlin, R. (1998). *The Immunoglobulines-Chapter-1-General-Characteristics-of-Immunoglobulin*. USA: Academic Press.

Ngom, B., Guo, Y., Wang, X., & Bi, D. (2010). Development and application of lateral flow test strip technology for detection of infectious agents and chemical contaminants: a review. *Analytical and Bioanalytical Chemistry, 397*(3), 1113-1135. doi:10.1007/s00216-010-3661-4

Nguyen, P. V., Lee, B., Yoo, M.-S., & Yoon, B. S. (2012). Development and Clinical Validation of a DNA Gyrase Subunit B Gene Based Loop-Mediated Isothermal Amplification Method for Detection of Melissococcus plutonius. *Journal of Apiculture*, 51-58.

OIE. (2016). Terrestrial manual. In *Terrestrial manual*: OIE (World Organization for Animal Health).

Olive, D. M., & Bean, P. (1999). Principles and applications of methods for DNA-based typing of microbial organisms. *Journal of Clinical Microbiology, 37*(6), 1661-1669.

Olsen, P. E., Grant, G. A., Nelson, D. L., & Rice, W. A. (1990). Detection of AFB using a monoclonal antibody specific to *Bacillus larvae* in an enzyme-linked immunosorbent assay. *Canadian Journal of Microbiology, 36*, 732-735.

Otte, E. (1973). Ein Beitrag zur Labordiagnose der bösartigen Faulbrut der Honigbiene unter besonderer Berücksichtigung der Immunofloureszenzmethode. *Apidologie, 4*(4), 331-339.

Pastucha, M., Odstrčilíková, E., Hlaváček, A., Brandmeier, J. C., Vykoukal, V., Weisová, J., . . . Farka, Z. (2021). Upconversion-Linked Immunoassay for the Diagnosis of Honeybee Disease American Foulbrood. *IEEE Journal of selected topics in Quantum Electronics, 27*(5), 11. doi:10.1109/JSTQE.2021.3049689

Peng, Y.-S., & Peng, K.-Y. (1979). A study on the possible utilization of immunodiffusion and immunofluorescence techniques as the diagnostic methods for American foulbrood of honeybees (*Apis mellifera*). *Journal of Invertebrate Pathology, 33*, 284-289.

Pinnock, D. E., & Featherstone, N. E. (1984). Detection and quantification of Melissococcus pluton infection by means of enzyme-linked immonosorbent assay. *Journal of Agricultural Research*, 168-170.

Poláchová, V., Pastucha, M., Mikušová, Z., Mickert, M. J., Hlaváček, A., Gorris, H. H., . . . Farka, Z. (2019). Click-conjugated photon-upconversion nanoparticles in an immunoassay for honeybee pathogen Melissococcus plutonius. *Nanoscale, 11*(17), 9. doi:10.1039/c9nr01246j

Pomastowski, P., Zloch, M., Rodzik, A., Ligor, M., Kostrzewa, M., & Buszewski, B. (2019). Analysis of bacteria associated with honeys of different geographical and botanical origin using two different identification approaches: MALDI-TOF MS and 16S rDNA PCR technique. *PLoS ONE, 14*(5), 20. doi:10.1371/journal.pone.0217078

Poppinga, L., Janesch, B., Funfhaus, A., Sekot, G., Garcia-Gonzalez, E., Hertlein, G., . . . Genersch, E. (2012). Identification and functional analysis of the S-layer protein SplA of Paenibacillus larvae, the causative agent of American Foulbrood of honey bees. *PLoS Pathogens, 8*(5), e1002716. doi:10.1371/journal.ppat.1002716

Rince, A., Flahaut, S., & Auffray, Y. (2000). Identification of general stress genes in Enterococcus faecalis. *International Journal of Food Microbiology*(55), 87-91.

Roetschi, A., Berthoud, H., Kuhn, R., & Imdorf, A. (2008). Infection rate based on quantitative real-time PCR of *Melissococcus plutonius*, the causal agent of European foulbrood, in honeybee colonies before and after apiary sanitation. *Apidologie, 38*, 362-371. doi:10.1051/apido:200819

Rossi, F., Amadoro, C., Ruberto, A., & Ricchiuti, L. (2018). Evaluation of Quantitative PCR (qPCR) Paenibacillus larvae Targeted Assays and Definition of Optimal Conditions for Its Detection/Quantification in Honey and Hive Debris. *Insects, 9*(4). doi:10.3390/insects9040165

Roy, C., & Franco, S. (2021). Investigation of an atypical case of European foulbrood in France. *Veterinary Record Case Reports*, 5. doi:10.1002/vrc2.45

Ryan, A., Lynch, M., Smith, S. M., Amu, S., Nel, H. J., McCoy, C. E., . . . Loscher, C. E. (2011). A role for TLR4 in Clostridium difficile infection and the recognition of surface layer proteins. *PLoS Pathogens, 7*(6), e1002076. doi:10.1371/journal.ppat.1002076

Safenkova, I., Zherdev, A., & Dzantiev, B. (2012). Factors influencing the detection limit of the lateral-flow sandwich immunoassay: a case study with potato virus X. *Analytical and Bioanalytical Chemistry, 403*(6), 1595-1605. doi:10.1007/s00216-012-5985-8

Sajid, M., Kawde, A.-N., & Daud, M. (2015). Designs, formats and applications of lateral flow assay: A literature review. *Journal of Saudi Chemical Society, 19*(6), 689-705. doi:10.1016/j.jscs.2014.09.001

Sakamoto, S., Putalun, W., Vimolmangkang, S., Phoolcharoen, W., Shoyama, Y., Tanaka, H., & Morimoto, S. (2018). Enzyme-linked immunosorbent assay for the quantitative/qualitative analysis of plant secondary metabolites. *Journal of Natural Medicines, 72*(1), 32-42. doi:10.1007/s11418-017-1144-z

Saleh, M., Soliman, H., Sorum, H., Fauske, A. K., & El-Matbouli, M. (2012). A novel gold nanoparticles-based assay for rapid detection of Melissococcus plutonius, the causative agent of European foulbrood. *Veterinary Record, 171*(16), 400. doi:10.1136/vr.101040

Sanchez-Campillo, M., Comanducci, M., Raggiaschi, R., Marzocchi, B., Pallini, V., & Ratti, G. (1999). Identification of immunoreactive proteins ofChlamydia trachomatis by Western blot analysisof a two-dimensional electrophoresis map withpatient sera. *Electrophoresis, 20*, 2269-2279.

Sanger F, N. S., Coulson AR. (1977). <DNA sequencing with chain-terminating inhibitors>. *Proceedings of the National Academy of Sciences of the United States of America, 74*(12), 5463–5467. doi:10.1073/pnas.74.12.5463

Saville, B. G. (2011). *Differentiation of Virulent and Biological Control Paenibacillus larvae Strains Associated with American Foulbrood in Bee Hives.* (PhD), The University of York,

Schäfer, M. O., Formella, N., Bettin, B., & Karger, A. (2016). Epidemiology of Paenibacillus larvae in Germany, using MALDI-TOF mass spectrometry. *The 7th European Conference of Apidology : 7-9 September 2016, Cluj-Napoca, Romania*.

Schäfer, M. O., Genersch, E., Funfhaus, A., Poppinga, L., Formella, N., Bettin, B., & Karger, A. (2014). Rapid identification of differentially virulent genotypes of Paenibacillus larvae, the causative organism of American foulbrood of honey bees, by whole cell MALDI-TOF mass spectrometry. *Veterinary Microbiology, 170*(3-4), 291-297. doi:10.1016/j.vetmic.2014.02.006

Sela-Culang, I., Kunik, V., & Ofran, Y. (2013). The structural basis of antibody-antigen recognition. *Frontiers in Immunology, 4*, 302. doi:10.3389/fimmu.2013.00302

Settem, R. P., Honma, K., Nakajima, T., Phansopa, C., Roy, S., Stafford, G. P., & Sharma, A. (2013). A bacterial glycan core linked to surface (S)-layer proteins modulates host immunity through Th17 suppression. *Mucosal Immunology, 6*(2), 415-426. doi:10.1038/mi.2012.85

Shrivastava, A., & Gupta, V. B. (2011). Methods for the determination of limit of detection and limit of quantitation of the analytical methods. *Chronicles of Young Scientists, 2*(1), 5. doi:10.4103/2229-5186.79345

Sleytr, E. B., Messner, P., Pum, D., & Sara, M. (2001). Crystalline bacterial cell surface layers. *Molecular Microbiology, 10*, 911-916.

Sleytr, U. B., Schuster, B., Egelseer, E. M., & Pum, D. (2014). S-layers: principles and applications. *FEMS Microbiology Reviews, 38*(5), 823-864. doi:10.1111/1574-6976.12063

Southwick, E. E., & Southwick, L. J. (1992). Estimating the economic value of honey bees (Hymenoptera: Apidae) as agricultural pollinators in the United States. *v. 85*.

Takamatsu, D., Okumura, K., Tabata, A., Okamoto, M., & Okura, M. (2020). Transcriptional regulator SpxA1a controls the resistance of the honey bee pathogen *Melissococcus plutonius* to the antimicrobial activity of royal jelly. *Environmental Microbiology, 22*(7), 20. doi:10.1111/1462-2920.15125

Takamatsu, D., Sato, M., & Yoshiyama, M. (2016). Infection of *Melissococcus plutonius* clonal complex 12 strain in European honeybee larvae is essentially confined to the digestive tract. *Journal of Veterinary Medical Science, 78*(1), 29-34. doi:10.1292/jvms.15-0405

Tarr, H. L. A. (1937). Studies on American foul brood of bees I. The relative pathogenicity of vegetative cells and endospores of *Bacillus larvae* for the brood of the bee. *The Annals of Applied Biology*, 377-384.

Teixeira, É. W., Ferreira, E. A., Luz, C. F. P. d., Martins, M. F., Ramos, T. A., & Lourenço, A. P. (2020). EFB in stingless bees in brazil: Old disease, renewed threat. *Journal of Invertebrate Pathology, 172*, 10. doi:10.1016/j.jip.2020.107357

Teixera-Gomes, A. P., Cloeckaert, A., & Zygmunt, M. S. (2000). Characterization of Heat, Oxidative, and Acid Stress Responses in Brucella melitensis. *Infection and Immunity, 68*(5).

Theodore, C. M., Stamps, B. W., King, J. B., Price, L. S., Powell, D. R., Stevenson, B. S., & Cichewicz, R. H. (2014). Genomic and metabolomic insights into the natural product biosynthetic diversity of a feral-hog-associated Brevibacillus laterosporus strain. *PLoS ONE, 9*(3), e90124. doi:10.1371/journal.pone.0090124

Thirumalai, D., & Lorimer, G. A. (2001). Chaperonin-mediatedprotein folding. *Annu Rev Biophys Bio*(30), 245–269.

Thompson, S. A. (2002). Campylobacter surface-layers (S-layers) and immune evasion. *Annals of Periodontology, 7*(1), 43-53. doi:10.1902/annals.2002.7.1.43

Tiergesundheitsjahresbericht. (2019). Tiergesundheitsjahresbericht. *Friedrich-Loeffler-Institute*, 30-31.

Tomkies, V., Flint, J., Johnson, G., Waite, R., Wilkins, S., Danks, C., . . . Brown, M. (2009). Development and validation of a novel field test kit for European foulbrood. *Apidologie, 40*, 63-72. doi:10.1051/apido:2008060

Tsan, M. F., & Gao, B. (2009). Heat shock proteins and immune system. *Journal of Leukocyte Biology, 85*(6), 6. doi:10.1189/jlb.0109005
van Belkum, A. (1999). Short sequence repeats in microbial pathogenesis and evolution. *Cellular and Molecular Life Sciences, 56*, 6. doi:10.1007/s000180050019
Völker, U., Engelmann, S., Maul, B., Riethdorf, S., Völker, A., Schmid, R., . . . Heckerl, M. (1994). Analysis of the induction of general stress proteins of Bacillus subtilis. *Microbiology, 140*, 741-752.
Wharton, D. R. A. (1927). Etiology of EFB of bees. *Science*.
White, A. (1912). The cause of European foul brood. *Washington: government printing office*.
White, G. F. (1906). *The bacteriology of bee diseases*. Retrieved from
White, G. F. (1920). American Foulbrood. *United States Department of Agriculture, 809*, 1-46.
Wilkins, S., Brown, M. A., & Cuthbertson, A. G. (2007). The incidence of honey bee pests and diseases in England and Wales. *Pest Management Science, 63*(11), 1062-1068. doi:10.1002/ps.1461
Winston, M. L. (1987). *The biology of the honey bee*: Harvard University Press.
Woodrow, A. W. (1942). Susceptibility of honeybee larvae to individual inoculations with spores of *Bacillus larvae*. *Journal of Economic Entomology, 35*(6), 892-895.
Woodrow, A. W., & Holst, E. C. (1942). The mechanism of colony resistance to American Foulbrood. *Journal of Economic Entomology, 35*(3), 327-330.
Xu, M., van Hoof, R. A., Hamers, A. R. M., de Rijk, T. C., Guo, Y., Bovee, T. F. H., & Peters, J. (2019). *Innovative lateral flow devices for the detection of pesticides harmful to bees*. https://research.wur.nl/en/publications/innovative-lateral-flow-devices-for-the-detection-of-pesticides-h
Yue, D., Nordhoff, M., Wieler, L. H., & Genersch, E. (2008). Fluorescence in situ hybridization (FISH) analysis of the interactions between honeybee larvae and *Paenibacillus larvae*, the causative agent of American foulbrood of honeybees (*Apis mellifera*). *Environmental Microbiology, 10*(6), 1612-1620. doi:10.1111/j.1462-2920.2008.01579.x
Zarschler, K., Janesch, B., Zayni, S., Schaffer, C., & Messner, P. (2009). Construction of a gene knockout system for application in Paenibacillus alvei CCM 2051T, exemplified by the S-layer glycan biosynthesis initiation enzyme WsfP. *Applied and Environmental Microbiology, 75*(10), 3077-3085. doi:10.1128/AEM.00087-09
Ziegler, I., Vollmar, P., Knupfer, M., Braun, P., & Stoecker, K. (2021). Reevaluating limits of detection of 12 lateral flow immunoassays for the detection of Yersinia pestis, Francisella tularensis, and Bacillus anthracis spores using viable risk group-3 strains. *Journal of Applied Microbiology, 130*(4), 1173-1180. doi:10.1111/jam.14863

8. Table index

9. Figure index

10. Formula index

Eigenständigkeitserklärung

Hiermit erkläre ich, dass diese Arbeit bisher von mir weder an der Mathematisch-Naturwissenschaftlichen Fakultät der Universität Greifswald noch einer anderen wissenschaftlichen Einrichtung zum Zwecke der Promotion eingereicht wurde.

Ferner erkläre ich, dass ich diese Arbeit selbstständig verfasst und keine anderen als die darin angegebenen Hilfsmittel und Hilfen benutzt und keine Textabschnitte eines Dritten ohne Kennzeichnung übernommen habe.

Sandra Ehrenberg

Appendix

Below, the tables show the used chemicals (Table S 1Table S 1 Chemicals), electronic equipment (Table S 2) and devices (Table S 3).

Table S 1 Chemicals

Chemicals	Supplier
1-Step™ Ultra TMB-ELISA Substrate Solution	Thermo Scientific, USA
acetic acid	Carl Roth GmbH, Karlsruhe
acrylamide	Carl Roth GmbH, Karlsruhe
agarose Lonza LE	Biozym, Vienna
agarose NuSieve 3:1	Biozym, Vienna
ammonium persulfate (APS)	Sigma-Aldrich, Steinheim
BactoAgar	BD Bioscience, USA
bicarbonate buffer pH 9.6 (CBB)	Senova, Weimar
bovine serum albumin fraction V, pH 7 (BSA)	SERVA, Heidelberg
Clarity™ Western ECL Blotting Substrates	Bio-Rad, USA
cOmplete™ Protease Inhibitor Cocktail	Merck, Schuchardt
Coomassie Brilliant Blue R-250	Thermo Scientific, USA
D-glucose	Carl Roth GmbH, Karlsruhe
dimethyl formamide (DMF)	Thermo Scientific, Germany
dimethylsulfoxid (DMSO)	Carl Roth GmbH, Karlsruhe
dipotassium phosphate (K2HPO4)	Carl Roth GmbH, Karlsruhe
ethanol 96 % denatured	Carl Roth GmbH, Karlsruhe
ethanol 99 %	Carl Roth GmbH, Karlsruhe
ethidium bromide (EtBr)	Carl Roth GmbH, Karlsruhe
ethylene diamine tetra acetic acid (EDTA)	Serva, Heidelberg
Freund's Adjuvant, Complete cell suspension (FCA)	Sigma-Aldrich, Steinheim
Freund's Adjuvant, Incomplete liquid (FICA)	Sigma-Aldrich, Steinheim
fructose	Carl Roth GmbH, Karlsruhe
GelRed 10 000 x in water	Biotium, USA
GeneRuler 100 bp Plus; 1kb; 1kb plus	Thermo Scientific, USA
GERBU Adjuvant MM™	GERBU Biotechnik GmbH, Heidelberg
glycerine 99%	Carl Roth GmbH, Karlsruhe
glycine	Carl Roth GmbH, Karlsruhe
HEPES	Carl Roth GmbH, Karlsruhe
Hi-Di™ Formamide	ThermoFisher Scientific
hydrochloric acid (HCl)	Carl Roth GmbH, Karlsruhe
IGEPAL CA-630	Sigma-Aldrich, Steinheim
imidazole	Sigma-Aldrich, Steinheim
isopropanol	Carl Roth GmbH, Karlsruhe
isopropyl-b-D-thiogalactopyranosid (IPTG)	MP Biomedicals, France
kanamycin	Carl Roth GmbH, Karlsruhe
L-cysteine	Carl Roth GmbH, Karlsruhe
loading dye 6x	ThermoFisher Scientific

lysozyme	Carl Roth GmbH, Karlsruhe
magnesium chloride (MgCl2)	Thermo Scientific
methanol	Carl Roth GmbH, Karlsruhe
milk powder	Hobbybäcker-Versand, Bellaberg
MRS Broth	Merck, Schuchardt
PageRuler™ Prestained Protein Ladder, 10 to 180 kDa	Thermo Scientific
Pierce™ Coomassie Brilliant Blue R-250	Thermo Scientific
polyethylene glycol 1500 (PEG 1500)	Sigma-Aldrich, Steinheim
potassium chloride (KCl)	Merck, Darmstadt
potassium dihydrogen phosphate (KH2PO4)	Merck, Darmstadt
potassium dihydrogen phosphate (KH2PO4)	Carl Roth GmbH, Karlsruhe
potassium sulphate (K2SO4)	Sigma-Aldrich, Steinheim
ready-to-use, nuclease-free DEPC water	Carl Roth GmbH, Karlsruhe
Roti®-CELL 10x Phosphate-Buffered Saline (PBS)	Carl Roth GmbH, Karlsruhe
royal jelly	Biozentrum GmbH & Co. KG
sodium acetate	Merck, Darmstadt
sodium chloride (NaCl)	Carl Roth GmbH, Karlsruhe
sodium dodecylsulphate (SDS)	Carl Roth GmbH, Karlsruhe
sodium hydrogen phosphate dihydrate ($Na_2HPO_4x2H_2O$)	Carl Roth GmbH, Karlsruhe
sodium hydroxide (NaOH)	Carl Roth GmbH, Karlsruhe
sodium phosphate	Sigma-Aldrich, Steinheim
starch	Carl Roth GmbH, Karlsruhe
Streptavidin-PolyHRP40, stock 1 mg/mL (SA-poly-HRP)	SDT GmbH, Germany
sucrose	Carl Roth GmbH, Karlsruhe
sulphuric acid 96 % (H2SO4)	Carl Roth GmbH, Karlsruhe
temed	Carl Roth GmbH, Karlsruhe
TERGITOL™	Sigma-Aldrich, Germany
Tris base	Thermo Fisher Scientific, USA
trypan blue staining	Sigma-Aldrich, Steinheim
TWEEN-20	Sigma-Aldrich, Steinheim
urea	Carl Roth GmbH, Karlsruhe
yeast extract	Thermo Scientific
β-Mercaptoethanol	Merck, Schuchardt

Table S 2 Electronic equipment

Electronic equipment	**Supplier**
AB Hitachi 3500 Genetic Analyzer	Applied Biosystems, Weiterstadt
balance handy H51	Sartorius AG, Göttingen
balance M-power	Sartorius AG, Göttingen
balance universal U6100D	Sartorius AG, Göttingen
centrifuge 5424	Eppendorf, Germany
centrifuge 5430 R	Eppendorf, Germany
centrifuge 5810R	Eppendorf, Germany
centrifuge Biofuge 13	Heraeus sepatech
centrifuge HSA 28001	biozym, USA

CO2 incubator MCO-19A/C	Sanyo, Japan
DNA/RNA work station	Kisker Biotech GmbH & Co. KG, Germany
flame device IBS Fireboy eco	Integra Biosciences AG, Switzerland
Flex cycler2	Analytik Jena GmbH, Germany
fraction collector Frac-920 Äkta	Amersham Biosciences Europe GmbH, Germany
freezer comfort	Liebherr, Germany
fridge profi line	Liebherr, Germany
Imaging system ChemiDoc	Bio-Rad Laboratories, Germany
Imaging system ChemiDoc MP	Bio-Rad Laboratories, Germany
incubation shaker Multitron HT	Infors AG, Switzerland
magnetic stirrer IKA-combimag RCO	Bachofer, Reutlingen
magnetic stirrer IKA-combimag REO	Bachofer, Reutlingen
magnetic stirrer IKAMAG RCT	Janke & Künkel GmbH & Co, Staufen
magnetic stirrer MR Hei standard	Heidolph, Schwabach
microplate reader F200 pro	Tecan, Switzerland
microplate reader infinite M200 pro	Tecan, Switzerland
microplate shaker Wallace 1296-001	Heidolph, Schwabach
microscope Axio LAB-A1	Carl Zeiss AG, Germany
microwave	Siemens
mixer M-925 Äkta	Amersham Biosciences Europe GmbH, Germany
Monitor UPC-900 Äkta	Amersham Biosciences Europe GmbH, Germany
NanoDrop 2000C	Thermo Scientific
pH bench top ORION 3 STAR	Thermo electron cooperation, Germany
pH bench top WTW series ph 720	Xylem Analytics Germany Sales GmbH & Co KG
power supply Major Science MP-3AP	biostep GmbH, Jahnsdorf
power supply, Power Pac basic	Bio-Rad Laboratories, Germany
pump P-920 Äkta	Amersham Biosciences Europe GmbH, Germany
safety workbench Safe 2020	Thermo Scientific
Secuflow SF-TA	Waldner Laboreinrichtungen GmbH & Co. KG, Wangen
sonifier 450 Branson	G. Heinemann Ultraschall- und Labortechnik, Germany
table light source	Messinstrumentebau GmbH, Erlangen
Thermal cycler CFX96 RT system	Bio-Rad Laboratories, Germany
Thermo stat plus	Eppendorf, Germany
Thermocycler C10000	Bio-Rad Laboratories, Germany
Thermomix 5436	Eppendorf, Germany
Thermomixer comfort	Eppendorf, Germany
Ultraflex TOF/TOF mass spectrometer	Bruker Corporation, USA
vacuum system BVC 21 NT	Vacuubrand GmbH & Co KG, Wertheim
vortex gene 2	Scientific Industries, USA
vortex K550-GE	Bachofer, Reutlingen
water bath U3	Bachofer, Reutlingen

Table S 3 Lab devices

Devices	Supplier
dispenser multipipette plus	Eppendorf, Germany
DynaMag™-2 Magnet	Thermo Fisher Scientific, Norway
electrophoresis cells Mini-Sub Cell GT Cell	Bio-Rad Laboratories, Germany
electrophoresis cells Sub-Cell GT Cell	Bio-Rad Laboratories, Germany
electrophoresis cells Wide Mini-Sub Cell GT Cell	Bio-Rad Laboratories, Germany
ELISA washer Nunc immuno wash 12	Thermo Scientific
Helber Bacteria Counting Chamber	Hawksley, UK
Mini-PROTEAN system short plates	Bio-Rad Laboratories, Germany
Mini-PROTEAN system spacer plates with 1mm spacers	Bio-Rad Laboratories, Germany
Mini-PROTEAN Tetra Vertical Electrophoresis Cell	Bio-Rad Laboratories, Germany
multi-channel pipette (200 µL)	Eppendorf, Germany
Oxoid AnaeroJar AG0025	Thermo Scientific
pipette (1000 µL, 200 µL, 100 µL, 10 µL)	Eppendorf, Germany
semi dry blotter unit V20-SDB	biostep GmbH, Jahnsdorf

Table S 4 Consumables

Consumables	Supplier
Amersham Protran 0.2µm nitrocellulose blotting membrane	Cytiva, USA
AnaeroGen sachet	Thermo Scientific
clot activator S-Monovette Z	Sarstedt Inc., USA
Corning membrane filter, 100 µm	Thermo Fisher Scientific, Germany
Corning® Axygen® PCR Tube Strips	Merck, Germany
disposable Luer-Lock syringes (10 mL, 50 mL)	BD biosciences
filter units Millex-GP, sterile, 0.22 µm	Merck, Germany
HisTrap HP Ni^{2+} column	Thermo Scientific, Sweden
HiTrap Protein G HP 1mL	Cytiva, USA
MaxiSorp Clear C-Shaped Immuno nonsterile 96-well plates	Thermo Scientific
Multiplate PCR plates white	Bio-Rad Laboratories, Germany
Nunc™ microplate lids	Thermo Scientific
Pierce™ Protein Concentrators, PES 10K	Thermo Scientific, USA
Pierce™ Protein Concentrators, PES 30K	Thermo Scientific, USA
Pipette tips (10 µL, 20 µL, 100 µL, 200 µL, 1000 µL)	Eppendorf, Germany
polystyrene serological pipettes	Thermo Scientific
Reaction tubes (1.5 mL, 2 mL)	Sarstedt Inc., USA
Reaction tubes Safelock (1.5 mL, 2 mL)	Eppendorf, Germany
Reagent tubes (15 mL, 50 mL)	Sarstedt Inc., USA
Whatmann gel blot paper	Cytiva, USA

Results of LFD validation described in chapter 4.6.

Table S 5 LFD: dilution series of the target bacteria

Sample concentration in cell/mL	Sample species	AFB-LFD	AFB-ERIC II-LFD	EFB-LFD
$1x10^7$	*M. plutonius*	negative	negative	positive
$5x10^6$	*M. plutonius*	negative	negative	positive
$1x10^6$	*M. plutonius*	negative	negative	negative
$5x10^5$	*M. plutonius*	negative	negative	negative
$1x10^5$	*M. plutonius*	negative	negative	negative
$5x10^6$	*P. larvae* ERIC I	positive	negative	negative
$1x10^6$	*P. larvae* ERIC I	positive	negative	negative
$5x10^5$	*P. larvae* ERIC I	positive	negative	negative
$1x10^5$	*P. larvae* ERIC I	positive	negative	negative
$5x10^4$	*P. larvae* ERIC I	negative	negative	negative
$5x10^6$	*P. larvae* ERIC II	positive	positive	negative
$1x10^6$	*P. larvae* ERIC II	positive	positive	negative
$5x10^5$	*P. larvae* ERIC II	positive	negative	negative
$1x10^5$	*P. larvae* ERIC II	positive	negative	negative
$5x10^4$	*P. larvae* ERIC II	negative	negative	negative

Table S 6 LFD results of bee-associated bacteria

reference number	Species	AFB-LFD	EFB-LFD
DSM 101882	*Parasaccharibacter apium*	negative	negative
DSM 12361	*Lactobacillus kunkeei*	negative	negative
DSM 18844	*Paenibacillus dendritiformis*	negative	negative
DSM 20478	*Enterococcus faecalis*	negative	negative
DSM 25	*Brevibacillus laterosporus*	negative	negative
DSM 27	*Bacillus pumilus*	negative	negative
DSM 29	*Paenibacillus alvei*	negative	negative

Table S 7 LFD results of M. plutonius strains

reference number	Species	AFB-LFD	EFB-LFD
2013_02	*M. plutonius*	negative	positive
2013_27	*M. plutonius*	negative	positive
2013_30	*M. plutonius*	negative	positive
2013_35	*M. plutonius*	negative	positive
2013_51	*M. plutonius*	negative	positive
CH 21.1	*M. plutonius*	negative	positive
CH 40.2	*M. plutonius*	negative	positive
CH 41.4	*M. plutonius*	negative	positive
CH 46.1	*M. plutonius*	negative	positive
CH 48.1	*M. plutonius*	negative	positive

CH 49.3	*M. plutonius*	negative	positive
CH 54.1	*M. plutonius*	negative	positive
CH 60	*M. plutonius*	negative	positive
CH 90	*M. plutonius*	negative	positive
CH 119	*M. plutonius*	negative	positive
LMG 20360	*M. plutonius*	negative	positive

Table S 8 LFD results of P. larvae strains

reference number	Species	ERIC-genotype	AFB-LFD	EFB-LFD
DSM 25719	*P. larvae*	ERIC I	positive	negative
DSM 25430	*P. larvae*	ERIC II	positive	negative
DSM 8443	*P. larvae*	ERIC III	positive	negative
DSM 3615	*P. larvae*	ERIC IV	positive	negative
DSM 106052	*P. larvae*	ERIC V	positive	negative
122-13	*P. larvae*	ERIC I	positive	negative
131-13	*P. larvae*	ERIC I	positive	negative
135-13	*P. larvae*	ERIC I	positive	negative
151-13	*P. larvae*	ERIC I	positive	negative
204-13	*P. larvae*	ERIC I	positive	negative
222-13	*P. larvae*	ERIC I	positive	negative
255-13	*P. larvae*	ERIC I	positive	negative
277-13	*P. larvae*	ERIC I	positive	negative
329-13	*P. larvae*	ERIC I	positive	negative
489-13	*P. larvae*	ERIC I	positive	negative
35-14	*P. larvae*	ERIC I	positive	negative
66-14	*P. larvae*	ERIC I	positive	negative
92-14	*P. larvae*	ERIC I	positive	negative
99-14	*P. larvae*	ERIC I	positive	negative
190-14	*P. larvae*	ERIC I	positive	negative
208-14	*P. larvae*	ERIC I	positive	negative
235-14	*P. larvae*	ERIC I	positive	negative
299-14	*P. larvae*	ERIC I	positive	negative
412-14	*P. larvae*	ERIC I	positive	negative
528-14	*P. larvae*	ERIC I	positive	negative
46-15	*P. larvae*	ERIC I	positive	negative
56-15	*P. larvae*	ERIC I	positive	negative
183-15	*P. larvae*	ERIC I	positive	negative
223-15	*P. larvae*	ERIC I	positive	negative
250-15	*P. larvae*	ERIC I	positive	negative
278-15	*P. larvae*	ERIC I	positive	negative
365-15	*P. larvae*	ERIC I	positive	negative
442-15	*P. larvae*	ERIC I	positive	negative
500-15	*P. larvae*	ERIC I	positive	negative
542-15	*P. larvae*	ERIC I	positive	negative
129-13	*P. larvae*	ERIC II	positive	negative

172-13	*P. larvae*	ERIC II	positive	negative
182-13	*P. larvae*	ERIC II	positive	negative
262-13	*P. larvae*	ERIC II	positive	negative
274-13	*P. larvae*	ERIC II	positive	negative
292-13	*P. larvae*	ERIC II	positive	negative
324-13	*P. larvae*	ERIC II	positive	negative
353-13	*P. larvae*	ERIC II	positive	negative
443-13	*P. larvae*	ERIC II	positive	negative
487-13	*P. larvae*	ERIC II	positive	negative
01-14	*P. larvae*	ERIC II	positive	negative
05-14	*P. larvae*	ERIC II	positive	negative
40-14	*P. larvae*	ERIC II	positive	negative
64-14	*P. larvae*	ERIC II	positive	negative
145-14	*P. larvae*	ERIC II	positive	negative
204-14	*P. larvae*	ERIC II	positive	negative
240-14	*P. larvae*	ERIC II	positive	negative
253-14	*P. larvae*	ERIC II	positive	negative
307-14	*P. larvae*	ERIC II	positive	negative
431-14	*P. larvae*	ERIC II	positive	negative
41-15	*P. larvae*	ERIC II	positive	negative
76-15	*P. larvae*	ERIC II	positive	negative
172-15	*P. larvae*	ERIC II	positive	negative
197-15	*P. larvae*	ERIC II	positive	negative
236-15	*P. larvae*	ERIC II	positive	negative
291-15	*P. larvae*	ERIC II	positive	negative
301-15	*P. larvae*	ERIC II	positive	negative
400-15	*P. larvae*	ERIC II	positive	negative
427-15	*P. larvae*	ERIC II	positive	negative
510-15	*P. larvae*	ERIC II	positive	negative
341-13	*P. larvae*	ERIC *	positive	negative
493-13	*P. larvae*	ERIC *	positive	negative
456-13	*P. larvae*	ERIC **	positive	negative
1201-14	*P. larvae*	ERIC **	positive	negative
252-18	*P. larvae*	atypical	positive	negative
282-18	*P. larvae*	atypical	positive	negative
100-19	*P. larvae*	atypical	positive	negative

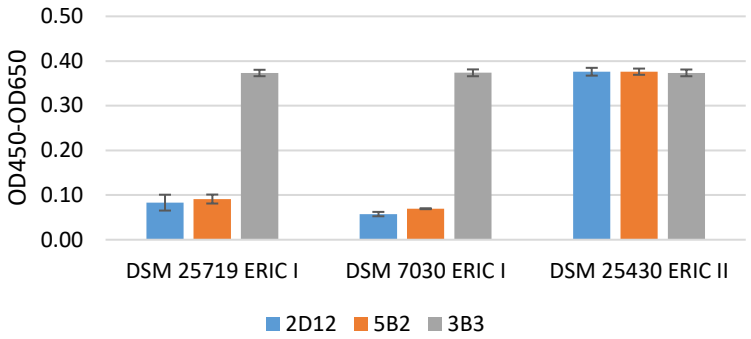

Figure S 1 Indirect ELISA of P. larvae reference strains

The indirect ELISA was performed with the anti-*P. larvae* mAb 3B3 and the two anti-ERIC II mAbs (2D12 and 5B2). Different ERIC I (DSM 25719; DSM 7030) and ERIC II (DSM 25430) reference strains were immobilized on ELISA plates (x-axis). The values of OD_{650} were subtracted from the values measured at OD_{450} (y-axis). The bars show the average of three technical replicates. The blue bars are representing 2D12, the orange bars are 5B2 and grey bars show the reactivity of 3B3. The error bars represent standard deviation of three technical replicates.